الجمهوريـة الجزائـريـة الديمقراطيـة الشعبيـة

People's Democratic Republic of Algeria

وزارة التعليــم العالـي والبحـث العلمـي

Ministry of Higher Education and Scientific Research

University of Mila

جـــامعة ميلـة

Faculty of Mathematics and Computer Sciences

Order N°: …………………

Registration number: …………….

Department: Mathematics

Field : Mathematics

Specialty: Applied Mathematics

Thesis

Submitted for the degree of
Doctorate LMD

Oligopolistic competition: Dynamic analysis and chaos control

Presented by: Azioune Mourad

Defended on: 23/07/2026

Jury Members:

Boudjedaa Badredine	Professor	University of Mila	Chairman
Abdelouahab Mohammed Salah	Professor	University of Mila	Supervisor
Hafirassou Zineb	MCB	University of Mila	Co-supervisor
Bazaniar Abdelghafour	MCA	University of Mila	Examiner
Laouira Widad	MCA	University of Mila	Examiner
Meddour Lotfi	MCA	Mentouri Brothers University of Constantine	Examiner
Menasri Abdellah	MCA	Higher National School of Forests, khenchela	Examiner

University year: 2025/2026

Acknowledgements

The completion of this thesis would not have been possible without the unwavering help, encouragement, and support of many individuals. Their guidance, inspiration, and willingness to share their expertise have profoundly shaped the progress and quality of this work. I am deeply grateful for their contributions, both academic and personal, which sustained me throughout this journey. To all of them, I extend my sincere appreciation and heartfelt gratitude. I am truly thankful to everyone who contributed in different ways to the realization of this work. Each of them played an important part in making this academic journey successful.

First and foremost, I would like to express my deep appreciation to my supervisor, Professor **Abdelouahab Mohammed Salah**, for his constant guidance, availability, and valuable advice throughout my research. His insightful suggestions and continuous encouragement helped me overcome many challenges and move forward with confidence. His dedication and generosity went far beyond his role as an academic advisor, and for that, I am sincerely grateful.

I also wish to thank the members of the jury for their interest in my research and for taking the time to evaluate this work. I am deeply grateful to the Chairman, **Badredine Boudjedaa**, my Supervisor, **Mohammed-Salah Abdelouahab**, and my Co-supervisor **Zineb Hafirassou**. I also extend my sincere thanks to the examiners: **Abdelghafour Bazaniar**, **Widad Laouira**, **Lotfi Meddour**, and **Abdellah Menasri**.

Their constructive feedback and thoughtful remarks have greatly improved the quality and clarity of my thesis. Their commitment to academic excellence has been a true source of inspiration.

My special thanks go as well to the administrative staff of the Doctoral School at the University of Mila for their continuous support and assistance. Their professionalism and dedication have contributed to creating a motivating and supportive environment for research and learning.

I would also like to express my appreciation to my fellow PhD colleagues for their collaboration, fruitful discussions, and friendly spirit. Sharing this journey with them made the process more enriching and enjoyable.

Finally, I extend my warmest thanks to all those who, directly or indirectly, contributed to the completion of this thesis. Their encouragement, kindness, and trust have been of great help throughout this endeavor. I am deeply thankful to all of them.

Dedication

To my dear parents,

whose boundless love, constant encouragement, and sacrifices
have been the foundation of all my achievements.

To my wonderful wife,

whose patience, understanding, and unwavering support
have given me strength and peace throughout this journey.

To my daughter,

whose joy, curiosity, and love
have brightened every step of my path.

To my teachers and mentors,

whose knowledge and guidance have shaped my academic path
and inspired my pursuit of learning and excellence.

And to my family and friends,

who have stood by me with kindness and faith,
this work is devoted to you with sincere gratitude.

Abstract

In oligopolistic markets, firms offer homogeneous or differentiated products. The Cournot and Bertrand models are the two classical frameworks used to describe competition in such markets. In the Cournot model, firms maximize their profits by choosing production quantities while taking their competitors' decisions into account. In the Bertrand model, firms maximize their profits by choosing prices while considering the pricing strategies of their competitors. The aim of this thesis is to develop and analyze discrete time oligopoly models based on realistic assumptions regarding firms' expectations and bounded rationality. The qualitative behavior of these models is investigated using stability and bifurcation theory. Particular attention is devoted to the emergence of complex dynamics, including periodic oscillations and chaotic behavior, resulting from variations in key model parameters. Several numerical tools, including bifurcation diagrams, phase portraits, and Lyapunov exponents, are employed to characterize the system dynamics and identify transitions from stability to chaos. Finally, different chaos control strategies are implemented to suppress unstable and chaotic trajectories and stabilize economically meaningful equilibria, thereby improving the predictability and reliability of the proposed models.

Keywords: Oligopolistic Markets, Cournot and Bertrand Models, Discrete Dynamical Systems, Stability Analysis, Bifurcation Theory, Chaos Control.

ملخص

في أسواق احتكار القلة، تقدم الشركات منتجات متجانسة أو متمايزة. ويُعد نموذجا كورنو وبرتراند الإطارين الكلاسيكيين الرئيسيين المستخدمين لوصف المنافسة في هذه الأسواق. ففي نموذج كورنو، تعمل الشركات على تعظيم أرباحها من خلال اختيار كميات الإنتاج مع مراعاة قرارات الشركات المنافسة. أما في نموذج برتراند، فتعمل الشركات على تعظيم أرباحها من خلال اختيار الأسعار مع الأخذ في الاعتبار استراتيجيات التسعير التي تعتمدها الشركات المنافسة. تهدف هذه الأطروحة إلى تطوير وتحليل نماذج احتكار القلة ذات الزمن المتقطع، اعتمادًا على فرضيات واقعية تتعلق بتوقعات الشركات ومحدودية العقلانية. ويُدرس السلوك النوعي لهذه النماذج باستخدام نظرية الاستقرار ونظرية التشعبات. ويُولى اهتمام خاص لظهور الديناميكيات المعقدة، بما في ذلك التذبذبات الدورية والسلوك الفوضوي، الناتجة عن تغير القيم الأساسية لمعاملات النموذج. ولتحليل ديناميكية هذه الأنظمة وتحديد الانتقالات من حالات الاستقرار إلى الفوضى، تُستخدم مجموعة من الأدوات العددية، من بينها مخططات التشعب، والفضاءات الطورية، وأُسس ليابونوف. وأخيرًا، تُطبَّق عدة استراتيجيات للتحكم في الفوضى بهدف القضاء على المسارات غير المستقرة والفوضوية وتثبيت حالات التوازن ذات الدلالة الاقتصادية، مما يسهم في تحسين القدرة التنبؤية للنماذج المقترحة وزيادة موثوقيتها.

الكلمات المفتاحية: أسواق احتكار القلة، نموذجا كورنو وبرتراند، الأنظمة الديناميكية المتقطعة، تحليل الاستقرار، نظرية التشعبات، التحكم في الفوضى.

Résumé

Dans les marchés oligopolistiques, les entreprises proposent des produits homogènes ou différenciés. Les modèles de Cournot et de Bertrand constituent les deux cadres classiques utilisés pour décrire la concurrence dans ces marchés. Dans le modèle de Cournot, les entreprises maximisent leurs profits en choisissant leurs quantités de production tout en tenant compte des décisions de leurs concurrents. Dans le modèle de Bertrand, les entreprises maximisent leurs profits en choisissant leurs prix tout en prenant en considération les stratégies de tarification de leurs concurrents. L'objectif de cette thèse est de développer et d'analyser des modèles oligopolistiques en temps discret fondés sur des hypothèses réalistes concernant les anticipations des entreprises et la rationalité limitée. Le comportement qualitatif de ces modèles est étudié à l'aide de la théorie de la stabilité et des bifurcations. Une attention particulière est accordée à l'apparition de dynamiques complexes, notamment des oscillations périodiques et des comportements chaotiques, résultant des variations des principaux paramètres du modèle. Plusieurs outils numériques, notamment les diagrammes de bifurcation, les portraits de phase et les exposants de Lyapunov, sont utilisés pour caractériser la dynamique des systèmes et identifier les transitions entre les régimes stables et chaotiques. Enfin, différentes stratégies de contrôle du chaos sont mises en œuvre afin de supprimer les trajectoires instables et chaotiques et de stabiliser des équilibres économiquement significatifs, améliorant ainsi la prédictibilité et la fiabilité des modèles proposés.

Mots-clés: Marchés oligopolistiques, modèles de Cournot et de Bertrand, systèmes dynamiques discrets, analyse de stabilité, théorie des bifurcations, contrôle du chaos.

Contents

General Introduction

Over the past decades, the theory of dynamical systems has become one of the most influential and interdisciplinary areas of modern science, with applications spanning mathematics, physics, biology, engineering, and economics [43, 61, 66]. It provides a rigorous mathematical framework for describing the evolution of systems over time according to deterministic laws. Among the different modeling approaches, discrete-time dynamical systems have attracted considerable attention because they naturally describe iterative processes and sequential decision-making mechanisms that frequently arise in engineering, biological, and economic applications [28, 31].

A discrete dynamical system is commonly represented by a difference equation that maps the current state of the system to its subsequent state through an iterative process [28, 31]. Depending on the system parameters and the nonlinear characteristics of the governing equations, the resulting dynamics may converge to an equilibrium, evolve toward periodic oscillations, or exhibit highly irregular chaotic behavior. Consequently, stability analysis plays a fundamental role in understanding the long-term behavior of discrete systems, while bifurcation theory provides the mathematical framework for explaining qualitative changes in system dynamics as parameters vary [43, 45, 60].

One of the most remarkable properties of nonlinear discrete dynamical systems is their ability to generate extremely rich behaviors from relatively simple mathematical models. As system parameters change, transitions from stable equilibria to periodic oscillations and eventually to chaos may occur through several classical bifurcation mechanisms, including period-doubling (Flip), Neimark–Sacker bifurcations, and intermittency [43, 60]. These phenomena have been extensively investigated because they explain how small parameter variations may drastically modify the qualitative behavior of a nonlinear system.

The study of nonlinear dynamics has found numerous applications in economics, where many decision-making processes naturally evolve in discrete time. In particular, oligopolistic markets provide an important framework for applying dynamical systems theory. In these markets, a small number of firms interact strategically while attempting to maximize their individual profits. The two classical models of oligopoly theory are the Cournot model, in which firms compete through production quantities [27], and the Bertrand model, where competition is based on prices [18]. These models constitute the theoretical foundation of modern nonlinear oligopoly analysis and have motivated numerous extensions incorporating adaptive expectations, bounded rationality, heterogeneous players, and delayed information [19, 54, 58].

When firms adjust their production or pricing strategies according to bounded rationality, they rely on local market information rather than perfect optimization. Their decisions are therefore updated iteratively through simple adaptive rules, leading naturally to nonlinear discrete dynamical systems [19, 54]. The dynamic behavior of these models strongly depends on adjustment speeds, production costs, substitution effects, and demand characteristics. While appropriate parameter values ensure convergence toward the Nash equilibrium, excessive adjustment speeds frequently destabilize the market, giving rise to periodic oscillations, bifurcations, and chaotic fluctuations [4, 20, 34]. Such complex behaviors are economically undesirable because they generate unpredictable prices, unstable production levels, and irregular profit patterns.

To overcome these instabilities, numerous chaos control techniques have been proposed during the past three decades. Among them, the Ott–Grebogi–Yorke (OGY) method remains one of the most influential approaches for stabilizing unstable periodic or equilibrium solutions through very small parameter perturbations [56]. Since its introduction, this method has been successfully adapted to many nonlinear economic models. For example, Sarafopoulos and Papadopoulos [59] investigated chaos control in a Bertrand duopoly with quadratic costs, while Elsadany and Awad [32] proposed stabilization strategies for Bertrand competition under environmental taxation. More recently, Azioune and Abdelouahab [10] demonstrated the suppression of chaos and mixed-mode oscillations in a Bertrand duopoly with homogeneous expectations, and Azioune *et al.* [12] successfully applied the OGY method to stabilize chaotic dynamics in a boundedly rational Cournot triopoly. Similar investigations have also been conducted for heterogeneous Cournot-Bertrand competition [3] and fractional-order Cournot models defined on complex networks [39], confirming the effectiveness of chaos control techniques in nonlinear economic systems.

Motivated by these developments, this thesis investigates the nonlinear dynamics of discrete oligopoly games with particular emphasis on stability analysis, bifurcation phenomena, and chaos control. The main objective is to analyze the dynamic interactions among boundedly rational firms operating in Cournot and Bertrand markets and to determine how variations in adjustment speeds, substitution rates, and production costs affect the qualitative behavior of market equilibria. Both local analytical techniques and extensive numerical simulations are employed to identify stability regions, characterize bifurcation scenarios, and detect the onset of chaotic dynamics.

To complement the theoretical analysis, several numerical tools are employed throughout this work, including bifurcation diagrams, phase portraits, and Lyapunov exponents [36]. These indicators provide a comprehensive description of the transition from stable equilibria to periodic and chaotic regimes. Furthermore, chaos control strategies, particularly the OGY method and state feedback control techniques, are implemented to suppress chaotic oscillations and recover the stability of economically meaningful Nash equilibria.

The organization of this thesis is presented as follows:

- **Chapter 1** presents generalities on discrete dynamical systems and chaos control. It introduces the mathematical foundations of discrete and continuous systems, the concept of stability, and the classification of bifurcations. It also reviews the main approaches to chaos control, focusing particularly on the OGY method and feedback-based techniques.

- **Chapter 2** discusses oligopolistic markets, their theoretical foundations, and key models. It reviews the classical Cournot, Bertrand, and Stackelberg models, explaining their assumptions, equilibrium concepts, and relevance to real-world market behavior. The chapter also highlights the role of game theory as a mathematical tool for modeling strategic interactions.

- **Chapter 3** analyzes the dynamic behavior of a bounded rational Bertrand duopoly framework incorporating homogeneous expectations and nonlinear (quadratic) cost functions. Through bifurcation diagrams and Lyapunov exponents, this chapter demonstrates how variations in adjustment speed and differentiation parameters can lead to mixed-mode oscillations and chaotic dynamics. The OGY control method is then applied to stabilize the system around its Nash equilibrium.

- **Chapter 4** extends the analysis to a Cournot triopoly game with bounded rationality. The chapter investigates the local stability of equilibrium points, identifies the occurrence of flip and Neimark–Sacker bifurcations, and studies the global dynamics of the system. It also illustrates how chaos can be controlled through the OGY method, ensuring stable and predictable market outcomes.

Scientific Publications: The research presented in this thesis has led to several peer-reviewed publications in international journals and conference proceedings. A substantial part of the results has already been disseminated through the following contributions:

1. M. Azioune, M.S. Abdelouahab, Controlling chaos and mixed mode oscillations in a Bertrand duopoly game with homogeneous expectations and quadratic cost functions, Mathematics and Computers in Simulation 233 (2025) 553–566.

2. M. Azioune, M.S. Abdelouahab, R. Lozi, Bifurcation analysis of a Cournot triopoly game with bounded rationality and chaos control via the OGY method, International Journal of Bifurcation and Chaos 35 (08) (2025) 2530019.

3. M. Azioune, M.S. Abdelouahab, L. Gardini, Complex nonlinear dynamics in a two-dimensional Cournot map: from stability to chaos via local and global bifurcation scenarios, Nonlinear Dynamics 114 (4) (2026) Art. 300.

4. M. Azioune, M.S. Abdelouahab, Dynamic analysis and chaos control of a Cournot triopoly game involving firms with bounded rationality, in: Springer Proceedings in Mathematics & Statistics, in press.

These publications constitute the principal scientific outcomes of this doctoral research and reflect the progressive development of the work presented throughout the thesis. They address complementary aspects of nonlinear economic dynamics, including bifurcation analysis, mixed-mode oscillations, chaos detection, and chaos control in Bertrand and Cournot oligopoly games.

Chapter 1

Generalities on Discrete Dynamical Systems and Chaos Control

1.1 Introduction

A dynamical system is a mathematical framework used to describe the evolution of a process or phenomenon over time. The theory of dynamical systems has undergone significant development since the nineteenth century and has become one of the fundamental branches of applied mathematics. The term *system* refers to a collection of state variables together with the rules governing their interactions and temporal evolution. Thus, every dynamical system is characterized by two essential components: its state and the law that determines its evolution over time [8].

Dynamical systems are widely employed to model real-world phenomena arising in physics, biology, engineering, economics, ecology, and many other scientific disciplines. Depending on the nature of time, these systems are classified as either continuous or discrete. In particular, discrete dynamical systems describe processes that evolve at successive time instants and are naturally represented by difference equations or iterative maps. Owing to their simplicity and computational efficiency, discrete models have become indispensable for investigating nonlinear phenomena.

One of the most remarkable features of nonlinear discrete systems is the emergence of complex behaviors, including bifurcations, periodic oscillations, and deterministic chaos. Although chaotic dynamics are generated by deterministic laws, they exhibit an extreme sensitivity to initial conditions, making long-term prediction practically impossible. Understanding the mechanisms leading to chaos and developing effective strategies to control or suppress it have therefore become important research topics with numerous practical applications.

Dynamic systems are generally classified into two types:

- **Discrete-time systems**, where state variables update at specific time intervals.
- **Continuous-time systems**, where state variables change continuously over time.

1.2 Foundations of Discrete and Continuous Dynamical Systems

Definition 1.2.1. (Discrete Autonomous Dynamical System) [47]

A discrete autonomous dynamical system of dimension m is described by the difference equation

$$x_{n+1} = f(x_n), \qquad x_0 = x(0), \tag{1.1}$$

where $f : \mathbb{R}^m \to \mathbb{R}^m$ is a differentiable map, $x_0 \in X \subset \mathbb{R}^m$ is the initial state, and $x_n \in X$ denotes the state vector at the n-th iteration. Furthermore,

- $x_1 = f(x_0)$ is the first iterate of x_0 under f.
- $x_2 = f(x_1) = f(f(x_0)) = f^2(x_0)$ is the second iterate of x_0.
- More generally,

  $$x_n = f^n(x_0),$$

  where f^n denotes the n-fold composition of the map f, i.e.,

  $$f^n = \underbrace{f \circ f \circ \cdots \circ f}_{n \text{ times}}.$$

The triplet $(X, \mathbb{N}, \varphi)$ defines a discrete autonomous dynamical system, where the function φ is given by:

$$\varphi(x_0, t) = f^t(x_0). \tag{1.2}$$

Definition 1.2.2. (Continuous Autonomous Dynamical System) [61]

In the continuous case, a dynamical system is represented through a set of differential equations given by:

$$\dot{x}(t) = f(x, \mu), \tag{1.3}$$

In this formulation, $x \in \mathbb{R}^n$ corresponds to the system's state vector, $\mu \in \mathbb{R}^m$ is a parameter vector, and the mapping $f : \mathbb{R}^n \times \mathbb{R}^m \to \mathbb{R}^n$ characterizes the evolution of the system over time.

Example 1.2.1. The dynamics of the Rössler system are governed by the following set of coupled differential equations:

$$\begin{cases} \dot{x} = -y - z, \\ \dot{y} = x + ay, \\ \dot{z} = z(x - c) + b, \end{cases}$$

where $x, y, z \in \mathbb{R}$ represent the system's state variables and $a, b, c \in \mathbb{R}$ are system parameters.

The Rössler system exhibits chaotic behavior for certain parameter values and is often used as a simpler alternative to the Lorenz system for studying chaos and strange attractors.

1.2.1 Transition from Continuous-Time to Discrete-Time Systems

To analyze continuous-time systems in a discrete-time framework [13], various discretization techniques are employed. One widely used method is the *Euler discretization*. Consider the first-order differential equation:

$$\frac{dx}{dt} = f(x_t), \tag{1.4}$$

where x_t represents the state of the system at time t. Instead of examining the system continuously, we aim to evaluate it at discrete time steps defined by:

$$t_n = t_0 + n\Delta t, \tag{1.5}$$

where Δt denotes the sampling interval. When Δt is sufficiently small, the derivative $\frac{dx}{dt}$ can be approximated using the finite difference method:

$$\frac{dx}{dt} \approx \frac{x(t_{n+1}) - x(t_n)}{\Delta t}. \tag{1.6}$$

Substituting this approximation into the original differential equation yields the discrete-time representation:

$$x_{n+1} = x_n + \Delta t \cdot f(x_n). \tag{1.7}$$

This transformation allows the study of continuous dynamical systems in a discrete-time setting, facilitating numerical simulations and computational analysis.

1.2.2 Fixed Points and Their Orbits

In the following discussions [13], we primarily focus on first-order systems. Our goal is to describe the evolution of system states based on given initial conditions. To achieve this, it is essential to introduce the concepts of trajectory (orbit) and fixed points of the system.

Consider a first-order discrete dynamical system defined by the iteration of a function $f(x)$:

$$x_{n+1} = f(x_n), \quad x(0) = x_0, \quad n \in \mathbb{N}. \tag{1.8}$$

Definition 1.2.3. Fixed Points

A fixed point [13], often referred to as an equilibrium state, is a configuration of a dynamical system that remains unchanged as the system evolves over time. Formally, a point $\bar{x} \in \mathbb{R}^m$ is said to be a fixed point of the system if it satisfies:

$$\bar{x} = f(\bar{x}), \tag{1.9}$$

where $f : \mathbb{R}^m \to \mathbb{R}^m$ is a differentiable function governing the system's dynamics.

Geometric Interpretation (One-Dimensional Case): In a one-dimensional system, fixed points correspond to the intersections of the function $f(x)$ with the diagonal line $y = x$.

Key Properties:

- A point $\bar{x}$ is a fixed point when the mapping leaves it unchanged, that is, $f(\bar{x}) = \bar{x}$.
- It represents a state where the system does not evolve further under the given dynamics.

Example 1.2.2. The fixed points of the quadratic map $f(x) = x^2$ can be determined by solving the equation $x^2 = x$ or equivalently $x^2 - x = 0$. Solving this equation gives two fixed points: 0 and 1.

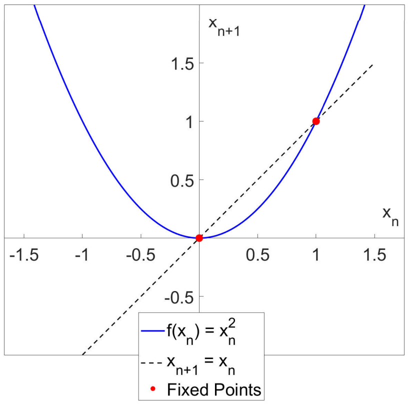

Figure 1.1: The fixed points of the quadratic map

Example 1.2.3. The map of Hénon is a famous two-dimensional discrete system used to study chaotic behavior, is given by the following formulation:

$$\begin{cases} x_{n+1} = 1 - ax_n^2 + y_n, \\ y_{n+1} = bx_n. \end{cases} \tag{1.10}$$

where $a, b \in \mathbb{R}$.

To find the fixed points, we solve:

$$\bar{x} = 1 - a\,\bar{x}^2 + \bar{y}, \quad \bar{y} = b\,\bar{x},$$

Substituting $\bar{y} = b\bar{x}$ into the first equation gives:

$$\bar{x} = 1 - a\bar{x}^2 + b\bar{x}. \tag{1.11}$$

Rearranging:

$$a\bar{x}^2 - (1 - b)\bar{x} + 1 = 0. \tag{1.12}$$

Solving this quadratic equation for $\bar{x}$:

$$\bar{x} = \frac{(1 - b) \pm \sqrt{(1 - b)^2 - 4a}}{2a}. \tag{1.13}$$

Once $\bar{x}$ is determined, $\bar{y}$ is found using $\bar{y} = b\bar{x}$.

Thus, the system can exhibit up to two fixed points, with their existence and location determined by the specific values of the parameters a and b.

Definition 1.2.4. (System Orbit)

The orbit (or trajectory) of the discrete dynamical system (1.8), starting from an initial condition x_0, is the sequence of iterates given by [13]:

$$O = \{x(0), x(1) = f(x(0)), x(2) = f^2(x(0)), x(3) = f^3(x(0)), \dots, x(t) = f^t(x(0)), \dots\}. \quad (1.14)$$

This sequence represents the evolution of the system state over time, providing insight into its long-term behavior.

Definition 1.2.5. (Periodic and Eventually Periodic Orbits) An orbit $O(x_0)$ is called **periodic** if there exists an integer $q > 1$ such that [13]:

$$x_{n+q} = x_n, \quad \forall n \in \mathbb{N}. \quad (1.15)$$

Additionally, an orbit is termed **eventually periodic** if there exist integers $p > 0$ and $N > 0$ such that the periodicity condition holds for all $n > N$.

Furthermore, a periodic orbit $O(x_0)$ consists entirely of periodic points, meaning each point in the sequence satisfies the periodicity condition. These points are referred to as **periodic points of period** p in the system.

1.2.3 Concept of Stability

The analysis of stability in a dynamical system focuses on determining whether an equilibrium point attracts or repels nearby trajectories for a given range of initial conditions. This examination helps in understanding both the local and, in some cases, global behavior of the system. Moreover, it allows for the evaluation of how small or even significant perturbations influence the system when it is near an equilibrium state.

Definition 1.2.6. (Stability of an Equilibrium Point [31]) Let $f : I \to I$ be a function, and let $\bar{x}$ be an equilibrium point of f, where $I \subset \mathbb{R}^n$. The stability of $\bar{x}$ is classified as follows:

- **Stability:** The equilibrium point $\bar{x}$ is *stable* if, for every $\epsilon > 0$, there exists $\delta > 0$

such that for all $x_0 \in I$,

$$\|x_0 - \bar{x}\| < \delta \implies \|f^n(x_0) - \bar{x}\| < \epsilon, \quad \forall n > 0.$$

If this condition is not satisfied, $\bar{x}$ is said to be *unstable*.

- **Repelling Fixed Point:** The equilibrium point $\bar{x}$ is a *repelling fixed point* if there exists $\epsilon > 0$ such that for any x_0 satisfying

$$\|x_0 - \bar{x}\| < \epsilon,$$

the inequality

$$\|f(x_0) - \bar{x}\| > \|x_0 - \bar{x}\|$$

holds, meaning that trajectories move away from $\bar{x}$.

- **Asymptotic Stability:** An equilibrium point $\bar{x}$ is said to be *asymptotically stable* (or *attracting*) if it is stable and, in addition, there exists a neighborhood of radius $\eta > 0$ around $\bar{x}$ such that any initial state x_0 within this neighborhood satisfies

$$\|x_0 - \bar{x}\| < \eta \implies \lim_{n\to\infty} x_n = \bar{x},$$

meaning that trajectories starting sufficiently close to $\bar{x}$ not only remain nearby but also converge to $\bar{x}$ as time progresses. If this holds for all $x_0 \in I$ ($\eta = \infty$), $\bar{x}$ is *globally asymptotically stable*, meaning all trajectories converge to it.

1.3 One-Dimensional First-Order Discrete Dynamical Systems

A discrete dynamical system is said to be **one-dimensional** if the state variable x is a scalar, meaning $x \in \mathbb{R}$ [31]. It is represented by the recurrence relation:

$$x_{n+1} = f(x_n). \tag{1.16}$$

In many cases, the function f depends on one or more parameters, often referred to as **bifurcation parameters**. When such dependencies exist, the system can be rewritten as:

$$x_{n+1} = f(x_n, a),$$

where $a = (a_1, a_2, \ldots, a_m) \in \mathbb{R}^m$ represents a vector of m parameters.

1.3.1 Linear One-Dimensional Dynamical Systems

After translating the origin [31], any first-order, one-dimensional linear dynamical system can be written as:

$$x_{n+1} = dx_n, \quad x \in \mathbb{R}. \tag{1.17}$$

The general solution for any initial condition x_0 is:

$$x_n = d^n x_0. \tag{1.18}$$

Fixed Point Analysis

- For $d \neq 1$, $x = 0$ is the *only* fixed point.
- For $d = 1$, *every* $x \in \mathbb{R}$ is a fixed point.

Stability Classification

The multiplier d determines the stability of the fixed point at $x = 0$:

Condition	Stability Type	Dynamics
$\lvert d \rvert < 1$	Attractive (Asymptotically stable)	$x_n \to 0$ for all x_0
$\lvert d \rvert > 1$	Repelling (Unstable)	$\lvert x_n \rvert \to \infty$ for $x_0 \neq 0$
$d = 1$	Neutral	Every point is fixed
$d = -1$	Period-2 behavior	$x_{n+2} = x_n$

Behavior Types

1. **Type 1 (Monotonic)**: If $d > 0$, the sequence maintains its sign:
$$\operatorname{sgn}(x_n) = \operatorname{sgn}(x_0).$$
2. **Type 2 (Oscillatory)**: If $d < 0$, the sequence alternates signs:
$$\operatorname{sgn}(x_{n+1}) = -\operatorname{sgn}(x_n).$$

Special Cases

- When $|d| = 1$:
  - $d = 1$: Identity map (every point is fixed).
  - $d = -1$: Perfect period-2 oscillation ($x_{n+1} = -x_n$).
- The case $x_{n+1} = d^2 x_n$ is redundant since it reduces to the $d > 0$ case when considering every other iteration.

Basin of Attraction

For $|d| < 1$, the basin of attraction of 0 is the entire real line:

$$\mathcal{B}(0) = \mathbb{R}.$$

For nonlinear systems, the basin is generally limited to a neighborhood of 0.

1.3.2 Nonlinear One-Dimensional Dynamical Systems

Consider the nonlinear dynamical system defined by:

$$x_{n+1} = f(x_n, a), \tag{1.19}$$

where $a \in \mathbb{R}^m$ represents the bifurcation parameters and $f(x, a)$ is a continuously differentiable (C^1) function of the real variable x that cannot be transformed into the linear form (1.17) through any linear change of variables [31].

The key questions we address are:

- Whether System (1.19) possesses a unique fixed point or multiple fixed points.
- The stability properties of these fixed points.
- The existence of periodic orbits, including their periods and stability characteristics.

Our analysis aims to fully characterize the dynamical behavior of System (1.19). The following discussion provides a framework to answer these fundamental questions.

Existence of Fixed Points and Periodic Orbits

The fixed points of the dynamical system (1.19) correspond to the solutions of the equation
$$x = f(x).$$
Similarly, the periodic points of period p are the solutions of
$$x = f^p(x),$$
that do not satisfy
$$x = f^m(x),$$
for any $m < p$.

Theorem 1.3.1. *[28] Let $h : [a, b] \to \mathbb{R}$ be a continuous function. Then, the image of h is a closed and bounded interval.*

Lemma 1.3.1. *[28] Let I be an interval and $f : I \to \mathbb{R}$ a function continuous at $x_0 \in I$. Suppose $|f(x_0)| < 1$ and let $k \in (|f(x_0)|, 1)$. Then, there exists $r > 0$ such that*
$$|f(x)| \leq k \quad \text{for all } x \in [x_0 - r, x_0 + r] \cap I.$$

Remark 1.3.1. [28] Lemma 1.3.1 also holds if the condition $|f(x_0)| < 1$ is replaced by $|f(x_0)| > 1$. More precisely, let I be an interval and let $f : I \to \mathbb{R}$ be continuous at $x_0 \in I$. If $|f(x_0)| > 1$ and $k \in (1, |f(x_0)|)$, then there exists $r > 0$ such that
$$|f(x)| \geq k, \qquad \forall\, x \in [x_0 - r, x_0 + r] \cap I.$$

Other fundamental concepts in calculus include the Mean Value Theorem and the Intermediate Value Theorem, stated below.

Theorem 1.3.2. *[Mean Value Theorem, [28]] Let $f : [a, b] \to \mathbb{R}$ be a function with $a < b$ that is continuous on the closed interval $[a, b]$ and differentiable on the open interval (a, b). Then, there exists at least one point $c \in (a, b)$ for which the derivative at c equals the average rate of change of f over $[a, b]$, that is,*
$$f'(c) = \frac{f(b) - f(a)}{b - a}.$$

Theorem 1.3.3. *[Intermediate Value Theorem, [28]] Let $f : [a, b] \to \mathbb{R}$ be a function continuous on the interval $[a, b]$. If u is any real number lying between $f(a)$ and $f(b)$, then there exists some point $c \in (a, b)$ such that*
$$f(c) = u.$$

The following two theorems are useful for analyzing the existence of fixed points in dynamical systems.

Theorem 1.3.4. *[28] Let $I = [a, b]$ be a closed interval, and let $f : I \to I$ be a continuous function. Then, f admits at least one fixed point in I; that is, there exists some $c \in I$ such that $f(c) = c$.*

Proof. Define the function $g(x) = f(x) - x$. Since f is continuous on I, it follows that g is also continuous on I.

If $f(a) = a$ or $f(b) = b$, then a or b is already a fixed point, and the theorem holds. Otherwise, suppose that $f(a) > a$ and $f(b) < b$, which gives

$$g(a) = f(a) - a > 0 \quad \text{and} \quad g(b) = f(b) - b < 0.$$

By the Intermediate Value Theorem (Theorem 1.3.3), there exists at least one $c \in (a, b)$ such that $g(c) = 0$. This immediately implies that $f(c) = c$.

Hence, the function f possesses at least one fixed point in the interval I. ■

Theorem 1.3.5. *[28] Let $f : I \to I$ be a function such that $|f'(x)| < 1$ for all $x \in I$. Then, f has a unique fixed point in I. Moreover,*

$$|f(x) - f(y)| < |x - y|,$$

for all $x, y \in I$ with $x \neq y$.

Proof. By Theorem 1.3.4, the function f has at least one fixed point in I. Assume, for contradiction, that x and y are two distinct fixed points of f, i.e., $x \neq y$ and $f(x) = x$, $f(y) = y$. By the Mean Value Theorem 1.3.2, there exists c between x and y such that

$$f'(c) = \frac{f(y) - f(x)}{y - x} = \frac{y - x}{y - x} = 1,$$

which contradicts the assumption that $|f'(x)| < 1$ for all $x \in I$. Hence, the fixed point must be unique.

To establish the second statement, we again apply the Mean Value Theorem 1.3.2. For any $x, y \in I$ with $x \neq y$, there exists c between x and y such that

$$|f(x) - f(y)| = |f'(c)|\,|x - y| < |x - y|,$$

since $|f'(c)| < 1$. This completes the proof. ■

Remark 1.3.2. [28]

1. The existence of periodic points of period p can be established using Theorems 1.3.4 and 1.3.5 by replacing f with f^p.

2. The existence of a periodic orbit of period 2 implies the existence of a fixed point. Indeed, if $x_1 = f(x_2)$ and $x_2 = f(x_1)$ with $x_1 \neq x_2$, we may assume $x_1 < x_2$. Then, $f(x_1) > x_1$ and $f(x_2) < x_2$, ensuring a fixed point exists in $[x_1, x_2]$.

Another important result concerning the existence of periodic orbits is given by Sharkovsky's Theorem.

Theorem 1.3.6 (Sharkovsky's Theorem, [28])**.** *Let I be an interval and let $f : I \to I$ be a continuous function. If f possesses a periodic point of period n, then it also has periodic points of every period m that comes after n in Sharkovsky's ordering.*

1.4 Two-Dimensional First-Order Discrete Dynamical Systems

We now examine systems where the state space is two-dimensional. While many results generalize to higher dimensions, the two-dimensional case provides essential insights while remaining tractable for analysis and visualization [31, 66].

1.4.1 Two-Dimensional First-Order Linear Dynamical Systems

General Form

A linear 2D discrete system has the form:

$$\mathbf{X}_{n+1} = A\mathbf{X}_n, \quad A = \begin{pmatrix} a_{11} & a_{12} \\ a_{21} & a_{22} \end{pmatrix}, \quad \mathbf{X}_n = \begin{pmatrix} x_n \\ y_n \end{pmatrix}. \tag{1.20}$$

Key Properties

- The origin is the unique fixed point when $\det(I - A) \neq 0$.
- Solutions satisfy $\mathbf{X}_n = A^n\mathbf{X}_0$.

- Behavior is classified by eigenvalues $\lambda_{1,2}$ of A.

When A has two linearly independent eigenvectors:

$$\mathbf{X}_n = c_1\lambda_1^n\mathbf{v}_1 + c_2\lambda_2^n\mathbf{v}_2. \tag{1.21}$$

Example 1.4.1. Independent Dynamics

For diagonal $A = \begin{pmatrix} 3 & 0 \\ 0 & 0.7 \end{pmatrix}$:

$$\begin{cases} x_n = 3^n x_0, \\ y_n = (0.7)^n y_0. \end{cases} \tag{1.22}$$

- x-direction: unstable ($|\lambda| = 3 > 1$).
- y-direction: stable ($|\lambda| = 0.7 < 1$).
- Saddle point at origin.

1.4.1.1 Jordan Matrix

This subsection summarizes fundamental linear algebra propositions used in deriving and qualitatively analyzing two-dimensional discrete dynamical systems.

Lemma 1.4.1. *[40] Let $A = (a_{ij})$ be a 2×2 matrix with $a_{ij} \in \mathbb{R}$ for all i, j:*

1. *If A has two distinct real eigenvalues $\{\lambda_1, \lambda_2\}$, then there exists a nonsingular 2×2 matrix Q and a diagonal matrix D such that $A = QDQ^{-1}$, where:*

$$D = \begin{pmatrix} \lambda_1 & 0 \\ 0 & \lambda_2 \end{pmatrix},$$

   and Q is an invertible 2×2 matrix whose columns are the eigenvectors of A.

2. *If A has a repeated real eigenvalue $\lambda_1 = \lambda_2 = \lambda$, then A is similar to a matrix D via some nonsingular matrix Q, that is, $A = QDQ^{-1}$, where:*

$$D = \begin{pmatrix} \lambda & 0 \\ 1 & \lambda \end{pmatrix}.$$

3. *If A has complex conjugate eigenvalues $\lambda_{1,2} = a \pm ib$ with associated eigenvectors $w = u \pm iv$, then there exists a nonsingular 2×2 matrix Q such that $A = QDQ^{-1}$ where:*

$$D = \begin{pmatrix} a & -b \\ b & a \end{pmatrix},$$

and $Q = (v, u)$ is an invertible 2×2 matrix.

Proof. See Hirsch and Smale (1974) [40]. ■

1.4.1.2 Characterization of Solutions for Linear Dynamical Systems

We analyze solutions to the 2D linear dynamical system:

$$X_{n+1} = AX_n \quad \text{where } X \in \mathbb{R}^2 \text{ and } A \text{ is } 2 \times 2. \tag{1.23}$$

Using the similarity transformation $X = QY$ and $D = Q^{-1}AQ$ (lemma 1.4.1), we study the equivalent system $Y_{n+1} = DY_n$.

Distinct Real Eigenvalues

For $D = \begin{pmatrix} \lambda_1 & 0 \\ 0 & \lambda_2 \end{pmatrix}$ with $\lambda_1 \neq \lambda_2 \in \mathbb{R}$:

- Solutions: $x_n = \lambda_1^n x_0$, $y_n = \lambda_2^n y_0$.
- Invariant curves: $y = cx^{\ln \lambda_2 / \ln \lambda_1}$.
- Stability cases:
  1. **Stable node** ($|\lambda_{1,2}| < 1$):
     - Type 1: Both $\lambda_i > 0$ (monotonic convergence).
     - Type 2: One $\lambda_i < 0$ (oscillation on one axis).
     - Type 3: Both $\lambda_i < 0$ (oscillation on both axes).
  2. **Unstable node** ($|\lambda_{1,2}| > 1$): Solutions diverge.
  3. **Saddle point** ($|\lambda_1| < 1 < |\lambda_2|$): Stable along one axis, unstable along another.

Repeated Real Eigenvalues

For a 2×2 matrix with a repeated eigenvalue λ, we distinguish two cases based on its geometric multiplicity:

- **Star Node (Proper Node):** If $D = \begin{pmatrix} \lambda & 0 \\ 0 & \lambda \end{pmatrix} = \lambda I$ (diagonalizable), every non-zero vector is an eigenvector. Solutions decay or grow exponentially without coupling terms: $x_n = \lambda^n x_0$ and $y_n = \lambda^n y_0$.
- **Improper Node (Defective Case):** If $D = \begin{pmatrix} \lambda & 0 \\ 1 & \lambda \end{pmatrix}$ (non-diagonalizable), there is only one independent eigenvector.
  - Solutions contain linear growth terms: $y_n = n\lambda^{n-1}x_0 + \lambda^n y_0$.
  - Asymptotic stability:
    * Asymptotically stable when $|\lambda| < 1$,
    * Unstable when $|\lambda| > 1$.

Complex Eigenvalues

For $D = r\begin{pmatrix} \cos\theta & -\sin\theta \\ \sin\theta & \cos\theta \end{pmatrix}$, where $\lambda_{1,2} = re^{\pm i\theta}$:

- Solutions: $x_n = r^n \rho_0 \cos(\phi_0 + n\theta)$, $y_n = r^n \rho_0 \sin(\phi_0 + n\theta)$.
- Cases:
  1. **Center** ($r = 1$): Solutions lie on invariant circles,
  2. **Stable focus** ($r < 1$): Spiral convergence to origin,
  3. **Unstable focus** ($r > 1$): Spiral divergence from origin.

  Rotation direction depends on θ sign (trigonometric if $b > 0$)

1.4.1.3 Classification via Trace and Determinant

The characteristic equation $\lambda^2 - \mathrm{tr}(A)\lambda + \det(A) = 0$ determines behavior:

Theorem 1.4.1. *Let $\lambda_{1,2}$ be eigenvalues of A:*

1. *Real eigenvalues ($(trA)^2 > 4\det A$):*
   - ***Saddle*** *if $P(1)P(-1) < 0$.*
   - ***Stable node*** *if $P(1) > 0$, $P(-1) > 0$, $\det A < 1$.*
   - ***Unstable node*** *if $P(1) < 0$, $P(-1) < 0$, $\det A > 1$.*

2. *Complex eigenvalues ($(trA)^2 < 4\det A$):*
   - ***Stable focus*** *if* $\det A < 1$.
   - ***Unstable focus*** *if* $\det A > 1$.

Remark 1.4.1.
- The stability domain covers the entire plane when $|\lambda_{1,2}| < 1$.
- When $|\lambda_1| = 1$, the system exhibits either:
  - A line of fixed points ($\lambda_1 = 1$).
  - Period-2 cycles ($\lambda_1 = -1$).

1.4.2 Stability of Nonlinear 2D Discrete Dynamical Systems

A nonlinear discrete system is given by:

$$\begin{pmatrix} x_{n+1} \\ y_{n+1} \end{pmatrix} = f\begin{pmatrix} x_n \\ y_n \end{pmatrix} = \begin{pmatrix} f_1(x_n, y_n) \\ f_2(x_n, y_n) \end{pmatrix}. \tag{1.24}$$

where f_1, f_2 are continuous nonlinear functions.

Fixed Points Analysis

For a fixed point $X^* = (x^*, y^*)$:

- Linear approximation via Jacobian:

$$J(X^*) = \begin{pmatrix} \frac{\partial f_1}{\partial x} & \frac{\partial f_1}{\partial y} \\ \frac{\partial f_2}{\partial x} & \frac{\partial f_2}{\partial y} \end{pmatrix}_{X^*}. \tag{1.25}$$

- Stability depends on eigenvalues λ_1, λ_2 of $J(X^*)$:

  Theorem 1.4.2.
  1. ***Stable***: *All $|\lambda_i| < 1$ (locally asymptotically stable).*
  2. ***Unstable***: *Any $|\lambda_i| > 1$.*
  3. ***Critical case***: *Eigenvalues on unit circle ($|\lambda_i| = 1$) require nonlinear analysis.*

Cycles and Higher Periodic Solutions

An *m-cycle* consists of m points $\{X_1, ..., X_m\}$ where:

- $X_{k+1} = f(X_k)$ for $k = 1, ..., m-1$.

- $X_1 = f(X_m)$.
- Stability analyzed via Jacobian of f^m (the m-th iterate).

Key Observations

- Nonlinear systems may exhibit multiple fixed points and cycles.
- Local stability can be determined through linearization when $|\lambda_i| \neq 1$.
- Critical cases ($|\lambda_i| = 1$) require advanced techniques (Lyapunov functions, center manifold theory).
- Nonlinear terms dominate behavior near critical cases.

1.5 Bifurcations and Chaotic Dynamics

1.5.1 Bifurcation Theory

Another valuable framework for analyzing dynamic systems is **bifurcation theory**. The term *bifurcation* was first introduced by Henri Poincaré in 1885. This theory examines families of dynamical systems, whether continuous or discrete, that depend on one or more parameters ($\mu \in \mathbb{R}^m$). Essentially, bifurcation theory investigates how the qualitative behavior of a system changes as these parameters vary [43].

1.5.1.1 Fundamental Concepts of Bifurcations

Consider a dynamical system dependent on parameters, given by:

$$x_{n+1} = f(x_n, \mu), \quad (2.1)$$

where $x \in \mathbb{R}^m$ denotes the state variables and $\mu \in \mathbb{R}^p$ represents the parameters, and p is the number of the parameters. When the parameters change, the system's phase portrait may also change. Two scenarios can occur: either the system remains topologically equivalent to its original form, or its topology undergoes a transformation.

Definition 1.5.1. [43] A **bifurcation** occurs when a variation in parameters results in a topologically distinct phase space structure.

In other words, a bifurcation signifies a change in the system's topological structure as the parameters cross a critical value μ_0.

Definition 1.5.2. [43] A **bifurcation diagram** partitions the parameter space based on topological equivalence, including representative phase portraits for each region. Ideally, this diagram emerges from a qualitative analysis of the system, compactly summarizing all possible dynamical behaviors and the transitions (bifurcations) between them as parameters vary. Note that the bifurcation diagram may vary depending on the phase space region under consideration.

1.5.1.2 Classification of Bifurcation Types in Discrete Dynamical Systems

Consider a two-dimensional system with one-parameter family of maps [43, 37, 60]:

$$F(\mu, X) : \mathbb{R} \times \mathbb{R}^2 \to \mathbb{R}^2, \tag{1.26}$$

where $X = (x, y) \in \mathbb{R}^2$, $\mu \in \mathbb{R}$, and $F \in C^r$ with $r \geq 5$. After centering at a fixed point $(0, 0)$ and applying the center manifold theorem, we obtain a one-dimensional map $f_\mu(x)$. The bifurcation types depend on the Jacobian matrix $J = D_X F(0, 0)$ eigenvalues:

Bifurcations with Eigenvalue 1

When J has eigenvalue 1, we observe:

1. **Saddle-Node (Fold) Bifurcation**

   Definition 1.5.3. [43, 37, 60] A fold bifurcation occurs when a simple positive multiplier crosses the unit circle ($\lambda_1 = 1$), characterized by creation/annihilation of fixed points.

   Conditions:
   $$\frac{\partial f}{\partial \mu}(0, 0) \neq 0 \quad \text{and} \quad \frac{\partial^2 f}{\partial x^2}(0, 0) \neq 0. \tag{1.27}$$

2. **Pitchfork Bifurcation** Conditions:
   $$\frac{\partial f}{\partial \mu}(0, 0) = 0 \quad \text{and} \quad \frac{\partial^2 f}{\partial x^2}(0, 0) = 0. \tag{1.28}$$

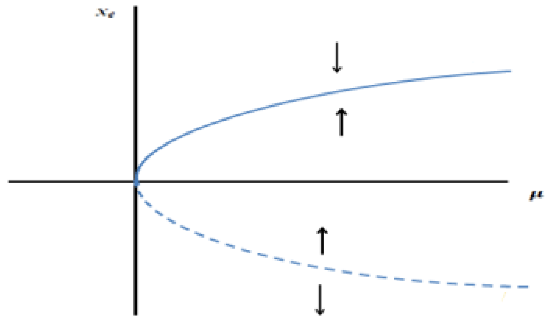

Figure 1.2: Diagram of a saddle-node bifurcation, indicating stable and unstable branches.

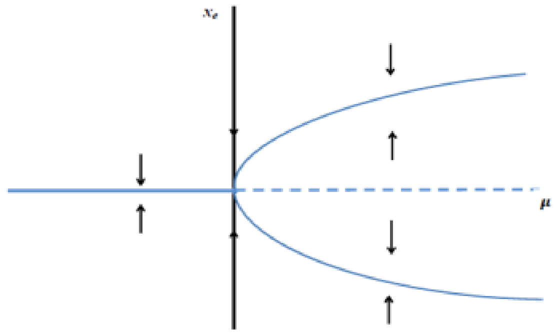

Figure 1.3: Supercritical pitchfork bifurcation diagram.

3. **Transcritical Bifurcation** Conditions:

$$\frac{\partial f}{\partial \mu}(0,0) = 0 \quad \text{and} \quad \frac{\partial^2 f}{\partial x^2}(0,0) \neq 0. \tag{1.29}$$

Bifurcations with Eigenvalue -1

4. **Period-Doubling (Flip) Bifurcation**

   Definition 1.5.4. [43, 37, 60] A flip bifurcation occurs when a simple multiplier crosses the unit circle at $\lambda_1 = -1$, leading to period-2 orbits.

   Conditions:

$$\left.\frac{\partial}{\partial x}[f(x,\mu) - x]\right|_{(0,0)} \neq 0, \quad \left.\frac{\partial^2 f}{\partial \mu \, \partial x} + \frac{1}{2}\frac{\partial f}{\partial \mu} \cdot \frac{\partial^2 f}{\partial x^2}\right|_{(0,0)} \neq 0, \quad \left.\frac{1}{3!}\frac{\partial^3 f}{\partial x^3} + \frac{1}{2}\left(\frac{\partial f}{\partial x}\right)^2\right|_{(0,0)} \neq 0. \tag{1.30}$$

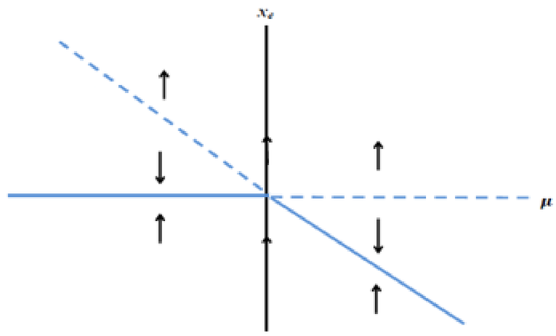

Figure 1.4: Transcritical bifurcation with stability exchange.

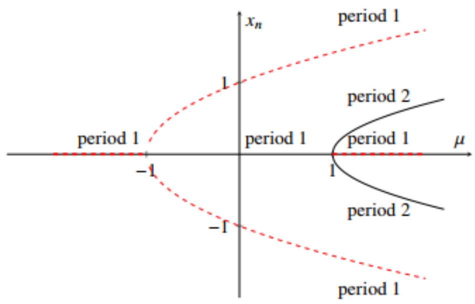

Figure 1.5: Period-doubling bifurcation diagram.

Bifurcations with Complex Eigenvalues

5. **Neimark-Sacker Bifurcation**

Definition 1.5.5. [43, 37, 60] A Neimark-Sacker bifurcation occurs when a pair of complex-conjugate eigenvalues crosses the unit circle, leading to invariant torus formation.

Theorem 1.5.1. *[43, 37, 60] For Neimark-Sacker bifurcation, the following must hold:*

- $|\lambda_{1,2}(\mu_0)| = 1$ *(complex eigenvalues on unit circle).*
- $\frac{d}{d\mu}|\lambda(\mu)| \neq 0$ *(transversality).*
- $\lambda_{1,2}^k(\mu_0) \neq 1$ *for* $k = 1, 2, 3, 4$ *(non-resonance).*

Example 1.5.1. Consider the discrete dynamical system defined by:

$$F : \begin{cases} x_{n+1} = \mu x_n(1 - y_n), \quad \mu > 0, \\ y_{n+1} = x_n. \end{cases} \tag{1.31}$$

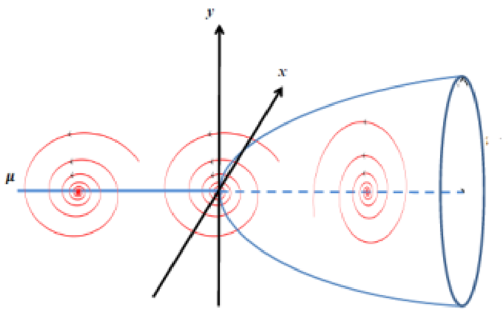

Figure 1.6: Neimark-Sacker bifurcation diagram.

This system possesses two fixed points:

$$\begin{cases} (\bar{x}_1, \bar{y}_1) = (0, 0), \\ (\bar{x}_2, \bar{y}_2) = \left(1 - \dfrac{1}{\mu}, 1 - \dfrac{1}{\mu}\right). \end{cases} \tag{1.32}$$

The Jacobian matrix evaluated at $(\bar{x}_2, \bar{y}_2)$ is:

$$J(\bar{x}_2, \bar{y}_2) = \begin{pmatrix} 1 & 1-\mu \\ 1 & 0 \end{pmatrix}. \tag{1.33}$$

The corresponding eigenvalues are:

$$\lambda_{1,2} = \frac{1}{2} \pm \sqrt{\frac{5}{4} - \mu}. \tag{1.34}$$

For $\mu > \frac{5}{4}$, the eigenvalues become complex with magnitude $|\lambda_{1,2}|^2 = \mu - 1$. At the critical value $\mu = 2$:

- The fixed point $(\bar{x}_2, \bar{y}_2)$ loses stability.
- The eigenvalues take the form $\lambda_{1,2} = e^{\pm i\pi/3}$.
- The system exhibits a Neimark-Sacker bifurcation.

1.5.2 Chaotic Systems

In everyday language, *chaos* refers to a state of complete disorder. However, in the context of chaos theory, the term has a more specific meaning it is strongly linked to

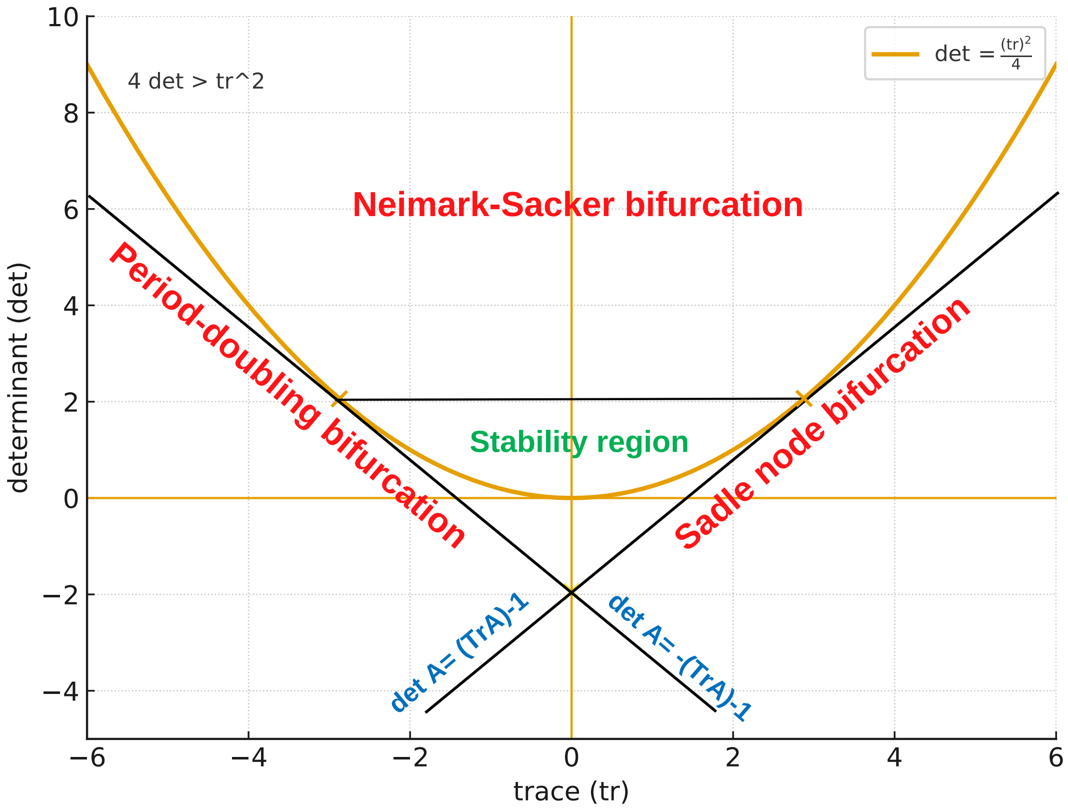

Figure 1.7: Summary of bifurcation types in two-dimensional systems.

unpredictability and the challenges of forecasting long-term behavior due to a system's extreme sensitivity to initial conditions [28].

Chaos theory is a mathematical discipline that studies complex, sensitive systems whose long-term behavior is inherently unpredictable. This is because minuscule variations in the starting conditions, often undetectable in practice, can amplify exponentially over time, leading to radically divergent results. Despite this apparent randomness, these systems are governed by deterministic rules and often contain hidden patterns, known as strange attractors.

1.5.2.1 Mathematical Foundations of Chaos

Various characterizations of chaos exist in the literature, with R. L. Devaney's formulation being among the first rigorous mathematical definitions [28]. Consider a compact metric space $(I \subset \mathbb{R}, d)$, where d denotes a distance metric, and a function defined by:

$$f : I \to I; \quad x_{k+1} = f(x_k); \quad x_0 \in I. \tag{1.35}$$

Definition 1.5.6 (Topological Transitivity [45])**.** A map f is *topologically transitive* on I if, for every pair of non-empty open sets $U, V \subset I$, an integer $k \geq 0$ exists for which $f^k(U) \cap V \neq \emptyset$. This signifies that the system's dynamics cannot be decomposed into disjoint invariant open sets.

The map is *totally transitive* if this condition is satisfied not only by f but by all its iterates f^n for $n > 1$.

Definition 1.5.7 (Sensitive Dependence on Initial Conditions)**.** A map f has *sensitive dependence on initial conditions* on I if a $\delta > 0$ exists with the following property: for any point $x \in I$ and any arbitrarily small neighborhood around it, there is a point y in that neighborhood and an integer $k > 0$ such that the orbits of x and y under f are separated by at least δ at time k.

This property is a foundational element of chaotic systems, often colloquially referred to as the "butterfly effect."

Definition 1.5.8 (Dense Set of Periodic Points)**.** The periodic points of f are said to be *dense* in I if for any $x \in I$ and any neighborhood $N_\epsilon(x)$, there exists a periodic point $p \in N_\epsilon(x)$ (i.e., $f^m(p) = p$ for some $m \in \mathbb{N}$).

Definition 1.5.9 (Devaney's Chaos [28])**.** A function $f : I \to I$ is said to be *chaotic* on the interval I if it satisfies the following three fundamental properties, which together generate a robust and unpredictable dynamical system:

1. **Sensitive Dependence:** The system exhibits the "butterfly effect," meaning arbitrarily small differences in initial conditions are amplified, leading to vastly different future states.

2. **Topological Transitivity:** The system is indecomposable and well-mixed; its orbit visits every region of the state space over time.

3. **Density of Periodic Points:** The system possesses a rich structure of regularity, as periodic orbits (cycles) are found arbitrarily close to any point in I.

These conditions ensure a blend of unpredictability, irreducibility, and underlying order.

1.5.2.2 Key Features of Chaotic Behavior

Chaotic systems exhibit several defining mathematical properties:

1. **Sensitivity to Initial Conditions**
   Discovered by Poincaré and later by Lorenz, this hallmark of chaos means infinitesimal changes in initial conditions lead to drastically divergent trajectories [57]. Quantified by:

2. **Lyapunov Exponents**
   These measure the exponential divergence rate of nearby orbits. For an n-dimensional system, there are n exponents matching the phase space dimension [57].

Theorem 1.5.2 (Lyapunov Exponent for 1D Maps [25]). *For $f : \mathbb{R} \to \mathbb{R}$ with $x_{n+1} = f(x_n)$, the Lyapunov exponent is:*

$$\lambda = \lim_{n\to\infty} \frac{1}{n} \sum_{i=0}^{n-1} \ln |f'(x_i)|. \tag{1.36}$$

Proof. Consider two nearby initial conditions x_0 and $x_0' = x_0 + d_0$, where $d_0 = |x_0' - x_0|$ denotes the initial distance between the two trajectories. After n iterations of the map f, the distance between the corresponding trajectories is $d_n = |f^n(x_0') - f^n(x_0)|$. For sufficiently small d_0, we obtain

$$\frac{d_n}{d_0} = \left| \frac{df^n}{dx}(x_0) \right| \approx e^{n\lambda}. \tag{1.37}$$

Taking the natural logarithm and dividing by n yields the Lyapunov exponent formula. The stability of the fixed point is determined by the sign of λ:

- $\lambda < 0$: Stable fixed point.
- $\lambda = 0$: Neutral stability.
- $\lambda > 0$: Chaotic behavior.

■

Example 1.5.2. Consider the logistic map

$$x_{n+1} = 4x_n(1 - x_n), \qquad x_n \in [0, 1].$$

The Lyapunov exponent is

$$\lambda = \lim_{N\to\infty} \frac{1}{N} \sum_{n=0}^{N-1} \ln |4(1 - 2x_n)|\,.$$

For the parameter value $r = 4$, one obtains

$$\lambda = \ln 2 > 0.$$

Since the logistic map possesses a bounded invariant interval and $\lambda > 0$, nearby trajectories separate exponentially fast, which is one of the fundamental signatures of chaotic dynamics.

Theorem 1.5.3 (Lyapunov Exponents for p-Dimensional Maps [25])**.** *For $f : \mathbb{R}^p \to \mathbb{R}^p$, with $\mathbf{x}_{n+1} = f(\mathbf{x}_n)$, there exist p Lyapunov exponents:*

$$\lambda_i = \lim_{n\to\infty} \frac{1}{n} \ln q_i(f^n(\mathbf{x}_0)), \quad i = 1, \dots, p. \tag{1.38}$$

where q_i are eigenvalues of the Jacobian $J_n(\mathbf{x}_0) = \prod_{k=0}^{n-1} J(\mathbf{x}_k)$.

Proof. For nearby points $\mathbf{x}_0$ and $\mathbf{x}'_0$, after n iterations:

$$\|\mathbf{x}_n - \mathbf{x}'_n\| \approx \|J_n(\mathbf{x}_0)\| \cdot \|\mathbf{x}_0 - \mathbf{x}'_0\| \tag{1.39}$$

Diagonalizing J_n yields the growth rates along eigendirections. ∎

Example 1.5.3 (Skinny–Baker Map)**.** Consider the Skinny–Baker map $B : [0,1]^2 \to [0,1]^2$ defined by

$$B(x,y) = \begin{cases} \left(\frac{x}{3}, 2y\right), & 0 \le y < \frac{1}{2}, \\ \left(\frac{x}{3} + \frac{2}{3}, 2y - 1\right), & \frac{1}{2} \le y \le 1. \end{cases}$$

For this piecewise linear map, the Jacobian matrix is constant almost everywhere and is given by

$$J = \begin{pmatrix} \frac{1}{3} & 0 \\ 0 & 2 \end{pmatrix}. \tag{1.40}$$

Hence, the Lyapunov exponents are obtained directly as

$$\lambda_1 = \ln\left|\frac{1}{3}\right| = -\ln 3 < 0 \quad \text{(contracting direction)},$$
$$\lambda_2 = \ln|2| = \ln 2 > 0 \quad \text{(expanding direction)}.$$

The existence of a positive Lyapunov exponent confirms the chaotic nature of the Skinny–Baker map.

3. **Fractal Dimensions**

   While Euclidean geometry effectively describes man-made structures with regular shapes, many natural phenomena like coastlines, clouds, and vegetation exhibit complex, irregular patterns that require fractal geometry for accurate characterization. These fractal objects display self-similarity across scales and possess non-integer dimensions, distinguishing them from classical geometric forms. In chaotic systems, various fractal dimensions - including capacity, information, and correlation dimensions - provide essential metrics for quantifying the intricate structure of strange attractors [45].

   Hausdorff Dimension:

   $$D_H = \sup\{s : H^s(A) = \infty\} = \inf\{s : H^s(A) = 0\}. \tag{1.41}$$

   where H^s is the s-dimensional Hausdorff measure [22].

   Lyapunov Dimension:

   $$D_L = j + \frac{\sum_{i=1}^{j} \lambda_i}{|\lambda_{j+1}|}. \tag{1.42}$$

   where $\lambda_1 \geq \cdots \geq \lambda_p$ and j is the largest index with $\sum_{i=1}^{j} \lambda_i \geq 0$ [57].

   Box-Counting Dimension:

   $$D_B = \lim_{\epsilon \to 0} \frac{\log N(\epsilon)}{\log(1/\epsilon)}. \tag{1.43}$$

   where $N(\epsilon)$ is the minimal covering by ϵ-boxes [45].

1.5.2.3 Routes to Chaos

A route to chaos refers to the characteristic sequence of bifurcations that transforms a predictable system (e.g., with stable fixed points) into a chaotic regime. Remarkably, these transition sequences often exhibit universal patterns across different systems. Three principal scenarios have been identified:

1. **Period-Doubling Route** [62]: The system evolves from stable equilibrium to chaos through successive period-doubling bifurcations. As the bifurcation parameter μ increases:

   - At $\mu = \mu_0$, a stable K-period cycle emerges.

- At $\mu = \mu_1$, this bifurcates to a $2K$-period cycle.
- The process continues until chaotic behavior dominates.

The accumulation point μ_∞ shows universal scaling properties.

2. **Intermittency** [57]: Characterized by alternating phases of:
   - Regular periodic motion (laminar phases).
   - Chaotic bursts (turbulent phases).

   As μ increases, the turbulent phases become more frequent until chaos prevails.

3. **Ruelle-Takens Scenario** [57]: Proceeds through quasi-periodic states:
   - Initial periodic behavior with frequency f_1.
   - Secondary frequency f_2 appears (f_2/f_1 irrational).
   - Additional frequencies emerge.
   - Chaos develops after three. incommensurate frequencies.

1.6 Controlling Chaotic Systems

Chaos control exploits the intrinsic properties of nonlinear dynamical systems to stabilize otherwise unpredictable behavior. Although chaotic systems exhibit sensitive dependence on initial conditions, they also possess a dense set of unstable periodic orbits, which can be stabilized through small and carefully designed perturbations [44, 56]. Two major control strategies have been widely developed. The first relies on parameter modulation, where one or more system parameters are slightly adjusted within prescribed bounds, whereas the second is based on feedback stabilization, in which corrective signals are introduced to drive the system toward a desired unstable orbit or equilibrium [1]. Both approaches require only minimal control effort and exploit the natural dynamics of the system rather than opposing them. The field of chaos control was initiated by the pioneering work of Ott, Grebogi, and Yorke in 1990, who demonstrated that chaotic trajectories can be stabilized through arbitrarily small parameter perturbations [56]. Since then, numerous control techniques have been developed and successfully applied in physics, engineering, biology, and economics, including laser stabilization, secure communications, cardiac rhythm regulation, and nonlinear market models [10, 12, 32, 44]. More recently, adaptive and intelligent control strategies incorporating optimization and machine learning have further expanded the capabilities of chaos control. In this thesis, we present the main representative control methods, with particular emphasis on the Ott–Grebogi–Yorke (OGY) method, which serves as the primary control strategy employed throughout this work.

1.6.1 The Ott–Grebogi–Yorke (OGY) Method

Developed in 1990 by Ott, Grebogi, and Yorke [56], this pioneering technique demonstrated that chaotic systems could be controlled with minimal energy input. The method exploits the fundamental property that chaotic attractors contain infinitely many unstable periodic orbits (UPOs). By applying precisely timed perturbations to an accessible system parameter, specific UPOs can be stabilized.

Theoretical Framework

Consider a nonlinear dynamical system:

$$\mathbf{x}_{n+1} = F(\mathbf{x}_n, p). \tag{1.44}$$

where $\mathbf{x}_n \in \mathbb{R}^n$ is the state vector and p is an externally adjustable control parameter. Let $\mathbf{x}_f$ denote an unstable fixed point satisfying $\mathbf{x}_f = F(\mathbf{x}_f, p_0)$.

Linearizing about $(\mathbf{x}_f, p_0)$ yields:

$$\delta\mathbf{x}_{n+1} = A\delta\mathbf{x}_n + B\delta p_n. \tag{1.45}$$

where:

- $A = D_x F|_{\mathbf{x}_f}$ (Jacobian matrix).
- $B = \partial F/\partial p|_{\mathbf{x}_f}$.
- $\delta\mathbf{x}_n = \mathbf{x}_n - \mathbf{x}_f$.
- $\delta p_n = p_n - p_0$.

The Jacobian A has stable ($|\lambda_s| < 1$) and unstable ($|\lambda_u| > 1$) eigendirections with corresponding eigenvectors $\mathbf{e}_s$, $\mathbf{e}_u$ and covariant vectors $\mathbf{f}_s$, $\mathbf{f}_u$.

Control Law Derivation

The OGY control strategy requires:

$$\mathbf{f}_u \cdot \delta\mathbf{x}_{n+1} = 0. \tag{1.46}$$

leading to the parameter adjustment:

$$\delta p_n = -\frac{\lambda_u}{\mathbf{f}_u B}\mathbf{f}_u \delta \mathbf{x}_n = -K\delta \mathbf{x}_n. \tag{1.47}$$

with $|\delta p_n| < \epsilon$ for some small $\epsilon > 0$.

Hénon Map Example

As a concrete illustration of the OGY method, we consider controlling the Hénon map, a canonical two-dimensional chaotic system described by:

$$\begin{cases} x_{n+1} = a - x_n^2 + by_n, \\ y_{n+1} = x_n. \end{cases} \tag{1.48}$$

where a and b are system parameters. For our control demonstration, we fix $(a, b) = (1.4, 0.3)$ to ensure chaotic behavior.

Fixed Point Analysis

The system's fixed points satisfy $x_{n+1} = x_n$ and $y_{n+1} = y_n$, yielding:

$$x_f = a - x_f^2 + bx_f \quad \Rightarrow \quad x_f = \frac{(b-1) \pm \sqrt{(1-b)^2 + 4a}}{2} \tag{1.49}$$

Substituting the parameter values gives two fixed points:

- $\mathbf{x}_{f1} = (0.8839, 0.8839)$ (saddle point).
- $\mathbf{x}_{f2} = (-1.5839, -1.5839)$ (saddle point).

We target stabilization of $\mathbf{x}_{f1}$ for this control example.

Control Implementation

The OGY control procedure involves five key steps:

1. **Jacobian Computation**: The system Jacobian at $\mathbf{x}_{f1}$ is:

$$A = \begin{pmatrix} -2x_f & b \\ 1 & 0 \end{pmatrix} = \begin{pmatrix} -1.7678 & 0.3 \\ 1 & 0 \end{pmatrix}. \tag{1.50}$$

with control matrix $B = \begin{pmatrix} 1 \\ 0 \end{pmatrix}$ when using a as the control parameter.

2. **Eigenvalue Analysis**: The characteristic equation $\det(\lambda I - A) = 0$ yields eigenvalues:

$$\lambda_{u,s} = -x_f \pm \sqrt{x_f^2 + b} \Rightarrow \begin{cases} \lambda_s = 0.1559 \text{ (stable)}, \\ \lambda_u = -1.9237 \text{ (unstable)}. \end{cases} \tag{1.51}$$

3. **Eigenvector Calculation**: Solving $(A - \lambda I)\mathbf{e} = 0$ gives the eigenvectors:

$$\mathbf{e}_s = \begin{pmatrix} \lambda_s \\ 1 \end{pmatrix}, \quad \mathbf{e}_u = \begin{pmatrix} \lambda_u \\ 1 \end{pmatrix}. \tag{1.52}$$

with corresponding covariant vectors $\mathbf{f}_s$, $\mathbf{f}_u$ satisfying $\mathbf{f}_i \mathbf{e}_j = \delta_{ij}$.

4. **Control Gain Determination**: The feedback gain is computed as:

$$K = \frac{\lambda_u \mathbf{f}_u}{\mathbf{f}_u B} = \begin{pmatrix} -1.9237 & 0.3011 \end{pmatrix}. \tag{1.53}$$

5. **Perturbation Application**: When the state enters an ϵ-neighborhood of $\mathbf{x}_{f1}$, we apply:

$$\delta p_n = \begin{cases} -K(\mathbf{x}_n - \mathbf{x}_{f1}) & \text{if } |K(\mathbf{x}_n - \mathbf{x}_{f1})| < \epsilon, \\ 0 & \text{otherwise.} \end{cases} \tag{1.54}$$

As shown in Figure (1.8), the OGY controller stabilizes the chaotic trajectory by applying small parameter perturbations near the saddle fixed point.

1.6.2 Feedback-Based Control Strategies

Feedback control systems pervade modern technology, from automotive braking systems to climate control in buildings. While engineers have empirically utilized feedback principles for decades, the formal mathematical framework for state feedback stabilization emerged in the 1960s. This approach dynamically adjusts control inputs u_n based on real-time system state measurements x_n to drive the system toward a desired trajectory. The method offers two key advantages [44]:

- Robust stability against parameter variations.
- Effective noise and disturbance rejection.

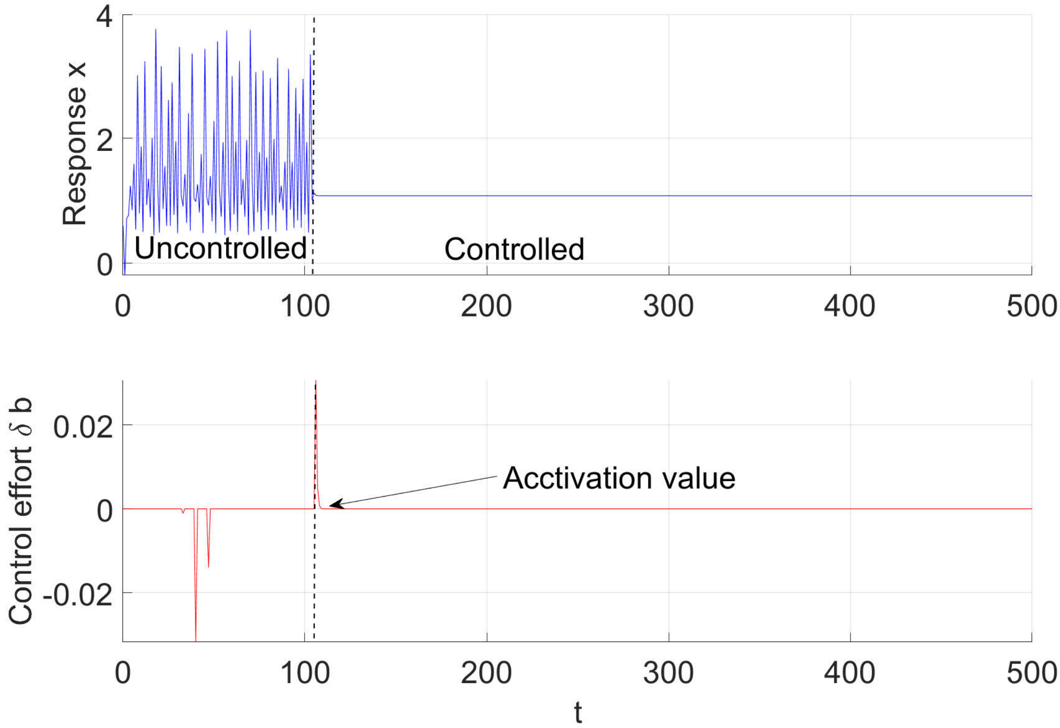

Figure 1.8: Stabilization of the Hénon map's saddle fixed point $\mathbf{x}_{f1}$ using OGY control. The controller activates when the trajectory enters the control region.

Mathematical Formulation

Consider the discrete-time control system:

$$x_{n+1} = f(x_n, u_n), \quad f : \mathbb{R}^k \times \mathbb{R}^m \to \mathbb{R}^k. \tag{1.55}$$

The control objective is to design a feedback law:

$$u_n = h(x_n). \tag{1.56}$$

such that the origin $\bar{x} = 0$ becomes a locally asymptotically stable equilibrium of the closed-loop system. We assume:

1. $f(0, 0) = 0$ (origin is an equilibrium).

2. f is C^1-smooth with Jacobians:

$$A = \frac{\partial f}{\partial x}(0,0) \quad (k \times k \text{ matrix}),$$
$$B = \frac{\partial f}{\partial u}(0,0) \quad (k \times m \text{ matrix}).$$

Theorem 1.6.1 (Nonlinear Stabilization). *If the matrix pair (A, B) is controllable, then the nonlinear system (1.55) is locally stabilizable. Specifically, for any stabilizing gain matrix K of (A, B), the control law:*

$$u_n = -Kx_n. \tag{1.57}$$

renders the origin asymptotically stable.

Proof. The controllability condition guarantees existence of K such that $A - BK$ has all eigenvalues inside the unit circle. Consider the closed-loop map:

$$g(x) = f(x, -Kx). \tag{1.58}$$

with linearization at the origin:

$$\left.\frac{\partial g}{\partial x}\right|_{x=0} = A - BK. \tag{1.59}$$

It follows from Lyapunov's indirect method that the local asymptotic stability of the nonlinear system is guaranteed by the asymptotic stability of its linearization, $\mathbf{y}_{n+1} = (A - BK)\mathbf{y}_n$, which holds by design. ■

Chapter 2

Oligopolistic Markets: Theory and Key Models

2.1 Oligopolistic competition

2.1.1 Definition and Fundamental Characteristics

An oligopoly represents a market structure dominated by a small number of firms that exert significant control over prices and output levels [42, 33]. According to economic theory, these firms may operate independently or engage in collusive behavior, which explicitly reduces market competition and is often illegal. Unlike perfect competition where numerous firms act as price takers, oligopolistic firms function as price makers, either collectively through cartel arrangements or by following industry price leaders.

The critical distinction between oligopoly and monopoly lies in the number of dominant market participants. While a monopoly features a single firm controlling the entire market, an oligopoly consists of several interdependent firms whose business decisions significantly impact competitors. This mutual interdependence constitutes the hallmark characteristic of oligopolistic markets, as no single firm can unilaterally dictate market conditions without considering rivals' potential responses.

2.1.2 Market Dynamics and Barriers to Entry

Oligopolies typically emerge in industries with substantial barriers to entry that prevent new competitors from entering the market. These barriers include significant economies of scale that give established firms cost advantages, stringent regulatory requirements that create compliance hurdles, control over essential distribution channels, and substantial capital investment requirements. Additionally, brand loyalty cultivated by incumbent firms through extensive marketing further reinforces market concentration.

Historical examples of oligopolistic industries include steel manufacturing, petroleum production, railroad operations, tire production, and wireless telecommunications. Such market structures raise economic concerns because they may stifle innovation, maintain artificially high prices, and limit consumer choice. The steel industry's evolution demonstrates how technological changes like offshore production and mini-mill development can disrupt established oligopolistic patterns.

2.1.3 Strategic Behavior and Game Theory

Oligopolistic firms frequently encounter strategic dilemmas modeled by game theory, particularly the prisoner's dilemma. This framework explains why firms may choose to cheat on collusive agreements despite mutual benefits from cooperation. When firms achieve Nash equilibrium, they reach a state where no participant can gain by unilaterally changing strategy given competitors' choices.

Firms employ various strategies to maintain market stability, including tacit coordination through price leadership or more overt mechanisms like contractual agreements. Some industries develop sophisticated coordination methods, such as using external signaling mechanisms to synchronize pricing changes without explicit communication that might violate antitrust laws.

2.1.4 Government Regulation and Policy Considerations

Governments typically monitor oligopolistic markets through antitrust legislation designed to prevent price-fixing and anti-competitive practices. However, regulatory approaches vary significantly across jurisdictions and economic systems. In mixed economies, oligopolistic firms often engage in political may engage in lobbying to shape favorable regulatory environments, sometimes resulting in government-sanctioned market protections.

The airline industry provides a compelling case study of regulatory intervention. Following the 1978 Airline Deregulation Act in the United States, the industry transitioned from utility-like regulation to an oligopolistic structure dominated by four major carriers. This shift produced mixed outcomes, including increased operational efficiency but also concerns about reduced competition and consumer choice.

2.1.5 Advantages and Disadvantages

Oligopolies present both benefits and drawbacks for market participants. The limited number of competitors allows firms to achieve higher profit margins and greater operational stability. Consumers may benefit from the reputation and reliability of established firms, along with the potential for coordinated industry standards.

Conversely, the high barriers to entry characteristic of oligopolies restrict market access for new competitors, potentially stifling innovation. Consumers often face limited product choices and may bear the cost of reduced price competition. The technology sector illustrates this tension, where dominant platforms like mobile operating systems create network effects while potentially limiting market diversity.

2.1.6 Contemporary Examples and Case Studies

OPEC is a classic example of a global oligopoly. Its member countries act like a group by coordinating how much oil they produce to control prices. More Conversational OPEC's market power stems from its collective share of global oil reserves rather than formal authority over members. This structure demonstrates how independent entities can exercise oligopolistic control through voluntary coordination.

In the media sector, concentration among major content producers like Disney and Warner Media illustrates domestic oligopoly dynamics, even as streaming platforms disrupt traditional distribution channels. Similarly, the smartphone operating system market, dominated by Google's Android and Apple's iOS, demonstrates how technological oligopolies can emerge in digital markets.

2.2 Fundamentals of Game Theory

2.2.1 Strategic-Form Game Assumptions

Game theory explores the strategic interactions among multiple decision-makers (players), each operating under a fixed set of rules and predictable outcomes. Every player is assumed to be rational and self-interested, aiming to select the optimal action based on their preferences. These preferences are unrestricted in nature and are defined by the player's consistent choices across different scenarios, not by their specific likes or dislikes [55].

Each player possesses a set A containing all feasible actions and has clear preferences. In each situation, a subset of A is presented, from which the player must select one element. The decision-maker accepts this subset as given, unaffected by their preferences. For instance, A might represent all consumable bundles, but actual choices depend on the player's current financial capacity.

Regarding preferences, we assume players can compare any two actions: either favoring one over the other or treating them as equally preferred. Additionally, we assume transitive consistency: if a player prefers action a to b and b to c, then they also prefer a to c. Altruistic preferences are not excluded, meaning a player might derive utility from the well-being of others.

2.2.2 Nash Equilibrium

A Nash Equilibrium refers to a set of strategies where no player can improve their payoff by deviating unilaterally. It provides a predictive solution for the outcome of strategic decision-making [41].

The existence of a unique Nash equilibrium does not automatically guarantee convergence toward it under dynamic adjustments. Convergence further depends on the stability of the underlying learning, information, and expectational dynamics. More generally, a game may possess no, one, or multiple equilibria.

- **Pure-Strategy Nash Equilibrium:** A strategy profile where no individual player can benefit by changing their strategy, assuming others stick to theirs.
- **Mixed-Strategy Nash Equilibrium:** A situation where players randomize over strategies, and no one can gain a higher expected payoff by unilaterally deviating.

2.2.3 Examples of Strategic Games

Given the players, their available strategies, and resulting payoffs, we can represent a game in its *normal form* (or *strategic form*). This format outlines the payoff for every possible combination of strategies. Each complete selection of strategies by all players is called a *strategy profile*, and the related payoffs can be organized in a matrix form. Consider the following matrix as an illustration [65]:

Basic Game with Nash Equilibrium in Pure Strategies

	A	**B**
A	**(8,8)**	(6,0)
B	(0,6)	(2,2)

It is easy to see that for Player 1, choosing strategy **A** always yields the highest payoff regardless of Player 2's choice. The same logic applies to Player 2. Thus, the strategy profile (A, A)-resulting in the payoff $(8, 8)$-is the only Nash equilibrium in this game.

Prisoner's Dilemma

	A	**B**
A	(6,6)	(0,8)
B	(8,0)	**(2,2)**

Although (A, A) gives both players a relatively high payoff, this outcome is unstable. If Player 1 selects **A**, Player 2 can increase her payoff by switching to **B**. If both end up playing **B**, the resulting equilibrium is (B, B) with payoffs $(2, 2)$. Despite being a Nash equilibrium, it is not Pareto optimal, since both players would prefer the outcome $(6, 6)$.

Matching Pennies

	A	**B**
A	(1,-1)	(-1,1)
B	(-1,1)	(1,-1)

This game has no pure strategy Nash equilibrium. For example, if Player 1 and Player 2 both choose **A**, Player 2 will prefer switching to **B** since it increases her payoff.

Similar reasoning applies to every other pure strategy pair, showing that all of them are unstable.

Suppose Player 1 believes Player 2 chooses **A** with probability p. Then, if Player 1 chooses **A**, the expected payoff is $2p - 1$. If Player 1 chooses **B**, the expected payoff becomes $1 - 2p$. Player 1 will be indifferent between **A** and **B** when these expected payoffs are equal, i.e., $2p-1 = 1-2p$, which yields $p = \frac{1}{2}$. Similarly, Player 2 randomizes if she also expects Player 1 to play each strategy with equal probability. Hence, the mixed strategy Nash equilibrium is $\left(\frac{1}{2}, \frac{1}{2}\right)$ for both players.

2.2.4 Sub-game Perfect Nash Equilibrium (SPNE)

In sequential games, where players move in turn, decisions depend on observing prior actions. These games are modeled using extensive-form trees [38].

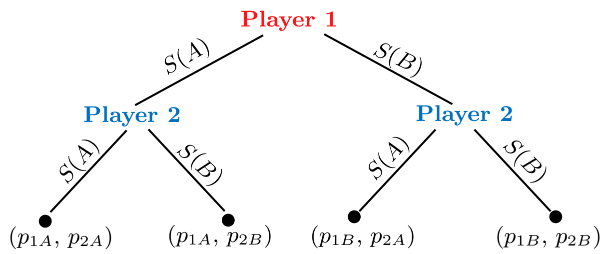

Figure 2.1: Generic Extensive form Game

A strategy profile is a Subgame Perfect Equilibrium only if it prescribes rational, optimal behavior in every possible subgame. The most common method for identifying these equilibria is backward induction, which solves the game by starting from the final moves and proceeding to the initial ones.

In a sample game tree, analyzing the last player's choices helps determine earlier optimal decisions. For example, if Player 1 knows that choosing action A leads to better payoffs regardless of Player 2's response, they will prefer A. Each player's optimal strategy forms the SPNE when combined.

2.3 Oligopoly Models

In this section, we explore how firms behave in oligopolistic markets, where only a few firms interact strategically. Unlike in perfectly competitive markets, firms in an oligopoly don't treat the market price as fixed. At the same time, unlike a monopoly, no single firm has complete control over the entire market. Our focus will be on oligopoly models in markets with **homogeneous goods**, where consumers see no difference between products offered by different firms.

An oligopoly is characterized by the presence of a limited number of firms and significant barriers to entry. These markets typically involve intense rivalry as each firm decides how much to produce, what price to charge, and how to promote its products to maximize profits [41, 54, 58].

Due to the small number of competitors, a firm's earnings are influenced not only by its own strategies but also by the actions of its rivals. This interdependence leads to a constant strategic balancing act where firms must anticipate and respond to one another's moves. Hence, strategic decision-making is central to the study of oligopoly.

Take the automotive industry, for example-each company's market position depends on how its pricing and production levels compare to its competitors. If Ford reduces its prices while others don't, it may capture a larger share of the market at the expense of its rivals.

Managers operating in oligopolistic markets usually assume that their competitors are rational and will react thoughtfully to any strategic changes. This assumption is crucial when predicting how other firms will respond.

The first formal analysis of oligopoly was developed by the French mathematician **Augustine Cournot** in 1838 [27]. His model, which anticipated Nash's concept of equilibrium by more than 100 years, laid the foundation for future research in this area.

Another influential model was proposed by **Joseph Bertrand**, also a French mathematician. He posed a key question: "What if each firm sets its price assuming the other firm's price is fixed?" This model, known as the *Bertrand model*, describes price competition in markets where firms produce identical goods [18].

A third model was introduced by **Heinrich von Stackelberg**, a German economist originally from Russia. In his 1934 work *Market Structure and Equilibrium*, Stackelberg presented a sequential-move game that revolutionized the analysis of duopolies by treating firm interaction as a leadership-followership game [64].

The final two models we'll examine are variants of the Cournot duopoly, but with **incomplete information**. In the fourth model, one firm lacks knowledge about its competitor's production cost. In the fifth, a firm is uncertain whether its rival knows its cost or not. These models introduce information asymmetry into oligopoly theory, deepening our understanding of strategic behavior in such settings.

2.3.1 Cournot's Model

2.3.1.1 General Model

Each firm is assumed to produce a single type of good. Let firm i have output level q_i, and its cost of production is described by a function $C_i(q_i)$ [55, 19]. This cost function is increasing, implying that higher production levels incur greater costs.

All units produced by a firm are sold at a market price determined by the total supply across all firms. Specifically, if total market output is $Q = \sum_{i=1}^{n} q_i$, then the corresponding price is given by $P(Q)$, where P denotes the inverse demand function. This function is assumed to be decreasing while $P(Q) > 0$, meaning prices fall as total output rises.

Each firm's revenue is calculated as $q_i P(Q)$, and so the profit for firm i becomes:

$$\pi_i(q_1, \ldots, q_n) = q_i P(q_1 + \cdots + q_n) - C_i(q_i).$$

The Cournot model treats this scenario as a strategic game, described as follows:

- **Players:** The n firms in the market.
- **Strategies:** Each firm selects an output level $q_i \geq 0$.
- **Payoffs:** Each firm's utility is identified with its profit.

2.3.1.2 Cournot Duopoly

In the simplified case of two competing firms, each firm i incurs a linear cost given by $C_i(q_i) = c_i q_i$, where c_i is the constant marginal cost [55, 15]. The inverse demand function is assumed to be linear and positive within a certain range, and is expressed as:

$$P(Q) = \begin{cases} \alpha - \beta Q & \text{if } \beta Q \leq \alpha, \\ 0 & \text{otherwise,} \end{cases}$$

where $\alpha > 0$, $\beta > 0$, and $c_i \geq 0$. To ensure that at least one firm can earn a positive profit, we assume that $c_i < \alpha$ for at least one firm. Otherwise, no firm could produce profitably, since market price never exceeds α. We also assume $\alpha - 2c_i + c_j > 0$, for $i, j \in \{1, 2\}$ with $i \neq j$.

To find the Nash equilibrium, we first determine each firm's best response function. Letting the firms' output quantities be q_1 and q_2, the market price is given by:

$$P(q_1 + q_2) = \begin{cases} \alpha - \beta(q_1 + q_2) & \text{if } \beta(q_1 + q_2) \leq \alpha, \\ 0 & \text{otherwise.} \end{cases}$$

Therefore, firm 1's profit can be written as:

$$\pi_1(q_1, q_2) = q_1(P(q_1 + q_2) - c_1) = \begin{cases} (\alpha - \beta(q_1 + q_2) - c_1)q_1 & \text{if } \beta(q_1 + q_2) \leq \alpha, \\ -c_1 q_1 & \text{otherwise.} \end{cases}$$

By symmetry, the profit of firm 2 can be expressed as:

$$\pi_2(q_1, q_2) = q_2(P(q_1 + q_2) - c_2).$$

Substituting the linear inverse demand function gives:

$$\pi_2(q_1, q_2) = \begin{cases} (\alpha - \beta(q_1 + q_2) - c_2)q_2 & \text{if } \beta(q_1 + q_2) \leq \alpha, \\ -c_2 q_2 & \text{otherwise.} \end{cases}$$

To identify firm 1's optimal output in response to any quantity q_2 produced by firm 2, we maximize firm 1's profit function. This involves taking the partial derivative of π_1 with respect to q_1 and solving the first-order condition:

$$\frac{\partial \pi_1}{\partial q_1} = \alpha - 2\beta q_1 - \beta q_2 - c_1 = 0.$$

Solving for q_1, we obtain firm 1's best response function:

$$\mathrm{BR}_1(q_2) = q_1(q_2) = \begin{cases} \dfrac{\alpha - \beta q_2 - c_1}{2\beta} & \text{if } q_2 \leq \dfrac{\alpha - c_1}{\beta}, \\ 0 & \text{if } q_2 > \dfrac{\alpha - c_1}{\beta}. \end{cases}$$

Since the cost functions are symmetric, we can derive firm 2's best response function in the same way:

$$\mathrm{BR}_2(q_1) = q_2(q_1) = \begin{cases} \dfrac{\alpha - \beta q_1 - c_2}{2\beta} & \text{if } q_1 \leq \dfrac{\alpha - c_2}{\beta}, \\ 0 & \text{if } q_1 > \dfrac{\alpha - c_2}{\beta}. \end{cases}$$

Each best response function links one firm's optimal output to the output level of its rival. Specifically, BR_1 maps outputs of firm 2 (horizontal axis) to outputs of firm 1 (vertical axis), while BR_2 does the reverse.

The intercept of $q_1(q_2)$ on the q_1-axis represents the quantity firm 1 would produce if firm 2 produced nothing. The intercept on the q_2-axis identifies the output level of firm 2 at which firm 1's optimal output becomes zero. Reversing axes gives equivalent intercepts for firm 2.

The point of intersection (q_1^*, q_2^*) of the best response functions corresponds to a state where each firm is optimizing its output based on the other's choice. That is, q_1^* is the best response to q_2^* and vice versa.

This mutual optimization defines the concept of a Nash equilibrium in pure strategies. Therefore, (q_1^*, q_2^*) is the Nash equilibrium of the Cournot duopoly game. To determine the equilibrium outputs q_1^* and q_2^*, we solve the system of best response functions:

$$q_1 = \frac{\alpha - c_1}{2\beta} - \frac{q_2}{2}, \quad q_2 = \frac{\alpha - c_2}{2\beta} - \frac{q_1}{2}.$$

By substituting the expression for q_2 into the equation for q_1, we reduce the system to a single-variable equation. Solving this yields:

$$q_1^* = \frac{\alpha - 2c_1 + c_2}{3\beta}, \quad .$$

Substituting q_1^* back into the second equation gives:

$$q_2^* = \frac{\alpha - 2c_2 + c_1}{3\beta}, \quad .$$

The total market output at equilibrium is:

$$Q = q_1^* + q_2^* = \frac{2\alpha - c_1 - c_2}{3\beta},$$

and the equilibrium price is:

$$P(q_1^* + q_2^*) = \frac{\alpha + c_1 + c_2}{3\beta}.$$

When α increases-indicating higher consumer willingness to pay-the market price and each firm's output also rise. In contrast, as a firm's marginal cost c_i increases, its output declines and the market price increases accordingly. Specifically, a unit rise in c_i results in a one-third unit increase in the equilibrium price.

2.3.1.3 Cournot's Model with n Firms

In the general Cournot framework with n firms, the profit of each firm i is determined by [55]:

$$\pi_i(q_1, \dots, q_n) = q_i P(q_1 + \cdots + q_n) - c_i q_i.$$

Here, a firm's payoff depends on its own output q_i and the aggregate production $Q = \sum_{j=1}^{n} q_j$, not on how total output is distributed among competitors.

Since the inverse demand function $P(Q)$ decreases with Q, a firm's payoff tends to shrink as the number of competitors rises. This structure can be represented as:

$$f_i(q_i, Q),$$

where f_i is decreasing in Q for a fixed q_i.

This formulation captures a wide class of strategic interactions over a shared resource, often referred to as "common property." A classic example is a communal pasture: the more farmers graze animals there, the less valuable the pasture becomes to each.

In Nash equilibrium, common resources are frequently over-utilized. That is, if all players were to scale back slightly from their equilibrium usage, each would benefit. In the farming analogy, if every farmer reduces grazing slightly, each one's herd would benefit more from the improved quality of the grassland.

The reasoning applies to Cournot competition as well: demand is the shared resource being over exploited. Each firm, by increasing output, reduces the market price, which negatively affects all firms.

2.3.2 Bertrand's Model

2.3.2.1 General Model

In contrast to Cournot's model, where firms compete by choosing output levels and prices adjust accordingly, the Bertrand model assumes that firms compete directly by setting prices to maximize profits [55].

Although the market setup remains similar to Cournot's-namely, n firms producing a single, homogeneous good-the key distinction lies in the nature of competition: firms select their own selling prices instead of production quantities.

Each firm can produce the good at a constant marginal cost c_i. Rather than specifying the price as a function of output (inverse demand), we define a direct demand function $D(p)$, which gives the quantity demanded at price p.

If firms set different prices, all customers buy from the firm offering the lowest price, and that firm is assumed capable of meeting total market demand. If several firms charge the same lowest price, they split the demand equally. Firms that charge a higher price than competitors receive zero demand.

Thus, the Bertrand oligopoly game is a strategic interaction defined as follows:

- **Players:** The firms.
- **Strategies:** Each firm selects a nonnegative price.
- **Preferences:** Profits represent each firm's payoff. If firm i is among m firms with the lowest price p_i, its profit is $\pi_i = \left(\frac{p_i D(p_i)}{m} - C_i\left(\frac{D(p_i)}{m}\right)\right)$. If some rival undercuts p_i, then $\pi_i = 0$.

2.3.2.2 Bertrand's Duopoly

Consider the case with two firms (firm 1 and firm 2). Each selects a price $p_i \geq 0$. Both firms produce identical goods and incur the same constant marginal cost c, i.e., $C_i(q_i) = cq_i$ for $i = 1, 2$ [55]. Assume that the market demand function is:

$$D(p) = \begin{cases} \frac{\alpha - p}{\beta} & \text{if } p \leq \alpha, \\ 0 & \text{if } p > \alpha, \end{cases}$$

where $\alpha, \beta > 0$ and $c < \alpha$.

Each firm's profit depends on its price relative to the competitor:

$$\pi_i(p_1, p_2) = \begin{cases} (p_i - c)\left(\frac{\alpha - p_i}{\beta}\right) & \text{if } p_i < p_j \\ \frac{1}{2}(p_i - c)\left(\frac{\alpha - p_i}{\beta}\right) & \text{if } p_i = p_j \\ 0 & \text{if } p_i > p_j \end{cases}$$

where j is the rival firm ($j = 2$ if $i = 1$, and vice versa). This profit function expresses how each firm's earnings depend on the difference between the price it charges per unit and its marginal cost, multiplied by the quantity that consumers demand at that price.

As previously mentioned, if one firm sets a price lower than its competitor, it captures the entire market demand and thus all the associated profit. If both firms choose the same price, the market demand is split equally, and each firm earns half the profit. On the other hand, a firm setting a higher price than its rival receives no demand and earns zero profit.

Similar to the Cournot setup, we identify Nash equilibria by determining each firm's best response to its competitor's pricing strategy.

Consider firm i. It would not set a price below the marginal cost c, since doing so would result in a loss. The same reasoning applies to firm j, so we establish that prices below c are never optimal. Thus, c serves as a natural lower limit for feasible prices.

Now, suppose one firm sets a price strictly above the other-say $p_i > p_j$. In this case, firm i (the higher-pricing firm) earns nothing, while firm j makes positive profit. This creates an incentive for firm i to reduce its price slightly-still above c-to attract consumers and gain a share of the market. Hence, no Nash equilibrium exists when prices differ and are both above c.

If $p_i = p_j > c$, both firms split the market and each earns positive profit. However, this is not a Nash equilibrium either. Each firm has a motivation to undercut the other marginally (setting a price slightly less than p_j or p_i but still above c) to capture the entire demand and profit.

This price-cutting competition continues until both firms reach the marginal cost $p_i = p_j = c$. At this point, if one firm deviates by lowering its price below c, it incurs losses. If it raises its price, it is undercut and earns nothing. Therefore, neither firm has an incentive to deviate.

Thus, both firms pricing at marginal cost c constitutes a Nash equilibrium. At this outcome, each firm earns zero profit, but any deviation would either reduce profit below zero or exclude the deviating firm from the market entirely.

This reasoning leads directly to the best response functions for both firms:

$$BR_i(p_j) = \begin{cases} p_i : p_j < c \le p_i & \text{if } p_j < c, \\ p_i : p_i \ge p_j & \text{if } p_j = c, \\ p_i : c \le p_i < p_j & \text{if } p_j > c. \end{cases} \quad BR_j(p_i) = \begin{cases} p_j : p_i < c \le p_j & \text{if } p_i < c, \\ p_j : p_j \ge p_i & \text{if } p_i = c, \\ p_j : c \le p_j < p_i & \text{if } p_i > c, \end{cases}$$

As a result, the only equilibrium outcome in this setting is:

$$p_1 = p_2 = c.$$

2.3.2.3 Bertrand's Paradox

This conclusion is known as Bertrand's paradox. It shows that even with only two firms, the outcome can replicate perfect competition, where the market price is equal to the marginal cost of production. Normally, we expect duopolies to set prices above marginal cost to earn profits, making this result quite counterintuitive [55].

There are a few ways to resolve this paradox, but each requires relaxing one of the original model's assumptions:

- The firms produce identical products.
- Each firm can satisfy total market demand on its own.
- Firms behave non-cooperatively in the short run.

The most common resolution is to assume that firms sell slightly different (differentiated) products. In this case, if a competitor slightly undercuts the price, a firm does not lose all its customers. Suppose both firms initially charge a price equal to marginal cost. If some buyers have a preference for firm i's product, then firm i can raise its price slightly and still retain part of its customer base. The same goes for firm j.

Both firms now have an incentive to increase their prices above cost. This continues until neither firm can benefit from raising or lowering its price, given the other's price. This defines a new equilibrium. The extent of price increase depends on how differentiated the products are. Greater differentiation allows for higher prices above cost. However, as more firms enter the market, differentiation diminishes and prices are pushed back toward marginal cost. Thus, even with product diversity, enough competition can still eliminate profits.

A second resolution to Bertrand's paradox involves dropping the assumption that any single firm can meet total market demand. In reality, firms often have capacity constraints, particularly in the short run. This idea is captured in the Bertrand-Edgeworth model, which assumes that no firm has the ability to serve the whole market alone.

In such a context, the incentive to undercut competitors vanishes because even if a firm sets a lower price, it cannot meet all of the demand. As a result, prices rise above marginal cost. Moreover, firms adopt mixed strategies-randomizing over several prices-since no pure-strategy Nash equilibrium exists. For instance, a firm might set a price of 20 with 10% probability or 25 with 15% probability, and so on.

Lastly, Bertrand's paradox can be addressed by removing the assumption of one-shot interaction. The original model assumes firms compete only once. However, in repeated interactions, firms may choose to avoid aggressive pricing in hopes that competitors will reciprocate. This leads to tacit collusion, where prices stay above marginal cost.

Still, economists argue that such collusion is fragile. Since prices are not part of a strict Nash equilibrium, each firm is tempted to deviate by cutting prices to gain market share-making long-term cooperation unstable without enforcement mechanisms.

2.3.3 Stackelberg's Model

2.3.3.1 General Model

Unlike previous models where firms act simultaneously without knowledge of competitors' decisions, the Stackelberg model introduces sequential decision-making [55]. Here, two firms produce a homogeneous good, but one firm moves first (the leader), and the second firm (the follower) observes this choice before making its own decision.

Both firms incur a cost of c per unit produced. The market price $P(Q)$ depends on the total quantity $Q = q_1 + q_2$. Although one firm moves first, this does not give it monopolistic power-the decisions happen rapidly enough that timing does not grant exclusivity.

Game Structure:

- *Players:* Two firms.
- *Actions:* Firm 1 selects a quantity $q_1 \in [0, \infty)$; Firm 2 responds with $q_2 \in [0, \infty)$ based on q_1.
- *Payoffs:* Each firm maximizes its own profit.

2.3.3.2 Stackelberg's Duopoly

Assume firm i moves first, and firm j follows. Each selects a non-negative production quantity: q_i and q_j [55]. The marginal cost is constant and identical for both firms: $C_i(q_i) = C_j(q_j) = cq$.

The market price is determined by:

$$P(Q) = \begin{cases} \alpha - \beta Q & \text{if } Q \leq \frac{\alpha}{\beta}, \\ 0 & \text{if } Q > \frac{\alpha}{\beta}, \end{cases}$$

with $\alpha > c$ to ensure profitability.

The strategic sets are:

- Firm i (leader) selects $q_i \in [0, \infty)$.
- Firm j (follower) reacts via a function $q_j(q_i)$, mapping each q_i to an optimal response.

This sequential setup changes the nature of strategic interaction: the leader anticipates the follower's best response and incorporates it when choosing its own output.

To find the sub-game perfect Nash equilibrium, we use backward induction. This means we start by figuring out what the second firm will do in the final stage. Once we know that, we can work backward to determine the first firm's best initial move, ensuring that neither firm has an incentive to deviate from this plan at any point in the game.

First, we determine firm j's profit function:

$$\pi_j = q_j[\alpha - \beta(q_i + q_j)] - cq_j.$$

To maximize profit, we compute the first-order condition (FOC) by taking the derivative with respect to q_j and setting it to zero:

$$\frac{d\pi_j}{dq_j} = \alpha - \beta q_i - 2\beta q_j - c = 0.$$

Solving this yields firm j's best response function:

$$BR_j(q_i) = \begin{cases} q_j = \frac{\alpha - \beta q_i - c}{2\beta} & \text{if } q_i \leq \frac{\alpha - c}{\beta}, \\ 0 & \text{otherwise.} \end{cases}$$

Next, we turn to firm i. Its profit is:

$$\pi_i = q_i[\alpha - \beta(q_i + q_j)] - cq_i.$$

Substituting firm j's optimal response into this expression:

$$\pi_i = q_i \left[\alpha - \beta \left(q_i + \frac{\alpha - \beta q_i - c}{2\beta} \right) \right] - cq_i.$$

Simplifying:

$$\pi_i = \frac{1}{2} q_i (\alpha - \beta q_i - c).$$

Now, we derive the FOC for firm i:

$$\frac{d\pi_i}{dq_i} = \frac{1}{2}(\alpha - 2\beta q_i - c) = 0.$$

Solving gives firm i's optimal output:

$$q_i^* = \frac{\alpha - c}{2\beta}.$$

Notice that this output depends only on constants and not on q_j, which contrasts with the Cournot model where each firm's output depends on the other's decision.

Since firm i makes its decision based solely on fixed parameters α, β, and the marginal cost c, its optimal output is independent of firm j's actions. Substituting

$q_i^* = \frac{\alpha - c}{2\beta}$ into firm j's best response gives:

$$q_j^* = \frac{\alpha - c}{4\beta}.$$

Thus, the sub-game perfect Nash equilibrium (SPNE) strategy profile is:

$$(q_i^*, q_j^*) = \left(\frac{\alpha - c}{2\beta}, \frac{\alpha - c}{4\beta} \right).$$

And the respective profits are:

$$\pi_i = \frac{(\alpha - c)^2}{8\beta}, \quad \pi_j = \frac{(\alpha - c)^2}{16\beta}.$$

2.3.3.3 Conclusions on the Stackelberg's Model

The Stackelberg framework shows that the firm moving first secures a strategic advantage. It earns higher output and greater profit than its rival, even though both face the same marginal cost.

Unlike the Cournot model, where identical firms share equal market outcomes, Stackelberg's sequential nature introduces an asymmetry-the leader firm leverages its early move to dominate. Though there's no exclusive market period, this structure mirrors real markets: early entrants often enjoy temporary monopolistic gains.

Such gains can be modeled by assuming firm j produces nothing, yielding firm i's monopoly profit:

$$\pi_i^m = \frac{(\alpha - c)^2}{4\beta}.$$

Chapter 3

From Chaos to Stability: Managing Complex Price Oscillations in a Bertrand Duopoly Game with Quadratic Cost Functions

3.1 Introduction

In economics, oligopoly models have been widely studied, with early research focusing on stability and equilibrium properties. Furth [34] analyzed how oligopolies reach a steady state, particularly regarding the stability of firm interactions. In duopoly settings, where two firms compete strategically, later studies shifted toward examining long-run dynamics. Bertrand-type models with differentiated goods have been well explored [18, 14, 10], with works by Bischi and Kopel [20], Al-Khedhairi [4], Yi and Zeng [67], and Chen and Jia [26] highlighting bifurcations and chaotic dynamics under homogeneous expectations.

In practical markets, firms rarely know the full demand structure, relying instead on local demand estimates and cost information, as discussed by Naimzada and Ricchiuti [52] and Askar [9]. Boundedly rational firms update strategies through discrete gradient adjustments based on marginal profit approximations. This approach, studied by Azioune and Abdelouahab [10], Azioune et al. [12], Meskine et al. [51], Al-Khedhairi [4], Bischi and Lamantia [21], and Tramontana [63], reduces the need for full knowledge of global market functions.

Analysis of these models shows that the Nash equilibrium undergoes a flip bifurcation, which destabilizes the steady state and gives rise to oscillatory or chaotic price dynamics, while Neimark–Sacker bifurcations are absent. As adjustment speeds and product differentiation rise, the system develops chaos and mixed-mode oscillations, confirmed via numerical simulations. While chaotic dynamics may sometimes play constructive roles in economics [48], in this context they undermine market predictability and stability. To address this issue, we investigate a state feedback control method that successfully eliminates chaos and restores equilibrium stability. The method defines three boundary conditions that enclose a triangular stability region, with their intersections determining viable parameter ranges. Numerical simulations confirm the control scheme's effectiveness in stabilizing the duopoly system.

3.2 Formulation of the Model

In this work, we adopt the framework introduced by Georges Sarafopoulos and Kosmas Papadopoulos [59], where firms produce differentiated goods and determine their supply through an inverse demand relation. The aggregate output is given by $Q = \sum_{i=1}^{n} q_i$, which governs the market price $P_i(Q)$ for each firm. We restrict our analysis to a Bertrand-type duopoly operating in discrete time periods $t = 0, 1, 2, \ldots$, where two firms compete by setting prices for distinct products. At each stage, firms form expectations about their rival's future decision in order to maximize profit. Here, q_1 and q_2 denote the outputs of the firms, while p_1 and p_2 represent the corresponding prices. The representative consumer's preferences are described by the utility function:

$$U(q_1, q_2) = a \sum_{i=1}^{2} q_i - \tfrac{1}{2}\left(\sum_{i=1}^{2} q_i^2 + 2dq_1q_2\right), \tag{3.1}$$

where the parameter $a > 0$ reflects the market size and d ($-1 < d < 1$) indicates the degree of product differentiation. As $d \to 1$, the goods tend to be close substitutes, while as $d \to 0$, they become more distinct. If $d < 0$ corresponds to complementarity, with the extreme case $d = -1$ representing perfect complements.

The inverse demand functions can be obtained from (3.1) and are expressed as [19]:

$$p_i = \frac{\partial U}{\partial q_i}, \text{then we get:} \quad \begin{cases} p_1 = a - dq_2 - q_1, \\ p_2 = a - dq_1 - q_2. \end{cases} \tag{3.2}$$

From (3.2), one can derive the corresponding direct demand functions:

$$\begin{cases} q_1 = \dfrac{a(1-d) + dp_2 - p_1}{1-d^2}, \\[2ex] q_2 = \dfrac{a(1-d) + dp_1 - p_2}{1-d^2}, \end{cases} \tag{3.3}$$

where we denote $b = 1 - d^2$.

To investigate the system's dynamics, we introduce quadratic production cost functions with parameters $c_i,\ i = 1, \ldots, 6$. Such quadratic forms allow the model to incorporate nonlinearities in production costs, thereby offering a more realistic representation of firm behavior compared to linear specifications [46]. The explicit cost functions of the two firms are defined as:

$$C_1(q_1) = c_1 q_1^2 + c_2 q_1 + c_3, \qquad c_1 > 0,\ c_2 \geq 0,\ c_3 \geq 0,$$

$$C_2(q_2) = c_4 q_2^2 + c_5 q_2 + c_6, \qquad c_4 > 0,\ c_5 \geq 0,\ c_6 \geq 0.$$

The profit functions can be expressed mathematically as,

$$\Pi_1(p_1, p_2) = p_1 q_1 - C_1(q_1), \quad \Pi_2(p_1, p_2) = p_2 q_2 - C_2(q_2).$$

The marginal profit with respect to each firm's price is obtained by differentiation:

$$\phi_1 = \frac{\partial \Pi_1}{\partial p_1} = \frac{(b + 2c_1)(1-d)a + dp_2(b + 2c_1) - 2p_1(b + c_1) + c_2 b}{b^2}, \tag{3.4}$$

$$\phi_2 = \frac{\partial \Pi_2}{\partial p_2} = \frac{(b + 2c_4)(1-d)a + dp_1(b + 2c_4) - 2p_2(b + c_4) + c_5 b}{b^2}. \tag{3.5}$$

Since the interaction takes place under incomplete information, firms cannot always determine the optimal response exactly. They therefore rely on adaptive strategies, such as bounded rationality [10, 12, 51]. In the present framework, both players are assumed to follow boundedly rational rules with homogeneous expectations. Given that each firm only observes a local estimate of its marginal profit ϕ_i, the decision rule is simple: if $\phi_i > 0$, the firm raises its price in the next period, whereas if $\phi_i < 0$, it decreases it. The updating process is formulated as

$$p_1(t+1) = p_1(t) + k_1 p_1(t)\phi_1, \quad p_2(t+1) = p_2(t) + k_2 p_2(t)\phi_2, \tag{3.6}$$

where $k_i > 0$ denotes the adjustment coefficient that controls the speed of reaction of firm i. This multiplicative adjustment implies that price changes are proportional to the current price level, reflecting a relative adjustment mechanism in which firms with a larger market presence or higher price level react more strongly to profit signals than firms operating at lower prices.

Thus, the two-dimensional discrete-time map describing the Bertrand duopoly evolves according to:

$$\begin{cases} p_1(t+1) = \left(1 + k_1 \dfrac{(b+2c_1)(1-d)a + dp_2(b+2c_1) - 2p_1(b+c_1) + c_2 b}{b^2}\right) p_1(t), \\ p_2(t+1) = \left(1 + k_2 \dfrac{(b+2c_4)(1-d)a + dp_1(b+2c_4) - 2p_2(b+c_4) + c_5 b}{b^2}\right) p_2(t). \end{cases} \tag{3.7}$$

In what follows, we will mainly study the case where the two adjustment speeds are almost identical, so that $k_1 \approx k_2$. For simplicity, we take them equal, i.e., $k_1 = k_2 = k$.

3.3 Stability Analysis and Bifurcations

We begin by determining the equilibrium states of system (3.7), this is done by imposing the fixed-point conditions $p_i(t+1) = p_i(t)$. This leads to the nonlinear algebraic system:

$$\begin{cases} \Big((b+2c_1)(1-d)a + dp_2(b+2c_1) - 2p_1(b+c_1) + c_2 b\Big).\, p_1(t) = 0, \\ \Big((b+2c_4)(1-d)a + dp_1(b+2c_4) - 2p_2(b+c_4) + c_5 b\Big).\, p_2(t) = 0. \end{cases} \tag{3.8}$$

Solving (3.8) yields the equilibrium points of system (3.7). They are given by:

$$E_0 = (0, 0),$$

$$E_1 = (0, \overline{p}_2) = \left(0,\ \frac{c_5 b + (1-d)(2c_4 + b)a}{2(c_4 + b)}\right),$$

$$E_2 = (\overline{p}_1, 0) = \left(\frac{c_2 b + (1-d)(2c_1 + b)a}{2(c_1 + b)},\ 0\right),$$

and

$$E_3 = (p_1^*, p_2^*),$$

with

$$p_1^* = \frac{2(c_4+b)\Big[c_2 b + (1-d)(2c_1+b)a\Big] + d(b+2c_1)\Big[c_5 b + (1-d)(2c_4+b)a\Big]}{A_1},$$

$$p_2^* = \frac{2(c_1+b)\Big[c_5 b + (1-d)(2c_4+b)a\Big] + d(b+2c_4)\Big[c_2 b + (1-d)(2c_1+b)a\Big]}{A_1},$$

where $A_1 = 4(b+c_1)(b+c_4) - d^2(b+2c_1)(b+2c_4)$.

The equilibria E_0, E_1, and E_2 are boundary solutions [10] and always exist, since $\overline{p}_1$ and $\overline{p}_2$ are positive for $d<1$. In contrast, E_3, which corresponds to the Nash equilibrium, is feasible only if the following condition is fulfilled:

$$A_1 > 0. \tag{3.9}$$

A local stability analysis of the equilibria is performed by computing the Jacobian matrix of system (3.7). This matrix, evaluated at a generic point (p_1, p_2), linearizes the system and its eigenvalues determine the stability of the equilibrium points. The Jacobian is given by:

$$J(p_1,p_2) = \begin{bmatrix} 1 + k\left(\dfrac{\partial \Pi_1}{\partial p_1} + p_1 \dfrac{\partial^2 \Pi_1}{\partial p_1^2}\right) & kp_1 \dfrac{\partial^2 \Pi_1}{\partial p_1 \partial p_2} \\ kp_2 \dfrac{\partial^2 \Pi_2}{\partial p_2 \partial p_1} & 1 + k\left(\dfrac{\partial \Pi_2}{\partial p_2} + p_2 \dfrac{\partial^2 \Pi_2}{\partial p_2^2}\right) \end{bmatrix}. \tag{3.10}$$

Local asymptotic stability of the equilibrium $E(\overline{p}_1, \overline{p}_2)$ is guaranteed when the absolute value of every eigenvalue from the Jacobian (3.10) is less than one, that is, $|\lambda_i| < 1$ for $i = 1, 2$.

3.3.1 The Stability Analysis of the Boundary Equilibria

Theorem 3.3.1. *At the equilibrium point E_0, the system exhibits repelling behavior, characteristic of an unstable node.*

Proof. Evaluating the Jacobian matrix (3.10) at E_0 yields

$$J(E_0) = \begin{bmatrix} \frac{c_2 b + (1-d)(2c_1+b)a}{b^2}k + 1 & 0 \\ 0 & \frac{c_5 b + (1-d)(2c_4+b)a}{b^2}k + 1 \end{bmatrix}.$$

Thus, the eigenvalues take the form

$$\lambda_1 = \frac{c_2 b + (1-d)(2c_1+b)a}{b^2}k + 1, \quad \lambda_2 = \frac{c_5 b + (1-d)(2c_4+b)a}{b^2}k + 1.$$

Since both $\lambda_1 > 1$ and $\lambda_2 > 1$, it follows that E_0 acts as an unstable repelling node. ■

Theorem 3.3.2. *For any $k > 0$, the boundary equilibrium E_1 is unstable. Specifically, it behaves as a saddle if $k < \frac{b^2}{(b+c_4)\overline{p}_2}$, while it becomes a repelling node whenever $k > \frac{b^2}{(b+c_4)\overline{p}_2}$.*

Proof. At $E_1 = (0, \overline{p}_2)$, the Jacobian matrix (3.10) is

$$J(E_1) = \begin{bmatrix} 1 + k\frac{(2c_1+b)(a(1-d)+d\overline{p}_2) + c_2 b}{b^2} & 0 \\ \frac{k\overline{p}_2 d(b+2c_1)}{b^2} & 1 - \frac{2k\overline{p}_2(b+c_4)}{b^2} \end{bmatrix}.$$

The eigenvalues are obtained as

$$\lambda_1 = 1 + k\frac{(2c_1+b)(a(1-d)+d\overline{p}_2) + c_2 b}{b^2}, \quad \lambda_2 = 1 - \frac{2k\overline{p}_2(b+c_4)}{b^2}.$$

Both are real, and clearly $\lambda_1 > 1$.

- For $k < \frac{b^2}{(b+c_4), \overline{p}_2}$, the eigenvalue λ_2 satisfies $|\lambda_2| < 1$, indicating that the equilibrium E_1 is a saddle point.
- For $k > \frac{b^2}{(b+c_4), \overline{p}_2}$, the eigenvalue λ_2 is less than -1, indicating that the equilibrium E_1 is a repelling node and thus unstable.

■

The equilibrium E_2 admits the same qualitative behavior as E_1, by symmetry.

Economically, boundary equilibria represent cases where one or both firms leave the market, leading to monopoly or complete exit. However, our main focus is the persistence of duopoly. Hence, the local stability of the interior Bertrand–Nash equilibrium E_3 will be the central object of study in the subsequent analysis.

3.3.2 The Stability Analysis of the Nash Equilibrium

The Jacobian matrix at the interior equilibrium $E_3 = (p_1^*, p_2^*)$ is given by

$$J(E_3) = \begin{bmatrix} 1 - \dfrac{2kp_1^*(b+c_1)}{b^2} & \dfrac{kp_1^* d(b+2c_4)}{b^2} \\ \dfrac{kp_2^* d(b+2c_1)}{b^2} & 1 - \dfrac{2kp_2^*(b+c_4)}{b^2} \end{bmatrix} = \begin{bmatrix} j_{11} & j_{12} \\ j_{21} & j_{22} \end{bmatrix}. \tag{3.11}$$

The corresponding characteristic polynomial of (3.11) is

$$P(\lambda) = \lambda^2 - \mathsf{T}\lambda + \mathsf{D}, \tag{3.12}$$

where T and D denote the trace and determinant of $J(p_1^*, p_2^*)$, respectively:

$$\mathsf{T} = 2\left(1 - \frac{kA_2}{b^2}\right),$$

where $A_2 = (b+c_1)p_1^* + (b+c_4)p_2^*$.

$$\mathsf{D} = 1 + \mathsf{T} + \frac{k^2 A_3}{b^4},$$

where $\Big(4(b+c_1)(b+c_4) - d^2(b+2c_1)(b+2c_4)\Big)p_1^* p_2^*$.

Per the Jury stability criterion [30], the Nash equilibrium E_3 is locally stable provided the following sufficient conditions are met:

$$\begin{cases} (i): \ TC = 1 - \mathsf{T} + \mathsf{D} > 0, \\ (ii): \ F = 1 + \mathsf{T} + \mathsf{D} > 0, \\ (iii): \ NS = 1 - \mathsf{D} > 0. \end{cases} \tag{3.13}$$

Failure of any of the three inequalities in (3.13) produces different bifurcation phenomena:

- $TC = 0$: Fold or transcritical bifurcation [10],

- $F = 0$: Flip bifurcation [10],
- $NS = 0$: This condition is necessary for a Neimark-Sacker bifurcation to occur [10, 11].

Rewriting the Jury inequalities, the stability requirements take the form

$$\begin{cases} (i): \ TC = \dfrac{k^2 A_3}{b^4} > 0, \\ (ii): \ F = 4 - \dfrac{4kA_2}{b^2} + \dfrac{k^2 A_3}{b^4} > 0, \\ (iii): \ NS = \dfrac{2kA_2}{b^2} - \dfrac{k^2 A_3}{b^4} > 0. \end{cases} \tag{3.14}$$

From (3.9), condition (i) automatically holds whenever E_3 exists.

Theorem 3.3.3. *Local asymptotic stability of the Nash equilibrium E_3 holds for*

$$k < k_1^f = \frac{4b^2(A_2 - \sqrt{\mathsf{T}^2 - 4\mathsf{D}})}{A_3}$$

and the system (3.7) experiences a period-doubling (flip) bifurcation at E_3 when $k = k_1^f$. Beyond this threshold ($k > k_1^f$), period-2 orbits branch from E_3 and further period-doubling may lead to chaotic dynamics.

Proof. The stability condition (ii) is violated when $F = 0$, leading to a period-doubling (flip) bifurcation. The two corresponding solutions of $F = 0$ are given by

$$k_1^f = \frac{4b^2\left(A_2 - \sqrt{\mathsf{T}^2 - 4\mathsf{D}}\right)}{A_3}, \quad k_2^f = \frac{4b^2\left(A_2 + \sqrt{\mathsf{T}^2 - 4\mathsf{D}}\right)}{A_3}. \tag{3.15}$$

The root of $NS = 0$ is

$$k^N = \frac{4b^2 A_2}{A_3},$$

where $k_1^f < k^N < k_2^f$. The sign variations of F and NS dictate when conditions (3.14) are met, as summarized in Table (3.1).

From Table (3.1), (3.14) holds simultaneously only if $k < k_1^f$. Thus, the Nash equilibrium E_3 is asymptotically stable for $k < k_1^f$, while instability arises for $k > k_1^f$.

At $k = k_1^f$, condition (ii) breaks down with $F(k_1^f) = 0$, leading to a flip bifurcation. For $k > k_1^f$, at least one requirement of (3.14) fails:

- $k_1^f < k < k^N$: $F < 0$.
- $k^N < k < k_2^f$: F and NS both negative.

k	0		k_1^f		k^N		k_2^f	
$F(k)$		$+$	0	$-$		$-$	0	$+$
$NS(k)$		$+$		$+$	0	$-$		$-$
Validity		*Satisfied*			*Not satisfied*			

Table 3.1: Sign diagram of F and NS versus k, showing satisfaction of (3.14).

- $k > k_2^f$: $NS < 0$.

Hence, conditions (3.14) cannot be satisfied across these ranges. Note that at $k = k_2^f$, even though $F = 0$, $NS < 0$, so no flip bifurcation occurs there.

Therefore, for $k > k_1^f$, the system (3.7) develops more complex dynamics, with period-2 cycles and subsequent chaos emanating from E_3. ■

Theorem 3.3.4. *A Neimark-Sacker bifurcation is ruled out at equilibrium E_3.*

Proof. For the polynomial in (3.12), the discriminant is

$$\mathsf{T}^2 - 4\mathsf{D} = \frac{4k^2}{b^4}\left[\left((b+c_1)\,p_1^* - (b+c_4)\,p_2^*\right)^2 + d^2 p_1^* p_2^* \cdot (b+2c_1)\,(b+2c_4)\right] > 0.$$

Even if $NS(k^N) = 0$ (with $F(k^N) < 0$ as well), the positive discriminant ensures that the Jacobian at E_3 has only real eigenvalues. Thus, a Neimark-Sacker bifurcation cannot occur (see [10]). ■

3.4 Visualizing Bifurcations and Quantifying Chaos

This section analyzes bifurcations and the emergence of chaotic dynamics in the Bertrand model (3.7), with a specific focus on the influence of the key parameters: the price adjustment speed k and the product differentiation parameter d. To comprehensively diagnose the system's behavior, we employ a suite of numerical tools:

- **Bifurcation diagrams** show how system states change with parameters.
- **Largest Lyapunov exponent** quantifies chaos (positive value = chaotic).
- **Phase portraits** visualize system trajectories.
- **Basins of attraction** display which initial conditions lead to which final states.

3.4.1 Analyzing Bifurcations and Chaos by Varying the Adjustment Speed k

To investigate the bifurcation and chaotic dynamics of the Bertrand duopoly model, we adopt two representative parameter sets chosen within economically reasonable ranges:

$$(a, c_1, c_2, c_3, c_4, c_5, c_6, d) = (5, 1, 0.75, 1, 0.8, 0.4, 0.5, 0.52), \tag{3.16}$$

$$(a, c_1, c_2, c_3, c_4, c_5, c_6, d) = (3.2, 0.6, 0.5, 1.2, 0.9, 0.7, 1, 0.22). \tag{3.17}$$

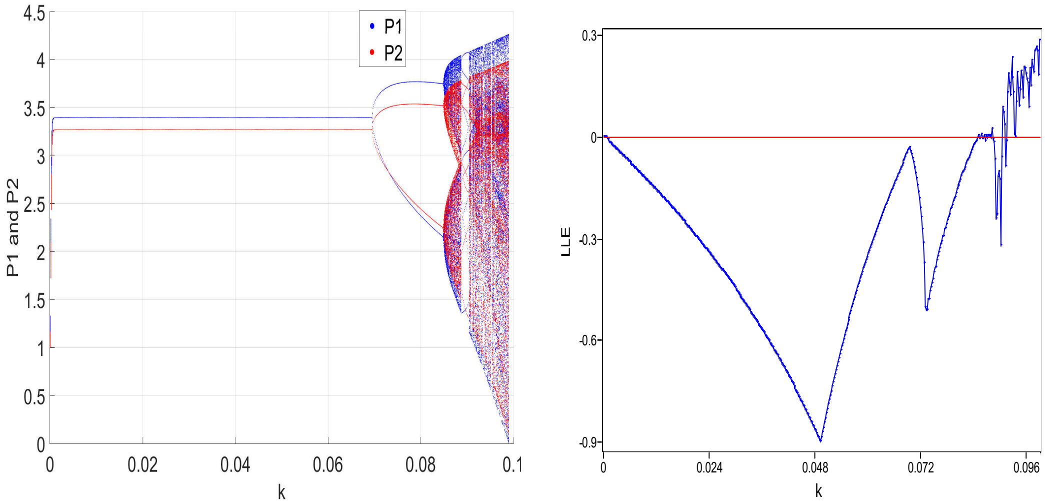

(a) **(b)**

Figure 3.1: (a) Diagram illustrating the bifurcation behavior of system (3.7) as a function of parameter k, computed with the parameter set defined in (3.16). (b) The related largest Lyapunov exponent.

To explore the dynamics of system (3.7), we generate bifurcation diagrams for $k \in (0, 0.1)$ under parameter sets (3.16) and (3.17), together with the largest Lyapunov exponents, shown in Figures (3.1) and (3.2) for a visual representation.

In Figure (3.1a), the Nash equilibrium is stable when $0 < k < k_1^f \approx 0.0695$, but it becomes unstable at the flip bifurcation point $k = k_1^f \approx 0.0695$. Beyond this threshold, successive period-doubling (flip) bifurcations occur, leading to chaotic behavior once the parameter k exceeds the critical value of 0.085. For small k, the firms' prices converge to equilibrium, whereas the positive Lyapunov exponent in Figure (3.1b) confirms chaotic behavior for higher k, in agreement with Theorem 3.3.3.

Similarly, in Figure (3.2a), the equilibrium is stable for $0 < k < k_1^f \approx 0.1902$, but loses stability at $k = k_1^f \approx 0.1902$. Subsequent period-doubling bifurcations lead to chaos for $k > 0.25$. The

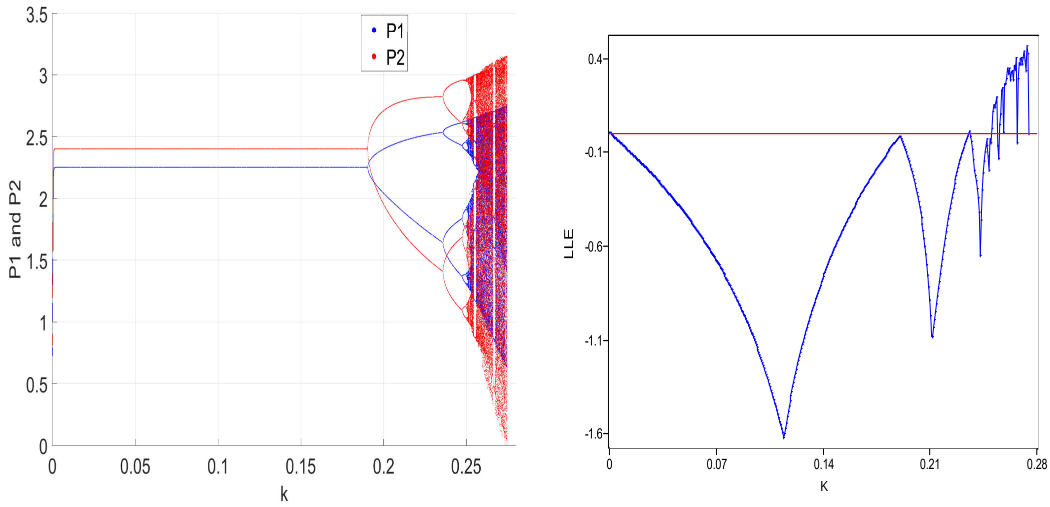

(a) **(b)**

Figure 3.2: (a) Diagram illustrating the bifurcation behavior of system (3.7) as a function of parameter k, computed with the parameter set defined in (3.17). (b) The related largest Lyapunov exponent.

corresponding Lyapunov exponent becomes zero during bifurcation and positive once chaos emerges, as shown in Figure (3.2b). Comparing bifurcation diagrams with their Lyapunov counterparts provides a clearer view of the model's (3.7) nonlinear dynamics.

Two hallmarks of chaos in system (3.7) are the strange attractor and the basin of attraction. These structures reveal the hidden geometry of chaotic states, highlighting order within randomness. Figure (3.6a) shows the phase portrait of system (3.7) for parameter set (3.16) and $k = 0.1$. Meanwhile, Figure (3.3) displays strange attractors for $k = 0.25, 0.256, 0.26$, and 0.273, using the parameter values in (3.17).

In addition, Figure (3.4) illustrates the basins of attraction under the same k values. Here, blue indicates the attraction domain, yellow the escape domain, and red the attractor. These attractors and basins confirm the intricate dynamics of Bertrand duopoly competition in chaotic regimes. Such unpredictable behavior hampers price forecasting, undermines consumer confidence, and complicates firms' strategic planning, potentially forcing weaker firms to exit the market. Resource allocation imbalances further destabilize duopolistic systems.

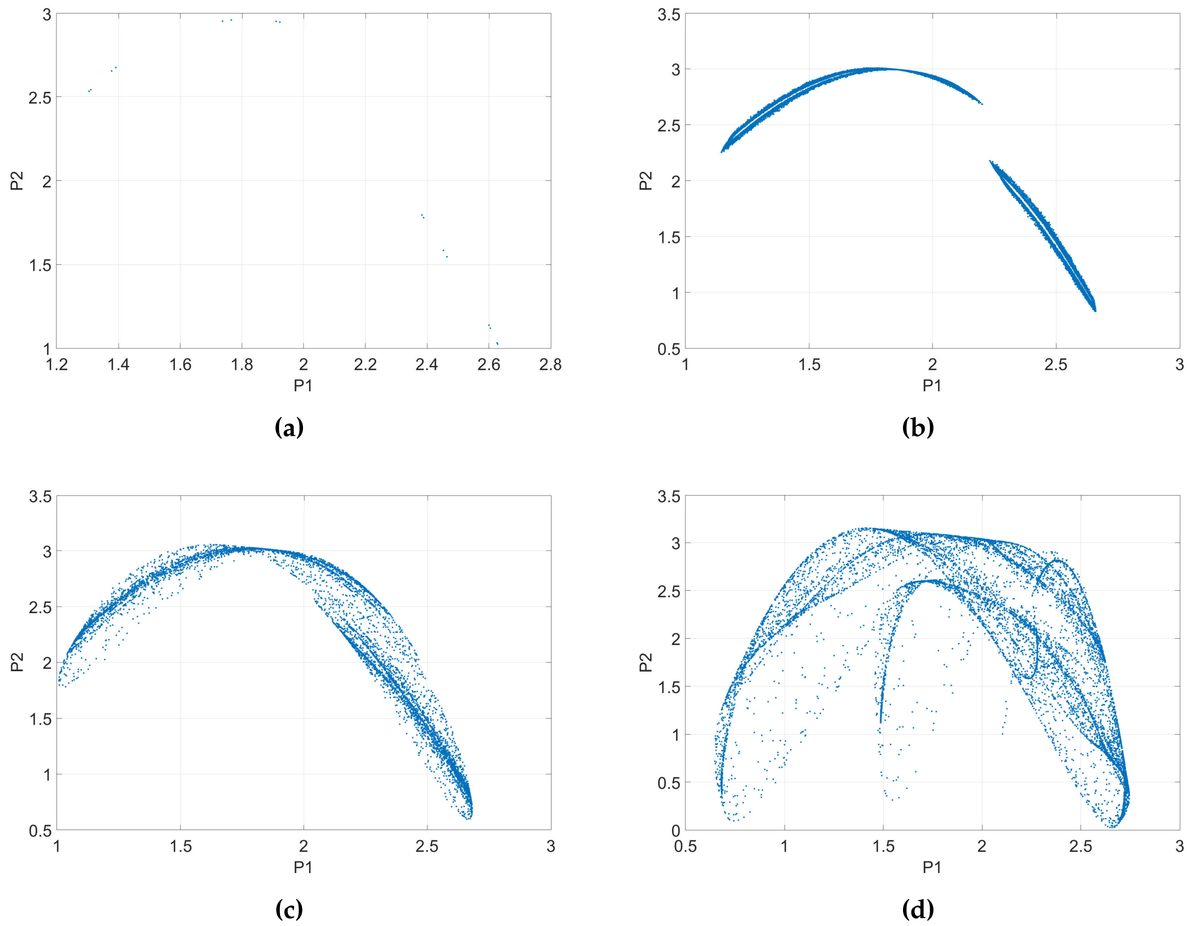

Figure 3.3: Progression of attractor dynamics in system (3.7) across different values of parameter k: (a) $k = 0.25$; (b) $k = 0.256$; (c) $k = 0.26$; (d) $k = 0.273$.

3.4.2 Analyzing Bifurcations and Chaos by Varying the differentiation parameter d

We now explore how the product differentiation parameter $d \in (-1, 1)$ affects the dynamics of system (3.7). For this analysis, we fix the parameters as

$$(\alpha, c_1, c_2, c_3, c_4, c_5, c_6, k) = (3.2, 0.6, 0.5, 1.2, 0.9, 0.7, 1, 0.1), \tag{3.18}$$

and treat d as the bifurcation parameter.

By substituting (3.18) into the stability conditions (ii) and (iii) of (3.14), we obtain:

$$\begin{cases} F = \dfrac{100d^{10}-1038.56d^8+47.84d^7+3362.9525d^6-237.94d^5-4461.03d^4+348.377d^3+2385.268d^2-134.98372d-391.66256}{(d^2-1)^3(25d^4-200d^2+304)}, \\ NS = \dfrac{-(29.44d^8+21.84d^7-261.0475d^6-99.992d^5+771.8763d^4+121.6069d^3-884.7316d^2-19.16372d+301.457344)}{(d^2-1)^3(25d^4-200d^2+304)}. \end{cases}$$

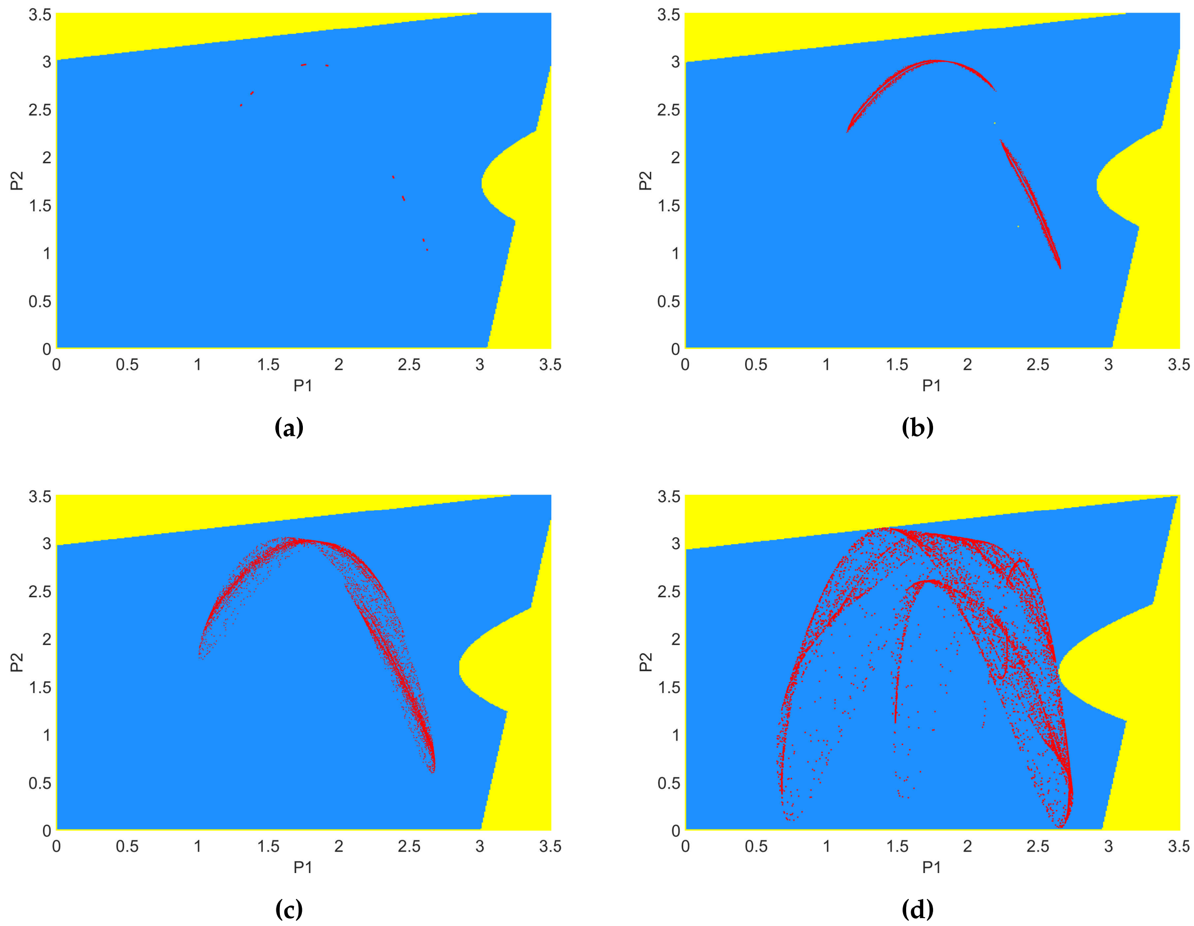

Figure 3.4: Basins of attraction of system (3.7) corresponding to various values of k: (a) $k = 0.25$; (b) $k = 0.256$; (c) $k = 0.26$; (d) $k = 0.273$.

The signs of F and NS determine whether conditions (3.14) are fulfilled. Solving $F(d) = 0$ in $(-1, 1)$ gives four roots: $d_1^f \approx -0.8473$, $d_2^f \approx -0.4920$, $d_3^f \approx 0.5872$, and $d_4^f \approx 0.9147$. Similarly, $NS(d) = 0$ yields two values: $d_1^N \approx -0.7234$ and $d_2^N \approx 0.8287$.

The sign changes of F and NS over $(-1, 1)$, together with the satisfaction of (3.14), are summarized in Table (3.2).

d	-1		d_1^f		d_1^N		d_2^f		d_3^f		d_2^N		d_4^f		1
$F(d)$		$+$	0	$-$		$-$	0	$+$	0	$-$		$-$	0	$+$	
$NS(d)$		$-$		$-$	0	$+$		$+$		$+$	0	$-$		$-$	
Satisfaction					*Not Satisfied*			*satisfied*				*Not satisfied*			

Table 3.2: Sign variation of F and NS in terms of d, and fulfillment of (3.14) for parameters (3.18).

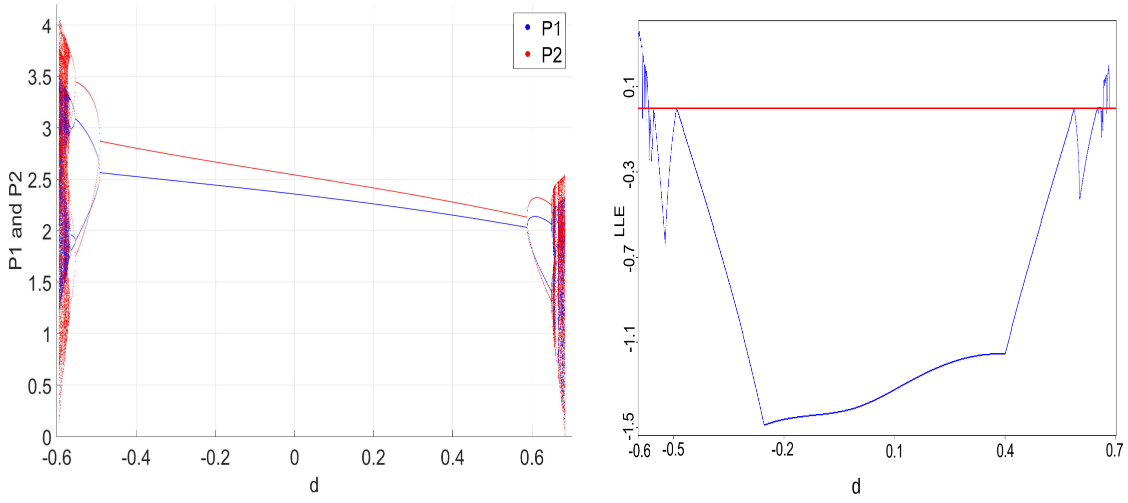

(a) **(b)**

Figure 3.5: (a) Diagram illustrating the bifurcation behavior of system (3.7) as a function of the parameter d. (b) The associated largest Lyapunov exponent.

For $d_2^f < d < d_3^f$, the Nash equilibrium E_3 exhibits asymptotic stability due to the positivity of both F and NS, while condition (3.14) is satisfied. At $d = d_{2,3}^f$, we have $F(d) = 0$, leading to a period-doubling (flip) bifurcation. By contrast, at $d = d_1^f$, d_1^N, d_2^N, and d_4^f, both conditions fail simultaneously, so no bifurcation is expected.

Numerical simulations confirm these results. Figure (3.5) shows the bifurcation diagram for d in the interval (-1,1) along with the Largest Lyapunov Exponent.

From Figure (3.5a), the system is chaotic when d in the interval (-0.6, -0.5675). Period-halving occurs for $-0.5675 < d < -0.4920$, ending at a period-doubling (flip) bifurcation near $d \approx -0.4920$. The system then stabilizes for $d \in (-0.4920, 0.5872)$, with both firms' prices declining. At $d \approx 0.5872$, another flip bifurcation initiates a period-doubling route for $0.5872 < d < 0.6420$, followed by chaos for $0.6420 < d < 0.68$.

The LLE in Figure (3.5b) is consistent with these observations: positive values in $(-0.6, -0.5675)$ confirm chaos, alternating zeros and negatives in $(-0.5675, -0.4920)$ indicate period-halving, and a zero at $d \approx -0.4920$ signals a flip bifurcation. Stability is confirmed by negative LLE in $(-0.4920, 0.5872)$. A zero at $d \approx 0.5872$ again signals a flip bifurcation, leading to period doubling for $(0.5872, 0.6420)$, and chaos for $(0.6420, 0.68)$.

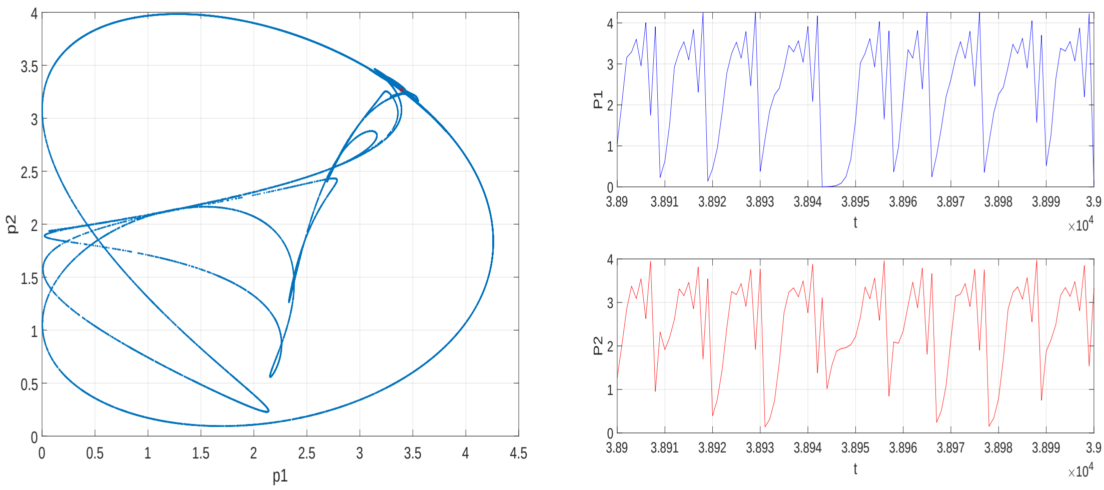

(a) **(b)**

Figure 3.6: (a) Phase trajectory of system (3.7). (b) Time evolution of p_1 exhibiting Mixed-Mode Oscillations (MMOs) of types $1^2 1^2 1^2 1^3$ and $1^2 1^2 1^2 1^3 1^3$ in the (p_1, t) plane.

3.5 Chaotic Behavior and Mixed-Mode Oscillation patterns with variation in k

Mixed-mode oscillations (MMOs) illustrate complex and highly structured dynamical behavior [10, 2]. In such phenomena, each oscillatory cycle generally combines one or more large-amplitude bursts with subsequent smaller peaks. This alternating pattern reflects the delicate balance of nonlinear effects present in the system.

As parameters change, MMOs frequently undergo bifurcations that give rise to additional cycles. Put differently, the oscillatory dynamics become progressively richer as new structures appear within each period, thereby increasing the overall complexity around the Nash equilibrium.

Figure (3.6a) presents a chaotic MMO trajectory for system (3.7) under the parameter set (3.16) with $k = 0.1$. The observed chaotic motion originates from a period-doubling cascade triggered by a flip bifurcation, ultimately producing a periodic orbit.

The irregular trajectory in panel Figure (3.6b), illustrates the system's chaotic nature. It avoids both the equilibrium and the folded singularity, reducing the frequency of large-amplitude epochs until they vanish. This transition leaves only a small-amplitude, indicating that variations in k shift the system from larger oscillations to finer-scale dynamics.

In the time series of Figure (3.6b), each cycle typically includes two or three MMOs with varying small-amplitude maxima and differing numbers of large-amplitude oscillations (LAOs). This highlights the intricate and non-uniform evolution of the system.

Close to the Nash equilibrium, even more elaborate oscillatory patterns appear. Sequential MMOs, denoted L^s, with L denotes the count of large-amplitude oscillations and s represents the number of small-amplitude oscillations, are organized in quasi-repetitive structures such as $L^sL^sL^sL^{s+1}$ or $L^sL^sL^sL^{s+1}L^{s+1}$. For instance, one sequence may look like $1^21^21^21^3$, while others may extend to $1^21^21^21^31^3$. These sequences are not strictly regular, as illustrated in Figure (3.6b).

3.6 Controlling the Instability of the Nash Equilibrium

As the adjustment speed parameter k rises, the system tends to fall into chaotic behavior, which creates serious issues for market stability. In a Bertrand duopoly, the onset of chaos distorts competition, causing unpredictability, instability, and negative outcomes for the economy. Such dynamics weaken consumer trust, hinder firms' long-term planning, and may even drive some firms to exit the market. Because of these harmful consequences, studying approaches to control chaos in economic systems becomes essential. A variety of methods have been developed, such as feedback control [32], adaptive control [29], and the OGY strategy [12, 7], as well as other methods [1, 24, 5, 6, 17, 50].

To address this challenge, we employ state feedback control methodologies [30]. The approach involves introducing a control input $u(t)$ into the system dynamics described in (3.7) and is applied to firm 1 only, which is sufficient to stabilize the system, where the first firm enhances its pricing strategy by integrating historical data from both market participants alongside the target equilibrium values. This control framework allows firms to monitor market deviations systematically and implement calibrated adjustments to maintain pricing stability.

The feedback mechanism operates by continuously comparing current market prices with the desired Nash equilibrium, generating corrective signals that modify the firm's pricing update rule. This ensures that any deviation from equilibrium triggers an appropriate response, gradually steering the system toward stable operation while preserving competitive market dynamics.

The control signal $u(t)$ is specifically formulated as a function of the difference between observed prices and equilibrium values, creating an autonomous self-correcting mechanism. Through continuous adjustment of pricing decisions based on real-time market data, firms can effectively counteract inherent instabilities in the competitive system without requiring external intervention.

This approach transforms unstable price dynamics into a controlled system where chaotic fluctuations are suppressed through strategic feedback. The method enables firms to maintain profitability while ensuring market convergence to the equilibrium, providing both theoretical stability guarantees and practical implementation advantages for real-world pricing systems.

This control method is both efficient and feasible. Firms can rely on computational resources and real-time data to track market evolution and make slight pricing adjustments. Likewise, external regulators may enforce simple price adjustment policies to reduce chaotic swings. Since the control action is minimal, it maintains practicality and adaptability for real applications. Overall, the approach demonstrates how chaos control tools can support stable and predictable competition in markets exposed to chaotic tendencies. The controlled dynamics are given by:

$$\begin{cases} p_1(t+1) = (1+k\phi_1)p_1(t) + u(t), \\ p_2(t+1) = (1+k\phi_2)p_2(t), \end{cases} \tag{3.19}$$

where $u(t)$ takes the form:

$$u(t) = -v_1(p_1(t) - p_1^*) - v_2(p_2(t) - p_2^*), \tag{3.20}$$

with (p_1^*, p_2^*) denoting the Nash equilibrium of (3.7), which remains unchanged in the controlled system (3.19). The constants v_1 and v_2 are the feedback coefficients.

The linearization of the controlled dynamics (3.19) yields the Jacobian matrix J_c, expressed by:

$$J_c(p_1^*, p_2^*) = \begin{pmatrix} j_{11} - v_1 & j_{12} - v_2 \\ j_{21} & j_{22} \end{pmatrix}, \tag{3.21}$$

with $j_{11}, j_{12}, j_{21}, j_{22}$ defined in (3.11).

The associated characteristic polynomial of $J_c(p_1^*, p_2^*)$ takes the form:

$$\lambda^2 - T_c\lambda + D_c = 0, \tag{3.22}$$

where

$$T_c = j_{11} + j_{22} - v_1,$$

$$D_c = j_{22}(j_{11} - v_1) - j_{21}(j_{12} - v_2).$$

We introduce the following coefficients:

$$\begin{cases} \alpha_1 = \frac{J_{22}}{J_{21}}, \quad \beta_1 = \frac{-j_{11}j_{22}+j_{12}j_{21}+1}{J_{21}}, \\ \alpha_2 = \frac{-1+j_{22}}{J_{21}}, \quad \beta_2 = \frac{j_{11}+j_{22}-1-j_{11}j_{22}+j_{12}j_{21}}{J_{21}}, \\ \alpha_3 = \frac{1+j_{22}}{J_{21}}, \quad \beta_3 = \frac{-j_{11}-j_{22}-1-j_{11}j_{22}+j_{12}j_{21}}{J_{21}}, \end{cases} \tag{3.23}$$

under the assumption $d \neq 0$, which guarantees $J_{21} \neq 0$.

Theorem 3.6.1. *The application of control rule (3.20) can stabilize the system (3.7) at its unstable Nash* *equilibrium $E_3 = (p_1^*, p_2^*)$, given the following provisions:*

$$\max\{\alpha_2 v_1 + \beta_2, \alpha_3 v_1 + \beta_3\} < v_2 < \alpha_1 v_1 + \beta_1. \tag{3.24}$$

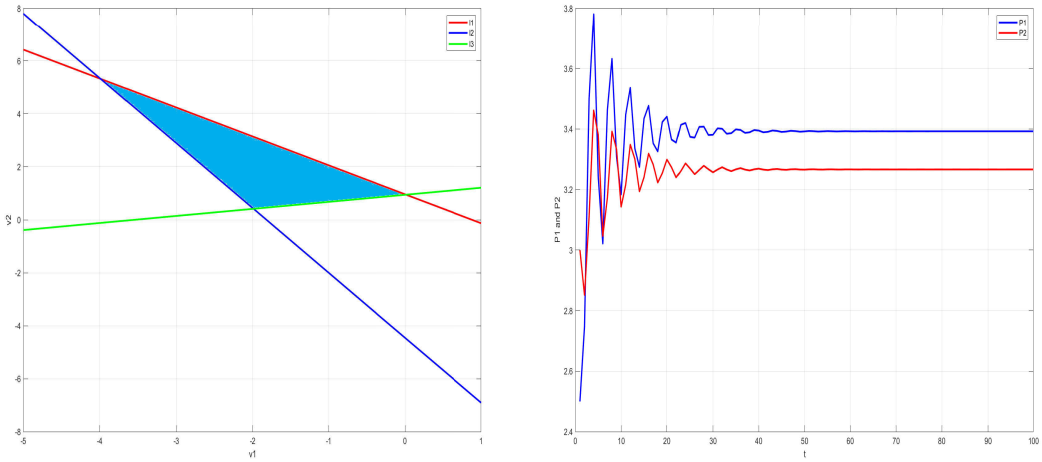

(a) **(b)**

Figure 3.7: (a) Stability domain in the (v_1, v_2) plane of system (3.19) for $k = 0.1$ with the parameter set (3.16). (b) Time evolution of $p_1(t)$ and $p_2(t)$ for system (3.19) using the parameter set (3.16), with $k = 0.1$ and $(v_1, v_2) = (-2, 2.9)$.

Proof.

(i) If $v_2 > \alpha_2 v_1 + \beta_2$, then $1 > -(j_{22}(j_{11} - v_1) - j_{21}(j_{12} - v_2)) + ((j_{11} + j_{22} - v_1)$, yielding $1 + D_c - T_c > 0$.

(ii) If $v_2 > \alpha_3 v_1 + \beta_3$, then $1 > -(j_{22}(j_{11} - v_1) - j_{21}(j_{12} - v_2)) - (j_{11} + j_{22} - v_1)$, implying $1 + D_c + T_c > 0$.

(iii) If $v_2 < \alpha_1 v_1 + \beta_1$, then $1 > j_{22}(j_{11} - v_1) - j_{21}(j_{12} - v_2)$, hence $1 - D_c > 0$.

From (i), (ii), and (iii), the Jury stability conditions [30] follow:

$$\begin{cases} 1 + D_c - T_c > 0, \\ 1 + D_c + T_c > 0, \\ 1 - D_c > 0. \end{cases} \tag{3.25}$$

These inequalities ensure both eigenvalues of (3.21) lie inside the unit circle. Consequently, the Nash equilibrium E_3 becomes locally asymptotically stable, showing that the system (3.7) can be stabilized at its originally unstable state under control law (3.20), provided v_2 satisfies (3.24).
■

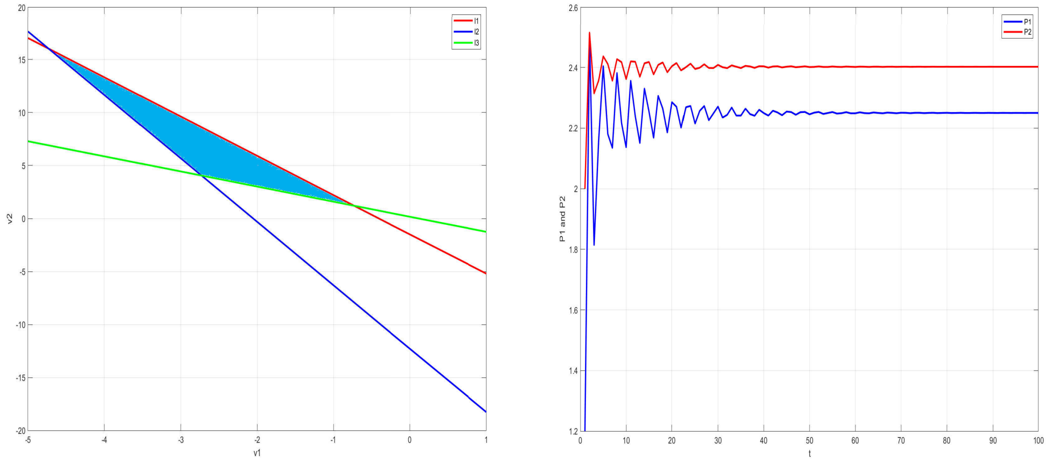

(a) **(b)**

Figure 3.8: (a) Stability domain in the (v_1, v_2) plane of system (3.19) for $k = 0.273$ with the parameter set (3.17). (b) Time evolution of $p_1(t)$ and $p_2(t)$ for system (3.19) using the parameter set (3.17), with $k = 0.273$ and $(v_1, v_2) = (-2, 5)$.

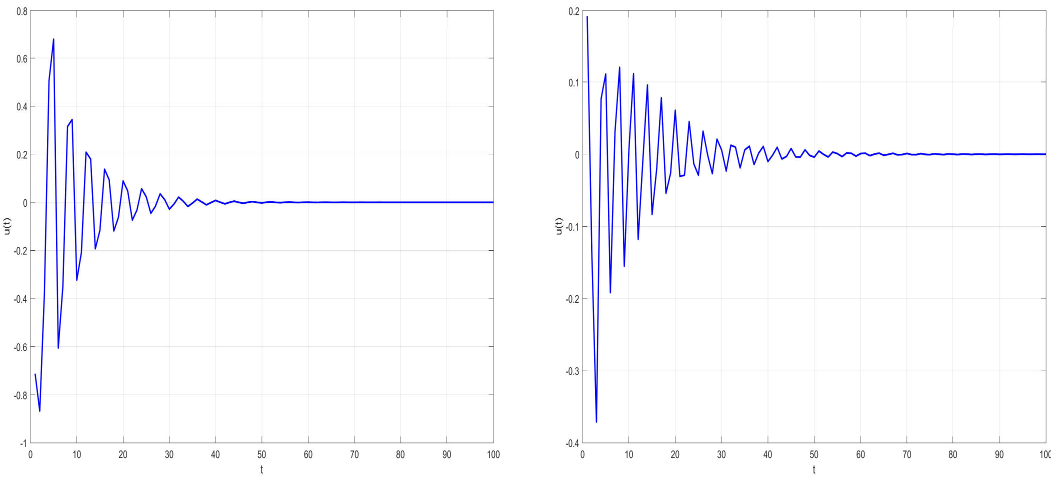

(a) **(b)**

Figure 3.9: Time-dependent behavior of the control force u: (a) linked to Figure (3.7), (b) linked to Figure (3.8).

Condition (3.24) from Theorem 3.6.1 establishes three marginal stability boundaries, forming a triangle in the (v_1, v_2) plane. This triangular region is depicted for two different cases: Figure (3.7a) uses parameter set (3.16) with $k = 0.1$, and Figure (3.8a) uses set (3.17) with

$k = 0.273$. Each line reflects a particular condition relevant to the stability analysis, and their intersections identify transitions between stable and unstable regimes. The triangular area indicates where the system remains stable, while points outside or on its edges suggest instability.

To evaluate how effectively the state feedback control stabilizes the Nash equilibrium, simulations were performed with fixed parameters. In the first case, using (3.16) and $k = 0.1$, the feedback gains were $v_1 = -2$ and $v_2 = 2.9$, with $(p_1(0), p_2(0)) = (2.5, 3.0)$. The stable eigenvalue region is shown in Figure (3.7a). In the second case, with (3.17) and $k = 0.273$, we set $v_1 = -2$ and $v_2 = 5$, with $(p_1(0), p_2(0)) = (1.2, 2.0)$. The stable region is again illustrated in Figure (3.8a). The simulations confirm that chaotic trajectories are successfully driven to the Nash equilibrium, as displayed in Figures (3.7b) and (3.8b). Moreover, the control function u is presented in Figures (3.9a) and (3.9b). These findings highlight the efficiency of state feedback in directing the system towards the desired equilibrium. As stabilization occurs, the control input tends to zero, underscoring its role in maintaining stability.

3.7 Summary and Conclusions

This study investigated the complex dynamics of a Bertrand duopoly game with product differentiation, where firms employ a boundedly rational gradient-based rule for price adjustments under quadratic cost structures. The analysis of the Nash equilibrium's local stability revealed that the market becomes susceptible to instability as firms react more aggressively (higher adjustment speeds) and as products become more distinct. This instability manifests through period-doubling bifurcations, where stable pricing cycles break down into periods of doubling. Numerical simulations confirm that this bifurcation cascade ultimately leads to a regime of chaotic dynamics, characterized by seemingly erratic price fluctuations and mixed-mode oscillations.

To address this market volatility, a state feedback control strategy was designed and proven effective in chaos suppression. The control method successfully stabilizes the system back to its Nash equilibrium, restoring predictable competitive pricing. The efficacy of this control is geometrically defined by three stability boundaries in the parameter space, which form a triangular region of stability. Each line of this triangle corresponds to a critical stability condition for the system, and their collective intersection delineates the precise domain of parameter values, specifically for adjustment speeds and differentiation levels, within which stable, equilibrium behavior is guaranteed.

Chapter 4

Dynamics of a Cournot Triopoly: Bifurcation, Chaos, and Stabilization using the OGY Method under Bounded Rationality.

4.1 Introduction

Oligopoly theory plays a crucial role in mathematical economics by modeling decision-making processes in markets dominated by a few strategic firms [55, 19]. Since the seminal contributions of Cournot [27] and Bertrand [18], dynamic market models have progressively replaced static formulations to reflect real-world economic interactions. In classical models, economic agents were assumed to possess complete market information and perfect rationality. However, modern market dynamics are more accurately described through bounded rationality, where firms adjust production levels using local gradient mechanisms based on marginal profit estimates [20, 4].

When boundedly rational firms update their outputs iteratively, the governing discrete dynamical system often undergoes stability loss. As key parameters such as the speed of adjustment or demand sensitivity exceed critical thresholds, the stable Nash equilibrium destabilizes through local bifurcations [67, 11]. In a Cournot triopoly, the interaction of three competing firms expands the dimensionality of the state space, resulting in period-doubling cascades, Neimark-Sacker bifurcations, and complex deterministic chaos [12, 51].

Although chaotic dynamics illustrate rich economic behavior, unmanaged fluctuations introduce severe market risk and operational instability. Therefore, controlling chaotic trajectories is essential for maintaining predictable equilibrium states. The Ott-Grebogi-Yorke (OGY) feedback control method [56] provides an effective mechanism for stabilizing unstable periodic orbits or steady states by applying small, targeted perturbations to an accessible parameter without altering the underlying game structure [1, 10].

This chapter investigates the three-dimensional dynamic behavior of a Cournot triopoly game under bounded rationality and linear costs. First, we establish the existence and local stability conditions for the interior Nash equilibrium. Second, we analyze the local and global bifurcation routes to chaos. Finally, we implement the OGY control scheme to eliminate chaotic oscillations and stabilize the market equilibrium.

4.2 The Cournot Triopoly Game Model

We consider a market with three competing firms indexed by $i = 1, 2, 3$, each producing a homogeneous product. Production decisions are made at discrete time steps $t = 0, 1, 2, \ldots$. The output of firm i at time t is denoted by $q_i(t)$, and the corresponding production cost is given by $C_i(q_i(t))$. The price $p_i(t)$ of each firm depends on the total market supply $Q(t) = \sum_{i=1}^{3} q_i(t)$, and follows the inverse demand functions:

$$\begin{aligned} p_1(t) &= 1 + a_1 q_2(t) + b_1 q_3(t) - q_1(t), \\ p_2(t) &= 1 + a_2 q_1(t) + b_2 q_3(t) - q_2(t), \\ p_3(t) &= 1 + a_3 q_1(t) + b_3 q_2(t) - q_3(t), \end{aligned} \tag{4.1}$$

where the constants $a_i, b_i > 0$ $(i = 1, 2, 3)$ capture the cross-effects of product substitution among the firms. Each firm is assumed to operate under a linear cost structure:

$$C_i\left(q_i(t)\right) = c_i q_i(t), \quad i = 1, 2, 3, \tag{4.2}$$

with $c_i > 0$ representing the marginal cost of production. Hence, the profit of each firm at time t can be written as

$$\begin{aligned} \pi_1(t) &= (1 - c_1 - q_1(t) + a_1 q_2(t) + b_1 q_3(t)) \cdot q_1(t), \\ \pi_2(t) &= (1 - c_2 - q_2(t) + a_2 q_1(t) + b_2 q_3(t)) \cdot q_2(t), \\ \pi_3(t) &= (1 - c_3 - q_3(t) + a_3 q_1(t) + b_3 q_2(t)) \cdot q_3(t). \end{aligned}$$

The marginal profits take the form

$$\begin{aligned}
\frac{\partial \pi_1(t)}{\partial q_1} &= 1 - c_1 - 2q_1(t) + a_1 q_2(t) + b_1 q_3(t), \\
\frac{\partial \pi_2(t)}{\partial q_2} &= 1 - c_2 - 2q_2(t) + a_2 q_1(t) + b_2 q_3(t), \\
\frac{\partial \pi_3(t)}{\partial q_3} &= 1 - c_3 - 2q_3(t) + a_3 q_1(t) + b_3 q_2(t).
\end{aligned} \tag{4.3}$$

The model assumes that firms behave with bounded rationality [10, 11]. In this setting, none of the producers has full knowledge of the market, and they instead adaptively update their strategies according to local estimates of marginal profit. The adjustment mechanism in this repeated Cournot triopoly is described as

$$q_i(t+1) - q_i(t) = k_i q_i(t) \frac{\partial \pi_i(q_1, q_2, q_3)}{\partial q_i(t)}, \quad i = 1, 2, 3, \tag{4.4}$$

where $k_i > 0$ reflects the relative adjustment speed of firm i.

By combining equations (4.3) and (4.4), one obtains the core three-dimensional discrete-time system that models the dynamics of a symmetric Cournot triopoly:

$$\begin{cases}
q_1(t+1) = [1 + k_1 (1 - 2q_1(t) + a_1 q_2(t) + b_1 q_3(t) - c_1)] \, q_1(t), \\
q_2(t+1) = [1 + k_2 (1 - 2q_2(t) + a_2 q_1(t) + b_2 q_3(t) - c_2)] \, q_2(t), \\
q_3(t+1) = [1 + k_3 (1 - 2q_3(t) + a_3 q_1(t) + b_3 q_2(t) - c_3)] \, q_3(t).
\end{cases} \tag{4.5}$$

The dynamic properties of system (4.5) are analyzed in the subsequent section.

4.3 Analysis of Equilibrium Points and Their Local Stability

To determine the equilibrium states of the dynamic Cournot triopoly, we impose the condition $q_i(t+1) = q_i(t)$ for each firm $i = 1, 2, 3$ in map (4.5). The equilibrium outputs are thus obtained from the nonnegative solutions of the following algebraic equations:

$$\begin{cases}
q_1(t) \, (1 - c_1 - 2q_1(t) + a_1 q_2(t) + b_1 q_3(t)) = 0, \\
q_2(t) \, (1 - c_2 - 2q_2(t) + a_2 q_1(t) + b_2 q_3(t)) = 0, \\
q_3(t) \, (1 - c_3 - 2q_3(t) + a_3 q_1(t) + b_3 q_2(t)) = 0.
\end{cases} \tag{4.6}$$

System (4.6) yields eight possible equilibrium points:

$$
\begin{aligned}
E_0 &= (0,0,0)\,,\\
E_1 &= \left(\tfrac{1-c_1}{2},0,0\right), \quad E_2 = \left(0,\tfrac{1-c_2}{2},0\right), \quad E_3 = \left(0,0,\tfrac{1-c_3}{2}\right),\\
E_4 &= \left(0,\ \frac{b_2-2c_2-b_2c_3+2}{4-b_2b_3},\ \frac{b_3-2c_3-b_3c_2+2}{4-b_2b_3}\right),\\
E_5 &= \left(\frac{b_1-2c_1-b_1c_3+2}{4-a_3b_1},\ 0,\ \frac{a_3-2c_3-a_3c_1+2}{4-a_3b_1}\right),\\
E_6 &= \left(\frac{a_1-2c_1-a_1c_2+2}{4-a_1a_2},\ \frac{a_2-2c_2-a_2c_1+2}{4-a_1a_2},\ 0\right),\\
E^* &= \left(q^*_{7,1},q^*_{7,2},q^*_{7,3}\right).
\end{aligned}
$$

Here, the interior Nash equilibrium E^* is explicitly given by

$$
\begin{cases}
q^*_{7,1} = \frac{2a_1+2b_1-4c_1+a_1b_2-2a_1c_2+b_1b_3-b_2b_3-2b_1c_3-a_1b_2c_3-b_1b_3c_2+b_2b_3c_1+4}{8-2a_1a_2-2a_3b_1-2b_2b_3-a_1a_3b_2-a_2b_1b_3},\\
q^*_{7,2} = \frac{2a_2+2b_2-4c_2+a_2b_1-a_3b_1+a_3b_2-2a_2c_1-2b_2c_3-a_2b_1c_3+a_3b_1c_2-a_3b_2c_1+4}{8-2a_1a_2-2a_3b_1-2b_2b_3-a_1a_3b_2-a_2b_1b_3},\\
q^*_{7,3} = \frac{2a_3+2b_3-4c_3-a_1a_2+a_1a_3+a_2b_3-2a_3c_1-2b_3c_2+a_1a_2c_3-a_1a_3c_2-a_2b_3c_1+4}{8-2a_1a_2-2a_3b_1-2b_2b_3-a_1a_3b_2-a_2b_1b_3}.
\end{cases}
$$

Thus, $E_0,\dots,E_6$ correspond to boundary equilibria, while E^* is the interior Nash equilibrium. The feasibility of equilibria E_1,E_2,E_3 requires

$$
c_i < 1, \quad i = 1,2,3. \tag{4.7}
$$

Similarly, E_4,E_5,E_6 are admissible if

$$
\begin{cases}
c_i < 1, \quad i = 1,2,3,\\
4-b_2b_3 > 0, \quad 4-a_3b_1 > 0, \quad 4-a_1a_2 > 0.
\end{cases} \tag{4.8}
$$

To assess the local stability of equilibria, we compute the Jacobian of system (4.5) at any state $(q_1(t),q_2(t),q_3(t))$, which is given by

$$
\begin{pmatrix}
J_{j,1} & k_1a_1q^*_{j,1} & k_1b_1q^*_{j,1}\\
k_2a_2q^*_{j,2} & J_{j,2} & k_2b_2q^*_{j,2}\\
k_3a_3q^*_{j,3} & k_3b_3q^*_{j,3} & J_{j,3}
\end{pmatrix}, \tag{4.9}
$$

with

$$\begin{cases} J_{j,1} = 1 + k_1\Big(1 + a_1 q_{j,2} - 4q_{j,1} - c_1 + b_1 q_{j,3}\Big), \\ J_{j,2} = 1 + k_2\Big(1 + a_2 q_{j,1} - 4q_{j,2} - c_2 + b_2 q_{j,3}\Big), \\ J_{j,3} = 1 + k_3\Big(1 + a_3 q_{j,1} - 4q_{j,3} - c_3 + b_3 q_{j,2}\Big). \end{cases}$$

The local stability of the system's equilibria depends critically on the eigenvalues of (4.9) evaluated at these points.

4.3.1 Local Stability of Boundary Equilibria

Theorem 4.3.1. *The origin E_0 acts as a repelling node whenever condition (4.7) holds.*

Proof. At $E_0 = (0,0,0)$, the Jacobian reduces to

$$\begin{pmatrix} 1 + k_1(1 - c_1) & 0 & 0 \\ 0 & 1 + k_2(1 - c_2) & 0 \\ 0 & 0 & 1 + k_3(1 - c_3) \end{pmatrix},$$

whose eigenvalues are $\lambda_i = 1 + k_i(1 - c_i),\ i = 1,2,3$. From (4.7), we observe that $|\lambda_i| > 1$, hence E_0 is unstable (repelling). ■

Theorem 4.3.2. *If E_1, E_2, E_3 are feasible and $k_i > \frac{2}{1-c_i}$ for $i = 1,2,3$, then each of these boundary equilibria is a repelling node.*

Proof. At $E_1 = (\frac{1-c_1}{2}, 0, 0)$, the Jacobian is

$$\begin{pmatrix} 1 - k_1(1 - c_1) & \frac{a_1 k_1 (1-c_1)}{2} & \frac{b_1 k_1 (1-c_1)}{2} \\ 0 & 1 + k_2\left(1 + \frac{a_2(1-c_1)}{2} - c_2\right) & 0 \\ 0 & 0 & 1 + k_3\left(1 + \frac{a_3(1-c_1)}{2} - c_3\right) \end{pmatrix}.$$

The eigenvalues are $\lambda_1 = 1 - k_1(1 - c_1),\ \lambda_2 = 1 + k_2(1 + \frac{a_2(1-c_1)}{2} - c_2),\ \lambda_3 = 1 + k_3(1 + \frac{a_3(1-c_1)}{2} - c_3)$. Clearly, $\lambda_2, \lambda_3 > 1$, and if $k_1 > \frac{2}{1-c_1}$ then $|\lambda_1| > 1$. Therefore, E_1 is unstable. Analogous reasoning applies to E_2 and E_3. ■

Theorem 4.3.3. *Boundary equilibria E_4, E_5, E_6 of system (4.5) are unstable under condition (4.8).*

Proof. At $E_4 = (0, q^*_{4,2}, q^*_{4,3})$, the Jacobian becomes

$$\begin{pmatrix} 1 + k_1(1 + a_1 q^*_{4,2} - c_1 + b_1 q^*_{4,3}) & 0 & 0 \\ k_2 a_2 q^*_{4,2} & 1 + k_2(1 - 4q^*_{4,2} - c_2 + b_2 q^*_{4,3}) & k_2 b_2 q^*_{4,2} \\ k_3 a_3 q^*_{4,3} & k_3 b_3 q^*_{4,3} & 1 + k_3(1 - 4q^*_{4,3} - c_3 + b_3 q^*_{4,2}) \end{pmatrix},$$

with $q^*_{4,2} = \frac{b_2-2c_2-b_2c_3+2}{4-b_2b_3}$ and $q^*_{4,3} = \frac{b_3-2c_3-b_3c_2+2}{4-b_2b_3}$.

The eigenvalues include $\lambda_1 = 1+k_1(1+a_1q^*_{4,2}-c_1+b_1q^*_{4,3})$. Since $1-c_1 > 0$ by (4.8), it follows that $\lambda_1 > 1$, hence E_4 is unstable. The same logic confirms instability of E_5 and E_6. ■

4.3.2 Analyzing the Nash Equilibrium's Local Stability

The stability of the Nash equilibrium E^* is now examined. To this end, we compute the Jacobian matrix (4.9) at E^*, yielding the following form, which characterizes the system's response to small perturbations:

$$\begin{pmatrix} J^*_{7,1} & k_1a_1q^*_{7,1} & k_1b_1q^*_{7,1} \\ k_2a_2q^*_{7,2} & J^*_{7,2} & k_2b_2q^*_{7,2} \\ k_3a_3q^*_{7,3} & k_3b_3q^*_{7,3} & J^*_{7,3} \end{pmatrix}, \tag{4.10}$$

where

$$\begin{cases} J^*_{7,1} = 1 + k_1\left(1 + a_1q^*_{7,2} - 4q^*_{7,1} - c_1 + b_1q^*_{7,3}\right), \\ J^*_{7,2} = 1 + k_2\left(1 + a_2q^*_{7,1} - 4q^*_{7,2} - c_2 + b_2q^*_{7,3}\right), \\ J^*_{7,3} = 1 + k_3\left(1 + a_3q^*_{7,1} - 4q^*_{7,3} - c_3 + b_3q^*_{7,2}\right). \end{cases}$$

The characteristic polynomial associated with (4.10) is expressed as

$$f(\lambda) = \lambda^3 + R_2\lambda^2 + R_1\lambda + R_0, \tag{4.11}$$

where the coefficients are

$$\begin{aligned} R_2 =& - J^*_{7,1} - J^*_{7,2} - J^*_{7,3}, \\ R_1 =& J^*_{7,1}J^*_{7,2} + J^*_{7,1}J^*_{7,3} + J^*_{7,2}J^*_{7,3} - a_1a_2k_1k_2q^*_{7,1}q^*_{7,2} - a_3b_1k_1k_3q^*_{7,1}q^*_{7,3} - b_2b_3k_2k_3q^*_{7,2}q^*_{7,3}, \\ R_0 =& - J^*_{7,1}J^*_{7,2}J^*_{7,3} + J^*_{7,3}a_1a_2k_1k_2q^*_{7,1}q^*_{7,2} + J^*_{7,2}a_3b_1k_1k_3q^*_{7,1}q^*_{7,3} + J^*_{7,1}b_2b_3k_2k_3q^*_{7,2}q^*_{7,3} \\ & - a_1a_3b_2k_1k_2k_3q^*_{7,1}q^*_{7,2}q^*_{7,3} - a_2b_1b_3k_1k_2k_3q^*_{7,1}q^*_{7,2}q^*_{7,3}. \end{aligned}$$

According to [35], local stability of the Nash equilibrium $E^*$is guaranteed if and only if the following Jury conditions are satisfied:

$$\begin{cases} (i) : 1 + R_2 + R_1 + R_0 > 0, \\ (ii) : 1 - R_2 + R_1 - R_0 > 0, \\ (iii) : 1 - R_1 + R_2R_0 - R_0^2 > 0, \\ (iv) : |R_0| < 1. \end{cases} \tag{4.12}$$

The economic interpretation of these conditions is closely tied to bifurcation theory. Specifically: - Condition (i) corresponds to the presence of the eigenvalue +1, typically associated with saddle-node, pitchfork, or transcritical bifurcations. - Condition (ii) relates to an eigenvalue at -1, which triggers a flip (period-doubling) bifurcation. - Condition (iii) is linked to the case of complex conjugate eigenvalues crossing the unit circle, leading to a Neimark-Sacker bifurcation. - Condition (iv) simply requires that the product of the three eigenvalues satisfies $|R_0| < 1$.

In practice, since (iv) always holds when the first three inequalities are satisfied, stability analysis usually focuses on conditions (i)-(iii).

Moreover, condition (i) in (4.12) is always valid. Thus, bifurcations of fold or pitchfork type cannot occur. More explicitly,

$$(i): J^*_{7,1}(J^*_{7,2}-1)+J^*_{7,2}(J^*_{7,3}-1)+J^*_{7,3}(J^*_{7,1}-1)-J^*_{7,1}J^*_{7,2}J^*_{7,3}+J^*_{7,3}(1-a_1a_2k_1k_2q^*_{7,1}q^*_{7,2})$$

$$+J^*_{7,2}(1-a_3b_1k_1k_3q^*_{7,1}q^*_{7,3})+J^*_{7,1}(1-b_2b_3k_2k_3q^*_{7,2}q^*_{7,3})+k_1k_2k_3q^*_{7,1}q^*_{7,2}q^*_{7,3}(-a_1a_3b_2-a_2b_1b_3)>0.$$

Theorem 4.3.4. *The Cournot-Nash equilibrium E^* loses stability when $k_1 = k^f$, at which point system (4.5) undergoes a flip bifurcation. For $k_1 > k^f$, a stable period-2 orbit bifurcates from E^*.*

$$k^f = \frac{-2D_1}{D_1D_2 + (D_3 + D_4)q^*_{7,1}}, \tag{4.13}$$

with

$$D_1 = 1 + J^*_{7,2} + J^*_{7,3} + J^*_{7,2}J^*_{7,3} - b_2b_3k_2k_3q^*_{7,2}q^*_{7,3}, \quad D_2 = a_1q^*_{7,2} - 4q^*_{7,1} - c_1 + b_1q^*_{7,3} + 1,$$

$$D_3 = -a_1a_2k_2q^*_{7,2} - a_3b_1k_3q^*_{7,3} - J_3a_1a_2k_2q^*_{7,2}, \qquad D_4 = -J_2a_3b_1k_3q^*_{7,3} + a_1a_3b_2k_2k_3q^*_{7,2}q^*_{7,3} + a_2b_1b_3k_2k_3q^*_{7,2}q^*_{7,3}.$$

Proof. A flip bifurcation arises when condition (ii) in (4.12) is violated, i.e., when $1 - R_2 + R_1 - R_0 = 0$. Solving this equality for k_1 yields $k_1 = k^f$. Therefore, E^* is destabilized through a period-doubling bifurcation at this critical parameter value, and for $k_1 > k^f$ the system admits a stable 2-cycle. ■

Theorem 4.3.5. *Consider the discriminant of the cubic polynomial (4.11) [23]:*

$$\Delta = 18ABC - 4B^3 + B^2A^2 - 4A^3C - 27C^2.$$

1. *If $\Delta > 0$, the polynomial has three distinct real roots.*
2. *If $\Delta = 0$, multiple roots exist (at least two coincide), thus a Neimark-Sacker bifurcation cannot occur.*

3. *If* $\Delta < 0$*, one real root and a complex conjugate pair exist, allowing a Neimark-Sacker bifurcation at* E^{*}*.*

Proof. The proof follows standard results on cubic discriminants; for details, see Appendix A in [12]. ∎

4.4 Bifurcation and Chaos

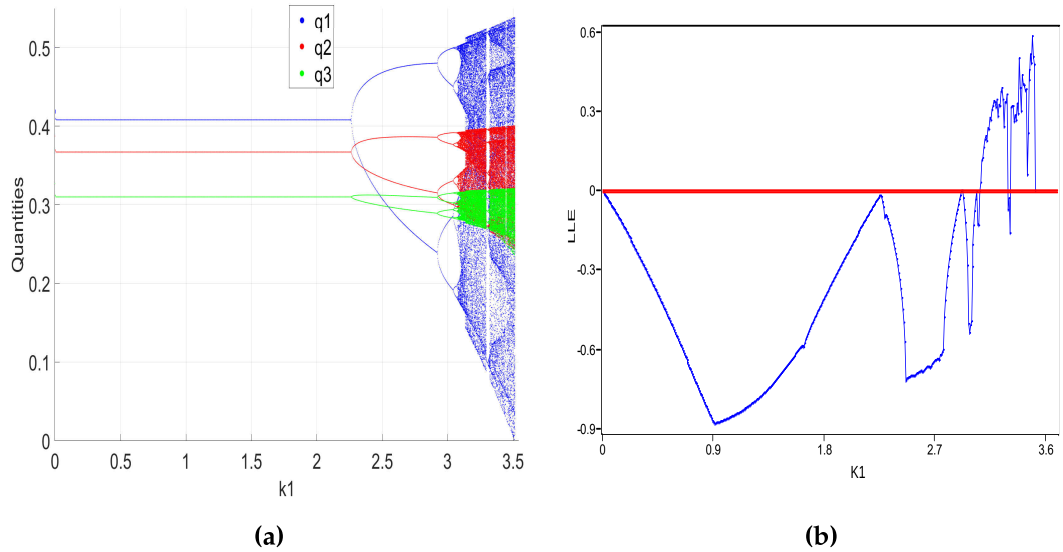

Figure 4.1: (a) Bifurcation diagram of system (4.5) with respect to k_1, for the parameter set in (4.14). (b) The associated LLE corresponding to (4.1a).

This section investigates the influence of the key parameters, the adjustment speed k_1 and the demand intercept a_1, on the complex dynamics of the system while holding all other parameters constant. To systematically explore this relationship, we employ numerical simulations by varying one parameter and observing the resulting evolutionary path of the system. The analysis is primarily visualized through bifurcation diagrams, which reveal qualitative changes in system behavior, and the corresponding *largest Lyapunov exponent* (LLE), which quantitatively distinguishes between periodic dynamics (negative LLE) and chaotic regimes (positive LLE). Furthermore, we identify and characterize the emergence of *strange chaotic attractors*, which signify a regime of bounded, deterministic, yet seemingly random motion within the system.

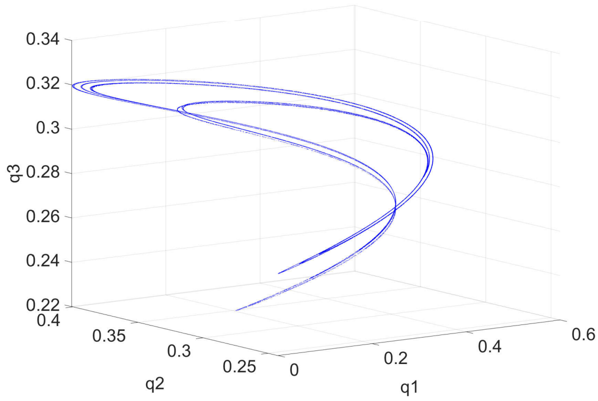

Figure 4.2: Chaotic attractor of system (4.5) when $k_1 = 3.5$.

4.4.1 Flip Bifurcation Around the Nash Equilibrium with Respect to k_1

Figure (4.1) investigates the influence of varying the parameter $k_1 \in (0, 3.5)$, with all other parameters fixed as:

$$\begin{aligned} a_1 = 0.4, \quad a_2 = 0.38, \quad a_3 = 0.3, \quad b_1 = b_2 = b_3 = 0.32, \\ c_1 = 0.43, \quad c_2 = 0.52, \quad c_3 = 0.62, \quad k_2 = 1.8, \quad k_3 = 1.5. \end{aligned} \tag{4.14}$$

The results indicate that the firms' outputs remain stable at the Nash equilibrium for $0 < k_1 < k^f = 2.2695$. Beyond this point, stability is lost and the system experiences a period-doubling route to chaos, a classic pathway where stable oscillations successively double in period before breaking down into deterministic chaos. The LLE is used to confirm these transitions. Figure (4.2) illustrates a chaotic attractor for $k_1 = 3.5$.

4.4.2 Neimark-Sacker Bifurcation Around the Nash Equilibrium with Respect to k_1

We now demonstrate a Neimark-Sacker bifurcation around the Cournot-Nash equilibrium of system (4.5). From Theorem 4.3.5, if $\Delta < 0$, complex conjugate eigenvalues arise, triggering such bifurcations. Solving equation (iii) in (4.12), namely $1 - B + AC - C^2 = 0$, yields $k_n = 1.025$. The other parameters are

$$\begin{aligned} a_1 = 0.79, \quad a_2 = 0.1, \quad a_3 = 0.7, \quad b_1 = 0.7, \quad b_2 = 0.72, \quad b_3 = 0.21, \\ c_1 = 0.5, \quad c_2 = 0.45, \quad c_3 = 0.45, \quad k_2 = 1.7, \quad k_3 = 1.43, \end{aligned} \tag{4.15}$$

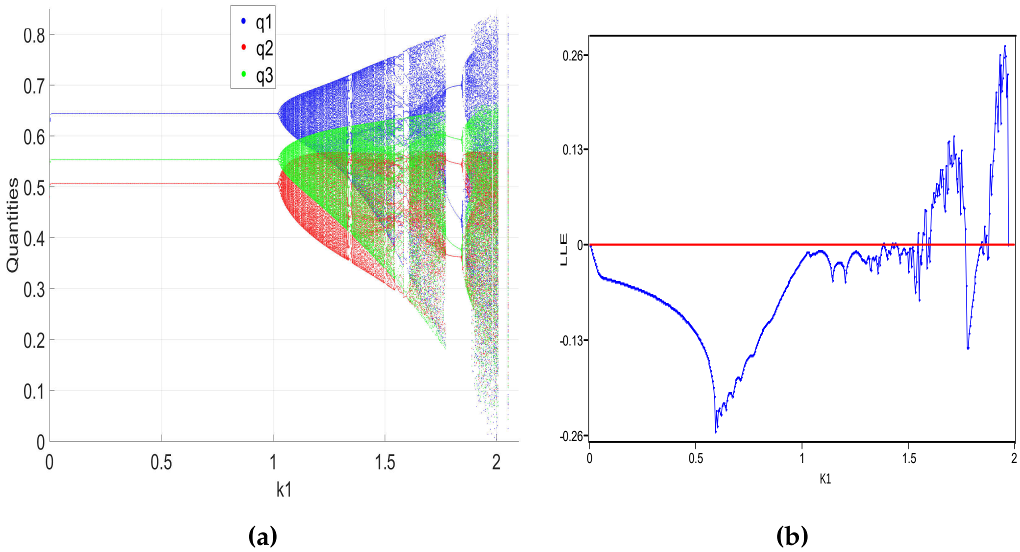

Figure 4.3: (a) Bifurcation diagram of system (4.5) with respect to k_1, under the parameters in (4.15). (b) Corresponding LLE of (4.3a).

and give $\Delta = -0.83 < 0$. The eigenvalues of the characteristic polynomial are $\lambda_1 = -0.9542 - 0.2775i$, $\lambda_2 = -0.9542 + 0.2775i$, and $\lambda_3 = 0.2955$. Their magnitudes, $|\lambda_{1,2}| = 1$ and $|\lambda_3| = 0.2955$, confirm a Neimark-Sacker bifurcation at $E^* = (0.6406, 0.5058, 0.5523)$.

For these parameter values, conditions (i)-(iv) in (4.12) are satisfied when $k_1 < k_n$. Once $k_1 > k_n$, the third condition fails, so the Nash equilibrium becomes unstable. Hence, the system transitions into chaotic dynamics beyond the critical value $k_n = 1.025$.

Figure (4.3) shows that the system (4.5) is stable for $k_1 < 1.025$, but becomes unstable at $k_1 = 1.025$, where a Neimark-Sacker bifurcation emerges. As depicted in Figure (4.3b), a zero LLE corresponds to quasi periodicity, while positive LLE values indicate chaos.

In Figure (4.4), several phase portraits are plotted in three-dimensional space (q_1, q_2, q_3) under different adjustment speeds. The invariant cycle in (4.4a) evolves into double chaotic attractors (4.4b), and then into fractal strange attractors (4.4c). The basin of attraction is also presented in (4.4d).

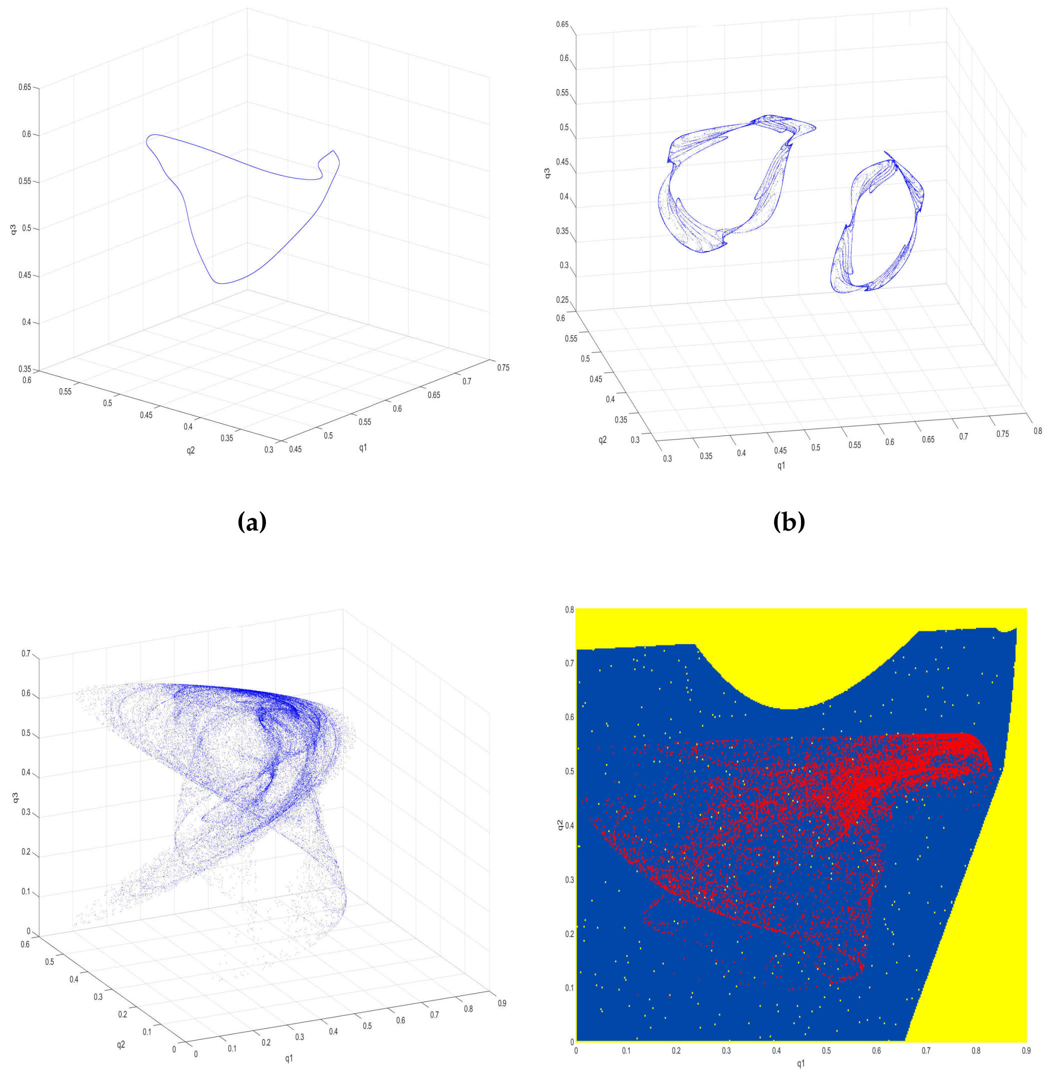

(a) **(b)**

(c) **(d)**

Figure 4.4: Evolution of attractors in system (4.5): (a) a smooth invariant cycle for $k_1 = 1.35$, (b) two chaotic attractors for $k_1 = 1.88$, (c) fractal-like attractor for $k_1 = 1.96$, (d) basin of attraction of the triopoly map in the $q_1 - q_2$ plane with $q_3 = 0.43$ when $k_1 = 1.96$.

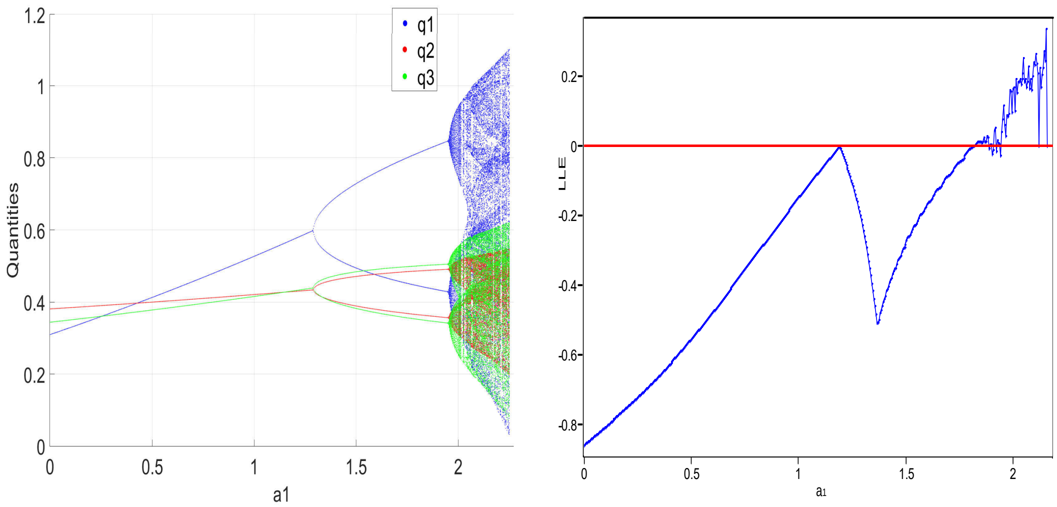

(a) **(b)**

Figure 4.5: (a) Bifurcation diagram of system (4.5) with respect to a_1. (b) The corresponding LLE for (4.5a).

4.4.3 Bifurcation and Lyapunov Exponent with Respect to the Substitution Parameter a_1

Figure (4.5) presents the bifurcation diagram and LLE with respect to $a_1 \in (0, 2.26)$ for the parameter set:

$$\begin{aligned} a_2 = 0.3, \quad a_3 = 0.6, \quad b_1 = 0.2, \quad b_2 = 0.2, \quad b_3 = 0.32, c_1 = 0.45, \\ c_2 = 0.4, \quad c_3 = 0.62, \quad k_1 = 1.3, \quad k_2 = 1.8, \quad k_3 = 1.5. \end{aligned} \tag{4.16}$$

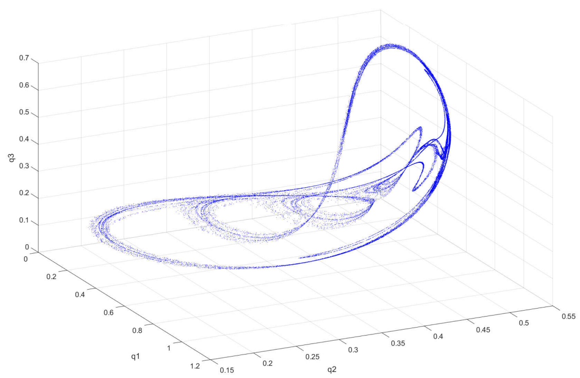

Figure 4.6: Chaotic attractor of system (4.5) for $a_1 = 2.24$.

The diagram in (4.5a) shows that the system (4.5) is stable for $0 \leq a_1 \leq 1.29$. As a_1 grows, firms' output quantities increase significantly, until a flip bifurcation occurs for $a_1 > 1.29$, producing chaotic oscillations. The LLE plot (4.5b) supports this by displaying stable, periodic, and chaotic phases, showing loss of stability of the Nash equilibrium. Figure (4.6) shows a strange attractor when $a_1 = 2.24$.

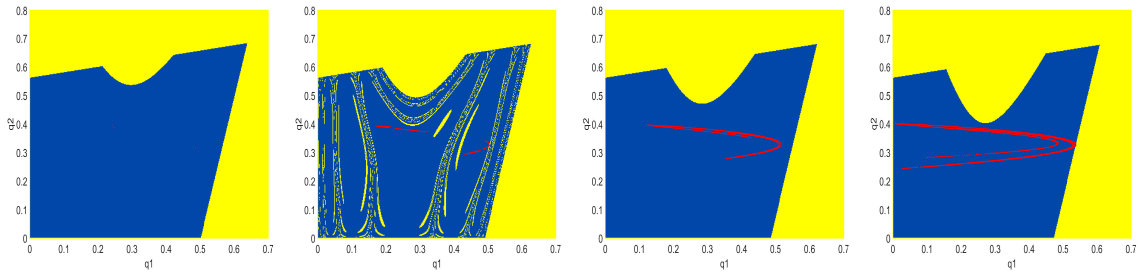

(a) **(b)** **(c)** **(d)**

Figure 4.7: Basins of attraction of the triopoly map in $q_1 - q_2$ plane with $q_3 = 0.28$: (a) $k_1 = 2.9$, (b) $k_1 = 3.1$, (c) $k_1 = 3.2$, (d) $k_1 = 3.5$.

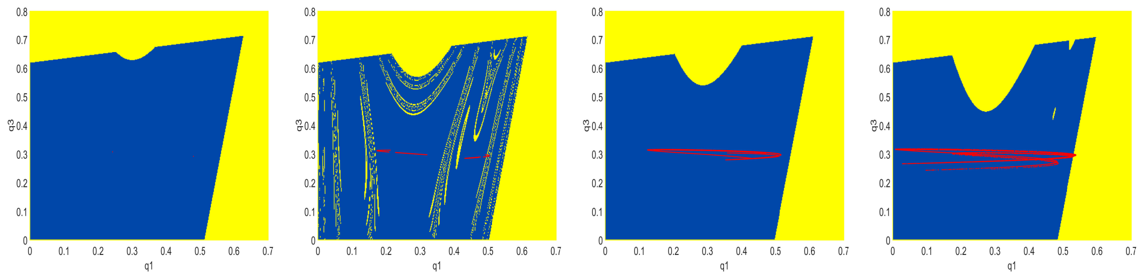

(a) **(b)** **(c)** **(d)**

Figure 4.8: Basins of attraction of the triopoly map in $q_1 - q_3$ plane with $q_2 = 0.34$: (a) $k_1 = 2.9$, (b) $k_1 = 3.1$, (c) $k_1 = 3.2$, (d) $k_1 = 3.5$.

4.5 Global Stability Analysis of the System

To study how adjustment speed influences global stability, we employ the concept of basins of attraction, which include the attraction domain, attractor, and escape region. The attraction domain represents the collection of initial output values that eventually converge to the same attractor after several iterations. When the attractor corresponds to an equilibrium point, this domain can be viewed economically as a safe zone. That is, if the initial outputs fall inside this

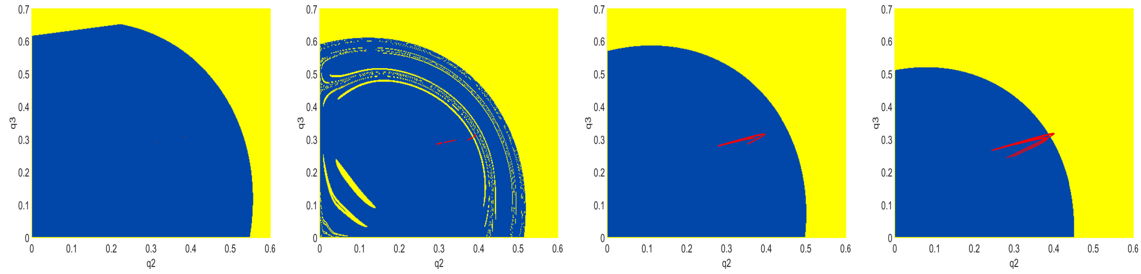

Figure 4.9: Basins of attraction of the triopoly map in $q_2 - q_3$ plane with $q_1 = 0.3$: (a) $k_1 = 2.9$, (b) $k_1 = 3.1$, (c) $k_1 = 3.2$, (d) $k_1 = 3.5$.

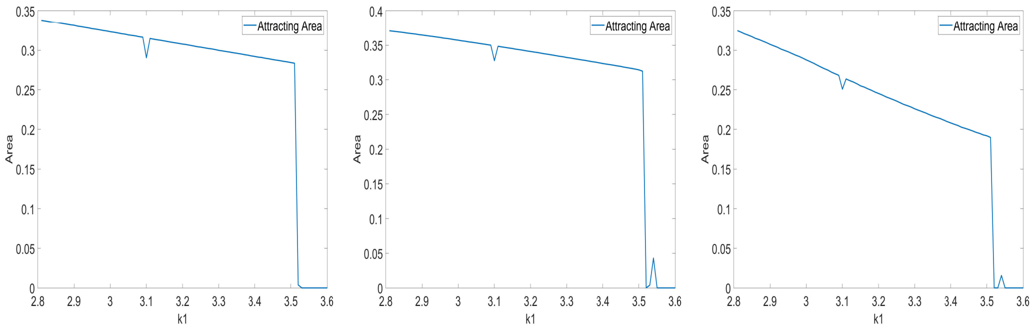

Figure 4.10: Curves of the basin areas corresponding to the attraction domain of the triopoly system (4.5): (a) for (4.7), (b) for (4.8), and (c) for (4.9).

region, the system remains stable after multiple iterations. Conversely, if the initial condition lies in the escape region, the system diverges over time.

The basins of attraction are displayed in the $q_i - q_j$ plane while fixing q_s (with $i, j, s \in \{1, 2, 3\}$, $i \neq j \neq s$). Parameters are chosen according to (4.14), and the speed parameter k_1 takes values 2.9, 3.1, 3.2, and 3.5. A total of twelve attraction basins of system (4.5) are presented in Figures (4.7a-4.9d). In these illustrations, the blue regions denote the attraction domain, red points show the attractor, and yellow points identify the escape set.

First, in the $q_1 - q_2$ plane with $q_3 = 0.28$: In Figure (4.7a), when $k_1 = 2.9$, the system exhibits a period-2 cycle, and the attraction domain has the shape of an irregular quadrilateral. In Figure (4.7b), with $k_1 = 3.1$, the system remains in a period-2 state, implying that initial values within this domain lead to alternating outputs. In Figures (4.7c) and (4.7d), at $k_1 = 3.2$ and $k_1 = 3.5$, the attraction domain is again irregular, but chaotic attractors emerge.

Next, in the $q_1 - q_3$ plane with $q_2 = 0.34$: In Figure (4.8a), at $k_1 = 2.9$, the system has a period-

2 cycle, with the attraction domain shaped as an irregular quadrilateral. In Figure (4.8b), for $k_1 = 3.1$, the system remains in the same state, where trajectories alternate if starting inside the domain. In Figures (4.8c) and (4.8d), for $k_1 = 3.2$ and 3.5, the domain retains an irregular quadrilateral form, accompanied by chaotic attractors.

Finally, in the $q_2 - q_3$ plane with $q_1 = 0.3$: In Figure (4.9a), when $k_1 = 2.9$, the system again shows a period-2 cycle, with the attraction domain approximating an irregular circle. In Figure (4.9b), at $k_1 = 3.1$, this period-2 behavior persists. In Figures (4.9c) and (4.9d), when $k_1 = 3.2$ and 3.5, the irregular circular domain persists, but chaotic attractors arise.

By varying the parameter k_1, we plot the area curve of the attraction domain in Figures (4.10a), (4.10b), and (4.10c), corresponding to the basins shown in Figures (4.7), (4.8), and (4.9). Results indicate that as k_1 increases, the attraction domain's area does not remain constant but undergoes significant changes. Specifically, the domain area generally decreases with larger k_1. This shrinking suggests that fewer initial conditions converge to the attractor, implying reduced stability and higher sensitivity to initial values. Such contraction of the attraction domain may signal the system's transition toward chaotic dynamics, where tiny variations in starting conditions yield diverging outcomes.

4.6 Stabilizing the Unstable Cournot-Nash Equilibrium via the OGY Method

In economics, chaotic dynamics are considered harmful since they undermine investor confidence, slow economic growth, and create operational difficulties. This leads to heightened market volatility and financial risks. Because chaos in triopoly games reacts strongly to even minor errors, the players' strategies may become unpredictable. Therefore, there is significant interest in developing approaches to regulate and suppress chaos in such systems. Several control strategies have been proposed, such as the OGY method [12], adaptive control [29], feedback control [32], and others including [1], [10], [16] and [24]. In this work, we adopt the OGY approach because it is minimally invasive: it requires only slight, short-lived parameter tweaks to stabilize the game's evolution.

The OGY idea is to apply small, time-varying perturbations to a controllable system parameter to steer trajectories toward an unstable equilibrium, exploiting the stable manifold to guide the orbit to the target.

Assume the system takes the form

$$W_{i+1} = H(W_i, a_1), \quad W_i \in R^3,\ a_1 \in R^+. \tag{4.17}$$

Here H is sufficiently smooth, and a_1 is an adjustable positive parameter. Treat a_1 as a variable near the nominal value $\bar{a}_1 = 2.24$; at $a_1 = 2.24$ and with parameters in (4.16), this value of a_1 corresponds to chaos, the equilibrium is $E^* = (0.8720, 0.4837, 0.5290)$.

Our objective is to tune a_1 so that the chaotic attractor captures almost all initial conditions and the system's motion converges to the Nash equilibrium. Owing to the ergodicity of chaos, when the trajectory passes sufficiently close to the unstable equilibrium, a feedback law is triggered to push the state toward the desired (unstable) Nash point.

Let $W^*(a_1)$ denote the unstable equilibrium E^*. A first-order Taylor expansion of (4.5) yields

$$W_{i+1} - W^*(\bar{a}_1) = A(W_i - W^*(\bar{a}_1)) + B\,(a_1 - \bar{a}_1), \tag{4.18}$$

where A is the Jacobian of $H(w, a_1)$ with respect to $w = (q_1, q_2, q_3)$, i.e.

$$A = \begin{pmatrix} J^*_{7,1} & k_1 a_1 q^*_{7,1} & k_1 b_1 q^*_{7,1} \\ k_2 a_2 q^*_{7,2} & J^*_{7,2} & k_2 b_2 q^*_{7,2} \\ k_3 a_3 q^*_{7,3} & k_3 b_3 q^*_{7,3} & J^*_{7,3} \end{pmatrix}, \tag{4.19}$$

with

$$\begin{cases} J^*_{7,1} = 1 + k_1\Big(1 + a_1 q^*_{7,2} - 4q^*_{7,1} - c_1 + b_1 q^*_{7,3}\Big), \\ J^*_{7,2} = 1 + k_2\Big(1 + a_2 q^*_{7,1} - 4q^*_{7,2} - c_2 + b_2 q^*_{7,3}\Big), \\ J^*_{7,3} = 1 + k_3\Big(1 + a_3 q^*_{7,1} - 4q^*_{7,3} - c_3 + b_3 q^*_{7,2}\Big). \end{cases}$$

The matrix B is the derivative of $H(w, a_1)$ with respect to a_1:

$$B = \begin{pmatrix} k_1 q^*_{7,1} q^*_{7,2} \\ 0 \\ 0 \end{pmatrix}. \tag{4.20}$$

Substituting $E^* = (0.8720, 0.4837, 0.5290)$ and the model parameters into A and B gives

$$A = \begin{pmatrix} -1.2592 & 2.5303 & 0.2259 \\ 0.2609 & -0.7393 & 0.1739 \\ 0.4752 & 0.2534 & -0.5839 \end{pmatrix}, \qquad B = \begin{pmatrix} 0.5457 \\ 0 \\ 0 \end{pmatrix}. \tag{4.21}$$

We select a linear feedback on the parameter,

$$a_1 - \bar{a}_1 = -K^T(W_i - W_*(\bar{a}_1)), \tag{4.22}$$

so that

$$W_{i+1} - W_*(\bar{a}_1) = \Big(A - BK^T\Big)(W_i - W_*(\bar{a}_1)). \tag{4.23}$$

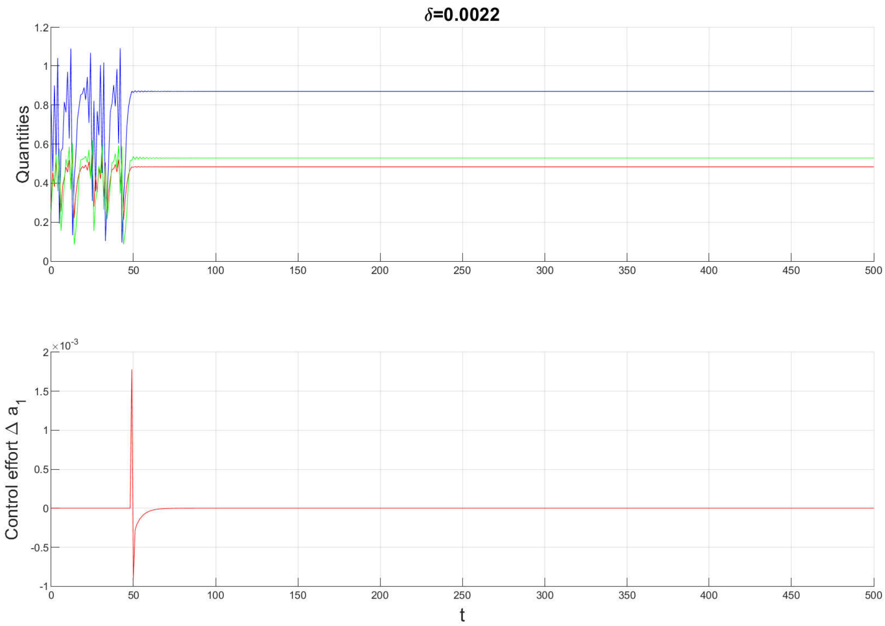

Figure 4.11: Chaos control for system (4.5) via the parameter a_1 using (4.16), evaluated at $a_1 = 2.24$.

The equilibrium $W^*(a_1)$ is stabilized provided all eigenvalues of $A - BK^T$ lie strictly inside the unit disk. Following [53], the controllability matrix is

$$D = \begin{pmatrix} B & AB & A^2B \end{pmatrix} = \begin{pmatrix} 0.5457 & -0.6872 & 1.2841 \\ 0 & 0.1424 & -0.2394 \\ 0 & 0.2593 & -0.4419 \end{pmatrix}. \tag{4.24}$$

We use pole placement; the gain K^T is chosen as

$$K^T \approx \begin{pmatrix} \alpha_3 - d_3 \\ \alpha_2 - d_2 \\ \alpha_1 - d_1 \end{pmatrix} T^{-1}, \qquad T = DQ, \tag{4.25}$$

with

$$Q = \begin{pmatrix} d_2 & d_1 & 1 \\ d_1 & 1 & 0 \\ 1 & 0 & 0 \end{pmatrix}. \tag{4.26}$$

The coefficients d_i $(i = 1, 2, 3)$ come from the characteristic polynomial of A:

$$\det(\lambda I - A) = \lambda^3 + d_1\lambda^2 + d_2\lambda + d_3, \tag{4.27}$$

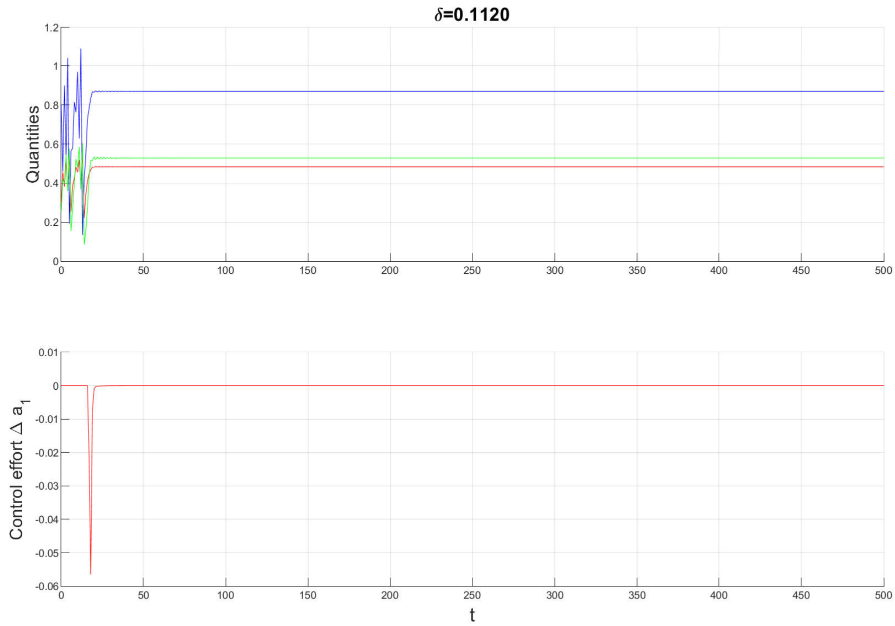

Figure 4.12: Stabilizing system (4.5) by modulating a_1 with parameters in (4.16), at $a_1 = 2.24$.

and direct computation gives

$$\det\begin{pmatrix} \lambda + 1.2592 & -2.5303 & -0.2259 \\ -0.2609 & \lambda + 0.7393 & -0.1739 \\ -0.4752 & -0.2534 & \lambda + 0.5839 \end{pmatrix} = \lambda^3 + 2.582\,\lambda^2 + 1.286\,\lambda - 0.2008. \tag{4.28}$$

Hence $d_1 = 2.582$, $d_2 = 1.286$, and $d_3 = -0.2008$. Let $\alpha_1, \alpha_2, \alpha_3$ be the coefficients of the characteristic polynomial of $A - BK^T$:

$$\det\Big(\beta I - (A - BK^T)\Big) = \beta^3 + \alpha_1\beta^2 + \alpha_2\beta + \alpha_3,$$

and

$$T = DQ = \begin{pmatrix} 0.5091 & -0.6100 & 1.1436 \\ 0 & 0.1613 & -0.2770 \\ 0 & 0.0896 & -0.0925 \end{pmatrix} \cdot \begin{pmatrix} 1.286 & 2.582 & 1 \\ 2.582 & 1 & 0 \\ 1 & 0 & 0 \end{pmatrix} = \begin{pmatrix} 0.2116 & 0.7219 & 0.5457 \\ 0.1282 & 0.1424 & 0 \\ 0.2277 & 0.2593 & 0 \end{pmatrix}.$$

Thus

$$T^{-1} = \begin{pmatrix} 0 & 315.2168 & -173.0675 \\ 0 & -276.7809 & 155.8208 \\ 1.8324 & 243.8945 & -139.0097 \end{pmatrix}. \tag{4.29}$$

The eigenvalues of A at $E^* = (0.8720, 0.4837, 0.5290)$ are approximately $\lambda_u \approx -1.8108$, $\lambda_{1s} \approx$

0.1239, and $\lambda_{2s} \approx -0.8954$. If μ_1, μ_2, μ_3 denote the desired closed-loop eigenvalues, then

$$\det\Big(sI - (A - BK^T)\Big) = s^3 - (\mu_1 + \mu_2 + \mu_3)s^2 + (\mu_1\mu_2 + \mu_2\mu_3 + \mu_1\mu_3)s - \mu_1\mu_2\mu_3, \tag{4.30}$$

which implies the coefficient relations

$$\alpha_1 = -(\mu_1 + \mu_2 + \mu_3), \qquad \alpha_2 = \mu_1\mu_2 + \mu_2\mu_3 + \mu_1\mu_3, \qquad \alpha_3 = -\mu_1\mu_2\mu_3. \tag{4.31}$$

Since K^T is non-unique, one convenient choice is $(\alpha_1, \alpha_2, \alpha_3) = \Big(-|\lambda_{1s}|, -|\lambda_{1s}|, 0\Big)$. Then

$$\begin{aligned} K^T &= \Big(0 - d_3, -|\lambda_{1s}| - d_2, -|\lambda_{1s}| - d_1\Big)\,T^{-1} \\ &= (0.2008, -1.239, -2.7059).\begin{pmatrix} 0 & 315.2168 & -173.0675 \\ 0 & -276.7809 & 155.8208 \\ 1.8324 & 243.8945 & -139.0097 \end{pmatrix} \\ &= \Big(-4.9582, -205.6478, 121.68734\Big). \end{aligned} \tag{4.32}$$

From $|a_1 - \bar{a}_1| < \delta$ and (4.22), it follows that $\Big|K_T\Big(W_i - W_*(\bar{a}_1)\Big)\Big| < \delta$. When W_i enters this band of width $2\delta/|K_T|$, the parameter is slightly perturbed; otherwise it is left unchanged. The parameter-update law is

$$a_1 - \bar{a}_1 = -K^T(W_i - W_*(\bar{a}_1))\; u\Big(\delta - \Big|K^T(W_i - W_*(\bar{a}_1))\Big|\Big), \tag{4.33}$$

where $\delta > 0$ is small and controls the activation timing. Figure 4.11 shows the controlled triopoly trajectories and the associated control input for $\delta = 0.0022$ with $\alpha_1 = \alpha_2 = -0.1239$, $\alpha_3 = 0$. As the state approaches the unstable equilibrium E^*, control activates around $t = 49$; during $t \in [46, 60]$, a_1 is perturbed with magnitude 10^{-3}. By $t = 60$, chaos is removed and the Cournot-Nash equilibrium is stabilized.

For $\delta = 0.0215$ and the same α-values, stabilization is achieved earlier, at $t = 21$, again driving the chaotic dynamics to the Cournot-Nash equilibrium (see Figure 4.12).

4.7 Conclusion

This work explored the dynamic behavior of a bounded rational triopoly game in which three firms produce homogeneous goods. The Cournot–Nash equilibrium was determined, and its local stability was analyzed. Numerical simulations revealed a variety of dynamic behaviors, including stable equilibria, periodic oscillations, quasiperiodicity, and chaos. The transition to chaos occurred through period-doubling and Neimark–Sacker bifurcations, as confirmed by bifurcation diagrams, the largest Lyapunov exponent, and the appearance of strange attractors and complex basins of attraction.

To control the chaotic motion, the OGY (Ott–Grebogi–Yorke) method was applied, demonstrating that small feedback perturbations can effectively stabilize the system at its Cournot–Nash equilibrium. This highlights the efficiency of the OGY approach in suppressing chaos and restoring stability. Overall, the study provides valuable insights into nonlinear dynamics and control in bounded rational oligopoly models and may serve as a foundation for future research involving heterogeneous agents or delayed information.

General Conclusion and Outlook

In this thesis, we have explored the complex dynamics arising in discrete-time oligopoly models through a combination of theoretical analysis, numerical simulations, and control techniques. By focusing on bounded rationality frameworks, our work contributes to the growing body of literature that bridges economics, nonlinear dynamics, and chaos theory. The study has shown that even relatively simple iterative maps representing firms' interactions can generate rich and unpredictable behaviors, including stable equilibria, bifurcations, and chaotic attractors.

We began by revisiting fundamental notions of discrete dynamical systems, such as fixed points, stability, bifurcation mechanisms, and chaos. This theoretical foundation provided the necessary tools to analyze the local and global stability properties of nonlinear maps describing economic competition. The transition from regular to chaotic regimes was investigated using analytical techniques, such as linear stability analysis and the Jury criterion, and numerical indicators like bifurcation diagrams, Lyapunov exponents, and basins of attraction.

In the second part, we examined oligopolistic market models, particularly Cournot and Bertrand games, under bounded rationality assumptions. These models capture how firms adjust their decisions based on limited information and adaptive expectations. By introducing realistic adjustment processes, we demonstrated how the equilibrium behavior of firms can lose stability through flip (period-doubling) or Neimark–Sacker bifurcations, leading to quasiperiodic or chaotic outcomes. Such results illustrate the sensitivity of economic systems to variations in adjustment speeds, cost parameters, or demand elasticities.

A major part of this work was devoted to the control of chaos. Using the Ott–Grebogi–Yorke (OGY) method and feedback-based techniques, we successfully stabilized unstable periodic orbits and restored the Cournot–Nash or Nash equilibrium when chaotic fluctuations emerged. These control strategies prove effective and practical, highlighting the relevance of chaos control in maintaining market predictability and efficiency. Moreover, the numerical experiments confirmed that slight parameter perturbations, if properly designed, can suppress irregular dynamics without altering the model's fundamental structure.

The numerical results, complemented by bifurcation diagrams, phase portraits, and time series plots, demonstrated a consistent correspondence between theoretical predictions and simulated behaviors. The coexistence of attractors, multistability, and mixed-mode oscillations further revealed the intricate interplay between competition intensity and agents' bounded rationality.

Outlook and Future Work

The results obtained in this thesis open several promising directions for future research. One possible extension concerns the incorporation of time delays, which often occur in real markets due to information lags or delayed responses to competitors' strategies. The inclusion of delay terms is expected to enrich the system's dynamics, potentially leading to new types of bifurcations and complex behaviors.

Another perspective involves extending the analysis to higher-dimensional models, such as multi-agent games, to capture the competitive dynamics among a larger number of firms. This could provide deeper insights into network effects, cooperation, and competition structures in realistic market environments.

From a methodological point of view, alternative chaos control techniques, such as adaptive, predictive, or hybrid feedback methods, can be explored to improve robustness and efficiency. In addition, the combination of control theory with optimization algorithms or machine learning approaches may offer innovative tools for real-time stabilization of economic systems.

Finally, the interdisciplinary nature of this research invites further investigation into the connections between nonlinear dynamics, game theory, and behavioral economics. Understanding how bounded rationality, learning, and expectations shape the global dynamics of markets remains a key challenge for both theorists and practitioners.

In conclusion, this work has demonstrated that discrete dynamical systems provide a powerful framework for studying the evolution, instability, and control of oligopolistic markets. By combining rigorous mathematical analysis with computational tools, we have deepened the understanding of how complex behaviors emerge and how they can be effectively managed. These findings contribute not only to the theoretical advancement of nonlinear economic modeling but also to the practical design of stable and efficient market mechanisms.

Bibliography

[1] M.S. Abd-Elouahab, N.E. Hamri, J. Wang, Chaos control of a fractional-order financial system, Mathematical Problems in Engineering 2010 (2010) 270646.

[2] M.S. Abdelouahab, R. Lozi, G. Chen, Complex canard explosion in a fractional-order FitzHugh-Nagumo model, International Journal of Bifurcation and Chaos 29 (2019) 1950111.

[3] R. Ahmed, M.Z.A. Qureshi, M. Abbas, N. Mumtaz, Bifurcation and chaos control in a heterogeneous Cournot-Bertrand duopoly game model, Chaos, Solitons & Fractals 190 (2025) 115757.

[4] A. Al-Khedhairi, Dynamics of a Cournot duopoly game with a generalized bounded rationality, Complexity 2020 (2020) 8903183.

[5] M.B. Almatrafi, M. Berkal, Bifurcation analysis and chaos control for prey-predator model with Allee effect, International Journal of Analysis and Applications 21 (2023) 131.

[6] M.B. Almatrafi, M. Berkal, Bifurcation analysis and chaos control for fractional predator-prey model with Gompertz growth of prey population, Modern Physics Letters B 39 (2025) 2550103.

[7] R. Amira, M.S. Abdelouahab, N. Touafek, M.B. Mesmouli, H.N. Zaidi, T.S. Hassan, Nonlinear dynamic in a remanufacturing duopoly game: Spectral entropy analysis and chaos control, AIMS Mathematics 9 (2024) 7711–7727.

[8] Y.V. Andreyev, Y.L. Belsky, A.S. Dmitriev, D.A. Kuminov, Information processing using dynamical chaos: Neural networks implementation, IEEE Transactions on Neural Networks 7 (1996) 290–299.

[9] S.S. Askar, Complex dynamic properties of Cournot duopoly games with convex and log-concave demand function, Operations Research Letters 42 (2014) 85–90.

[10] M. Azioune, M.S. Abdelouahab, Controlling chaos and mixed mode oscillations in a Bertrand duopoly game with homogeneous expectations and quadratic cost functions, Mathematics and Computers in Simulation 233 (2025) 553–566.

[11] M. Azioune, M.S. Abdelouahab, L. Gardini, Complex nonlinear dynamics in a two-dimensional Cournot map: From stability to chaos via local and global bifurcation scenarios, Nonlinear Dynamics 114 (2026) Art. 300.

[12] M. Azioune, M.S. Abdelouahab, R. Lozi, Bifurcation analysis of a Cournot triopoly game with bounded rationality and chaos control via the OGY method, International Journal of Bifurcation and Chaos 35 (2025) 2530019.

[13] A. Bacciotti, Discrete Dynamics: Basic Theory and Examples, Springer Nature (2022).

[14] M. Bai, Y. Gao, Chaos control on a duopoly game with homogeneous strategy, Discrete Dynamics in Nature and Society 2016 (2016) 7418252.

[15] A. Barkley, The Economics of Food and Agricultural Markets, New Prairie Press (2019).

[16] M. Berkal, M.B. Almatrafi, S. Azioune, M.S. Abdelouahab, Stability and bifurcation analysis of a discrete tumor-immune system with Allee effects, Mathematics 14 (2026) 713.

[17] M. Berkal, M.B. Almatrafi, B. Semmar, J.F. Navarro, Dynamical analysis of a generalized conformable incommensurate fractional-order modified SIR epidemic model: Stability, chaos and test, Journal of Applied Mathematics and Computing 72 (2026) 30.

[18] J. Bertrand, Review of théorie mathématique de la richesse sociale and of recherches sur les principes mathématiques de la théorie des richesses, Journal de Savants 67 (1883) 499.

[19] G.I. Bischi, C. Chiarella, M. Kopel, F. Szidarovszky, Nonlinear Oligopolies, Springer, Berlin (2010).

[20] G.I. Bischi, M. Kopel, Equilibrium selection in a nonlinear duopoly game with adaptive expectations, Journal of Economic Behavior & Organization 46 (2001) 73–100.

[21] G.I. Bischi, F. Lamantia, Nonlinear duopoly games with positive cost externalities due to spillover effects, Chaos, Solitons & Fractals 13 (2002) 701–721.

[22] R. Bououden, Systèmes dynamiques chaotiques: Application à l'optimisation, Doctoral Thesis, Brothers Mentouri University - Constantine 1 (2019).

[23] S. Bourafa, M.S. Abdelouahab, A. Moussaoui, On some extended Routh-Hurwitz conditions for fractional-order autonomous systems of order $\alpha \in (0, 2)$ and their applications to some population dynamic models, Chaos, Solitons & Fractals 133 (2020) 109623.

[24] T. Bouguettoucha, N. Boukhalfa, M.S. Abdelouahab, Nonlinear dynamics and chaos control of a discrete Rosenzweig-MacArthur prey-predator model, Journal of Innovative Applied Mathematics and Computational Sciences 5 (2025) 97–119.

[25] Eh. Boukhalfa, Sur le chaos et la synchronisation dans les systèmes dynamiques discrets, Doctoral Thesis, Badji Mokhtar University – Annaba (2017).

[26] H. Chen, W. Jia, Dynamics of quantum Bertrand duopoly games with asymmetric information, Quantum Information Processing 24 (2025) 177.

[27] A.A. Cournot, Researches into the Mathematical Principles of the Theory of Wealth, Macmillan, New York (1897).

[28] R.L. Devaney, An Introduction to Chaotic Dynamical Systems, 3rd ed., Chapman and Hall/CRC (2021).

[29] J. Ding, Q. Mei, H. Yao, Dynamics and adaptive control of a duopoly advertising model based on heterogeneous expectations, Nonlinear Dynamics 67 (2012) 129–138.

[30] S. Elaydi, An Introduction to Difference Equations, Springer, New York (2005).

[31] S.N. Elaydi, Discrete Chaos: With Applications in Science and Engineering, Chapman and Hall/CRC (2007).

[32] A.A. Elsadany, A.M. Awad, Dynamics and chaos control of a duopolistic Bertrand competitions under environmental taxes, Annals of Operations Research 274 (2019) 211–240.

[33] J. Friedman, Oligopoly theory, Handbook of Mathematical Economics 2 (1982) 491–534.

[34] D. Furth, Stability and instability in oligopoly, Journal of Economic Theory 40 (1986) 197–228.

[35] L. Gardini, N. Schmitt, I. Sushko, F. Tramontana, F. Westerhoff, Necessary and sufficient conditions for the roots of a cubic polynomial and bifurcations of codimension-1,-2,-3 for 3D maps, Journal of Difference Equations and Applications 27 (2021) 557–578.

[36] G.A. Gottwald, I. Melbourne, A new test for chaos in deterministic systems, Proceedings of the Royal Society A 460 (2004) 603–611.

[37] J. Guckenheimer, P. Holmes, Nonlinear Oscillations, Dynamical Systems, and Bifurcations of Vector Fields, Springer, New York (2013).

[38] R. Guo, Chapter 5 - Cross-border resource management: Methods, in: R. Guo (Ed.), Cross-Border Resource Management, 3rd ed., Elsevier (2018) pp. 109–137.

[39] F. Gurcan, N. Kartal, S. Kartal, Bifurcation and chaos in a fractional-order Cournot duopoly game model on scale-free networks, International Journal of Bifurcation and Chaos 34 (2024) 2450103.

[40] M.W. Hirsch, R.L. Devaney, S. Smale, Differential Equations, Dynamical Systems, and Linear Algebra, Vol. 60, Academic Press (1974).

[41] X. Jin, M. Dan, N. Zhang, W. Yu, X. Fu, S.K. Das, Game theory for infrastructure security: The power of intent-based adversary models, in: Handbook on Securing Cyber-Physical Critical Infrastructure, Elsevier (2012) pp. 31–53.

[42] R.E. Kuenne, Oligopolistic competition with scaling of characteristics, in: Price and Non-price Rivalry in Oligopoly: The Integrated Battleground, Palgrave Macmillan UK, London (1998) pp. 266–297.

[43] Y.A. Kuznetsov, Elements of Applied Bifurcation Theory, Vol. 112, Springer, New York (1998).

[44] W. Laouira, Contrôle des systèmes dynamiques chaotiques, Doctoral Thesis, Brothers Mentouri University – Constantine 1 (2018).

[45] G.C. Layek, An Introduction to Dynamical Systems and Chaos, Springer, New Delhi (2015).

[46] X. Li, L. Su, Local stability and convergence factors of nonlinear duopoly games with different types of players, Nonlinear Dynamics 112 (2024) 17627–17648.

[47] A.C. Luo, Regularity and Complexity in Dynamical Systems, Springer, New York (2012) pp. 49–59.

[48] A. Matsumoto, Let it be: Chaotic price instability can be beneficial, Chaos, Solitons & Fractals 18 (2003) 745–758.

[49] R.M. May, Simple mathematical models with very complicated dynamics, Nature 261 (1976) 459–467.

[50] M. Mechekef, L. Meddour, A novel 5D hyperchaotic system with multi-layer attractors: Sliding mode control and electronic circuit implementation, Archives of Control Sciences 35 (2025) 635–653.

[51] H. Meskine, M.S. Abdelouahab, R. Lozi, Nonlinear dynamic and chaos in a remanufacturing duopoly game with heterogeneous players and nonlinear inverse demand functions, Journal of Difference Equations and Applications 29 (2023) 1503–1515.

[52] A.K. Naimzada, G. Ricchiuti, Complex dynamics in a monopoly with a rule of thumb, Applied Mathematics and Computation 203 (2008) 921–925.

[53] K. Ogata, Modern Control Engineering, 5th ed., Prentice Hall (2010).

[54] K. Okuguchi, Expectations and Stability in Oligopoly Models, Vol. 138, Springer Science & Business Media (2013).

[55] M.J. Osborne, An Introduction to Game Theory, Vol. 3, Oxford University Press, New York (2004).

[56] E. Ott, C. Grebogi, J.A. Yorke, Controlling chaos, Physical Review Letters 64 (1990) 1196–1199.

[57] A. Ouannas, Sur la synchronisation des systèmes chaotiques discrets, Doctoral Thesis, Brothers Mentouri University – Constantine 1 (2015).

[58] T. Puu, I. Sushko, Oligopoly Dynamics: Models and Tools, Springer-Verlag (2002).

[59] G. Sarafopoulos, K. Papadopoulos, Complexity of a Bertrand duopoly game with homogeneous expectations, quadratic cost functions and chaos control, IFAC-PapersOnLine 54 (2021) 41–46.

[60] R. Seydel, Practical Bifurcation and Stability Analysis, 3rd ed., Springer (2010).

[61] T.C. Sideris, Ordinary Differential Equations and Dynamical Systems, Vol. 2, Atlantis Press, Paris (2013).

[62] D. Stauffer, H.E. Stanley, A. Lesne, From Newton to Mandelbrot: A Primer in Theoretical Physics, Springer-Verlag, Germany (2017).

[63] F. Tramontana, Heterogeneous duopoly with isoelastic demand function, Economic Modelling 27 (2010) 350–357.

[64] H. von Stackelberg, Marktform und Gleichgewicht, Springer, Vienna (1934).

[65] M. Wachs, Computer Science with Applications 2, Department of Computer Science, University of Chicago (2021).

[66] S. Wiggins, Introduction to Applied Nonlinear Dynamical Systems and Chaos, Springer, New York (2003).

[67] Q.G. Yi, X.J. Zeng, Complex dynamics and chaos control of duopoly Bertrand model in Chinese air-conditioning market, Chaos, Solitons & Fractals 76 (2015) 231–237.